Microseismic Monitoring of
Chocolate Bayou, Texas
The Pleasant Bayou No. 2
Geopressured/Geothermal Energy
Test Well Program

1982 Annual Progress Report

Prepared by
Frederick J. Mauk, Ph.D., and R. Alan Davis
Teledyne Geotech

DISCLAIMER

This report has been produced directly from the best available copy.

TABLE OF CONTENTS

ILLUSTRATIONS

TR 83-1

TR 83-1

TABLES

SUMMARY OF SIGNIFICANT RESULTS AND CONCLUSIONS
OF SEISMIC MONITORING THROUGH 1982

Seismological monitoring of the Chocolate Bayou region of Brazoria County, Texas, in the vicinity of the DOE Pleasant Bayou geopressured/geothermal design well has resulted in significant improvement in assessing the potential seismological hazards and risks associated with development of this alternative energy resource. Since the inception of the monitoring program in 1979, there hae been four periods during which significant volumes of brine have been produced from the Pleasant Bayou No. 2 well and subsequently reinjected into the Pleasant Bayou No. 1 well. Continuous seismic monitoring and analyses of the data through 1982 have resulted in the following observations and conclusions. (1) The temporal distribution of seismic events from 1979 through 1982 is not uniform. There is a pronounced increase in the frequency of occurrence of microearthquakes in the latter half of 1981. The distribution of events peaks in the fall months of 1981 and appears to be approximately Gaussian distributed about the peak. (2) Because the increased seismicity follows the Phase I short-term flow test with a delay of over two hundred days and occurs both during and following the aborted Phase II long-term flow test, the exact causality relationship between brine production and/or disposal and induction of microearthquakes is unclear. The conicidence of seismicity and times of brine production and the absence of seismicity in 1982 following a fourteen-month shut-in strongly suggest the existence of a correlation, however. If seismic activity resumes in mid 1983 following the reinitiation of the Phase II long-term flow test on 27 September 1982, there will be additional support for a hypothesized, delayed strain-release response of the local geologic column to the stress perturbation induced by the design well production. (3) The spatial distribution of the seismic epicenters from 1979 through 1982 cluster in the vicinity of proposed locations of growth faults at depths of 15,000 feet west and northwest of the Pleasant Bayou No. 2 well. Depths of the hypocenters are poorly constrained but suggest depths of origin less than that of the production reservoir. These data combined with the few unambiguously recorded first P-wave motions suggest that these microearthquakes occur as dip slip events along growth faults above the production horizon. The sense of block motion is dilitational (downward) at the seismograph stations. Because of the poor depth resolution, it is uncertain whether the events are more likely associated with brine production or brine injection. The preponderance of events have depths more strongly favoring brine injection than brine production as the causality agent; however, this evidence is extremely weak. (4) The characteristics of the observed seismicity do not indicate a high seismic risk associated with these events. No events with magnitudes greater than 2.0 have been observed. All events range in magnitude from 0.0 to 1.5. There is no obvious relationship between events which would suggest a normal foreshock, mainshock, or aftershock sequence as observed in other active tectonic regions. Even during the latter half of 1981, when event frequency was maximized, the total number of events was low ($\leq$10 events/5-day period). Although the number and size of these microearthquakes constitute a low seismic risk due to ground accelerations, the integrated displacement from many events along a single growth fault may constitute a significant subsidence hazard. The greatest benefit to be derived from microseismic moni-

toring of such production regions may be to identify which local faults display the greatest instability to slipping and thus constitute the regions which should be monitored most closely by other techniques for subsidence effects. (5) A variety of seismic signals which are significantly different from normal microearthquakes has been recorded. The frequency of occurrence of these signals, coupled with the fact that they are recorded by all other Gulf Coast microseismic arrays designed to monitor other design well projects, suggests that their occurrence is not uncommon. What, if any, significance can be placed on their role in stress release or understanding brine production and/or brine injection related phenomena is unknown at this time. (6) In conclusion, the results of seismic monitoring of the region around the Pleasant Bayou design well definitely demonstrate a correlation of increased local seismicity with high-volume brine transfer. The causality relationship and details of the induced activity remain areas requiring more extensive analyses and research.

TR 83-1

INTRODUCTION

The commercial feasibility of utilizing the vast quantities of geopressured/ geothermal brines underlying the Texas and Louisiana Gulf Coast is dependent upon high volumetric production and disposal rates. The production requirements for effective withdrawal and disposal of these environmentally hazardous fluids is generally $2 - 3 * 10^4$ barrel/day/well. Volumes of this order, by substantially altering the local state of subsurface stress, likely will cause ground subsidence and tilt in the immediate area of brine withdrawal. These withdrawals may activate preexisting growth faults as well as cause new fractures to occur.

To investigate the seismic risks associated with geopressured fluid production from the Pleasant Bayou No. 2 design well, Teledyne Geotech, with the authorization of the Texas Bureau of Economic Geology, has conducted a seismic monitoring program in the vicinity of the Brazoria County design wells since 1979. The monitoring program was designed first to establish the nature of the local ambient seismicity prior to production, and second to provide continued surveillence of the area during the well tests to determine if production altered ambient seismic conditions significantly.

Brine and gas are produced from the Pleasant Bayou No. 2 well at a depth of 14,647 - 14,707 feet (4464.4 m - 4482.7 m). The brines subsequently are reinjected in the Pleasant Bayou No. 1 well, approximately 152 meters from the production well, at a depth of 6226 - 6538 feet (1897.7 - 1892.8 m). The production history of the well has been extremely sporadic since the inception of the program. Prior to the formal testing program, 174,000 barrels of brine were produced from the well between 15 November and 3 December 1979. On 16 September 1980, the Phase I (short-term) flow test was initiated. Between 16 September and 31 October 1980, an additional 537,300 barrels of brine were produced. The wells remained shut-in until 2 July 1981 when a Phase II (long-term) flow test was begun. Due to a variety of problems, this flow test was aborted on 18 July 1981 after an additional 220,904 barrels of brine had been produced. The wells were again shut-in until 27 September 1982 when the Phase II flow test was reinitiated. By 1 October 1982, a total of 1,215,669 barrels of brine and 25,616 mcf of gas had been produced from the Pleasant Bayou No. 2 well since the beginning of the design well program. A total of 2,870,443 barrels of brine and 61,785 mcf of gas had been produced by 3 January 1983. This report describes the operation, data analyses, results and conclusions of the Brazoria seismic network during the operational period from 1 January through 31 December, 1982.

Results and conclusions drawn from analyses of the data are the opinions of the authors. Neither the Department of Energy, the Texas Bureau of Economic Geology, nor Teledyne Geotech necessarily endorse these opinions nor are they responsible for subsequent utilization of materials included in this document by other persons.

TR 83-1

THE BRAZORIA SEISMIC NETWORK, INSTRUMENTATION, DESIGN, AND SPECIFICATIONS

The Brazoria County seismic array consists of five seismograph stations in the Chocolate Bayou area of Brazoria County, Texas. The locations of these stations, local cultural features, and projected locations of growth faults at a depth of 16,000 feet are illustrated on figure 1. The aperture of the array is four kilometers. The latitudes, longitudes and elevations of the sensors are listed in table 1. Figure 2 is a block diagram illustrating the operation of the array. Each station consists of a Teledyne Geotech S-500 seismometer which is locked in a borehole at a depth of one hundred feet. The signal from the seismometer is magnified using a Teledyne Geotech 42.50 amplifier and then FM multiplexed to a voice-band carrier frequency for transmission to a common data collection point at Liverpool, Texas. Data transmission is via telephone telemetry circuits. At Liverpool, the signals from the five stations are amplitude conditioned and multiplexed together for transmission via ATT long lines to the Teledyne Geotech laboratory at Garland, Texas.

TABLE 1. BRAZORIA COUNTY TEXAS SEISMIC ARRAY

Site	Latitude(N) Deg	Min	Sec	Longitude(W) Deg	Min	Sec	Elevation Feet	Magnification X 1000 @ 5 Hz	VCO Hz
BEG1	29	17	28	95	16	53	-87	147	1360
BEG2	29	17	32	95	14	01	-87	138	2380
BEG3	29	16	54	95	15	22.5	-97	140	1020
BEG4	29	15	54	95	14	45.2	-90	164	2040
BEG5	29	15	53.4	95	16	10.3	-84	159	1700

In Garland, the five station signals are demultiplexed from their respective carriers using Teledyne Geotech 46.12 discriminators. The signals and precise time code then are recorded on magnetic tape and on 16-mm film using a Teledyne Geotech develocorder. The unity-gain velocity response of the system is illustrated in figure 3. The magnification at a frequency of five hertz of the individual stations is given in table 1. Variations in effective magnification reflect the variability of the ambient noise at the different sites.

In general, the maximum (O-P) ground displacements observable with the Brazoria seismograph instrumentation without significant distortion or clipping at one, five and ten hertz are respectively $7.4 * 10^{-5}$, $2.6 * 10^{-6}$, and $1.2 * 10^{-6}$ meters. The minimum (O-P) ground displacements observable are between $1 * 10^{-9}$ and $5 * 10^{-9}$ meters depending upon ambient ground noise conditions. These observation limitations correspond to events with seismic moments between 10^{17} and 10^{20} dyne-cm or approximate local magnitudes between -0.5 and 2.5 (see figure 4).

TR 83-1

FIGURE 1. BRAZORIA COUNTY TEXAS SEISMIC ARRAY

SCALE 1:62500
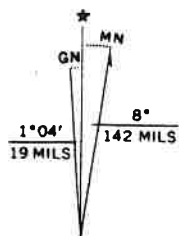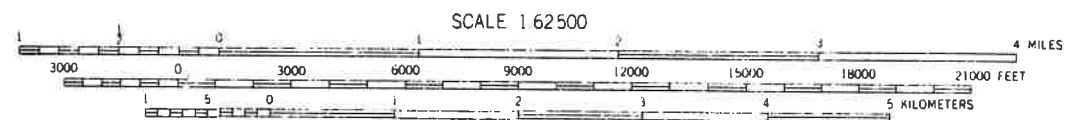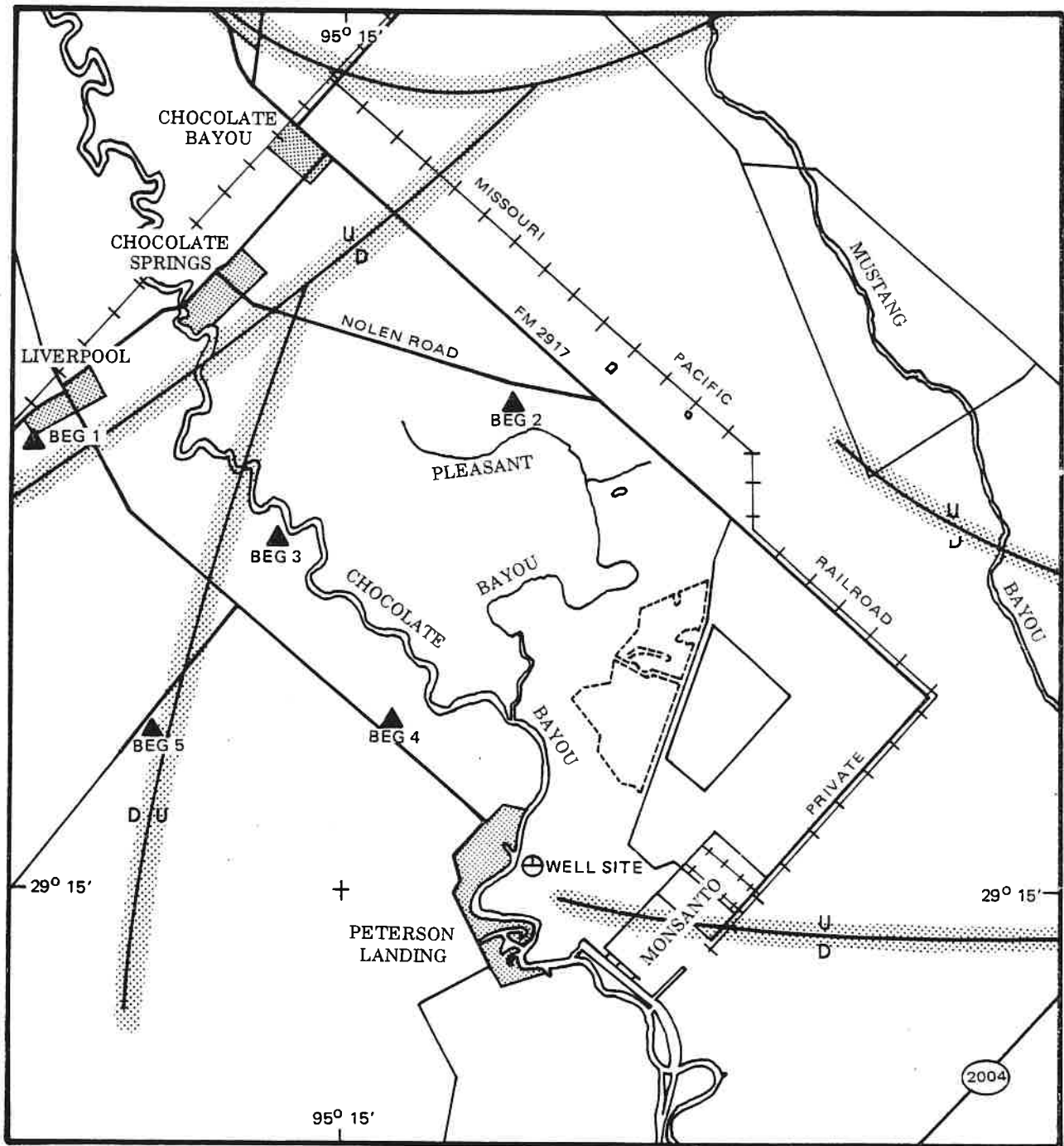
SEISMOGRAPH STATIONS

TEST WELL

GROWTH FAULTS AT 15000 FEET

TEXAS

QUADRANGLE LOCATION

G 11907

TR 83-1
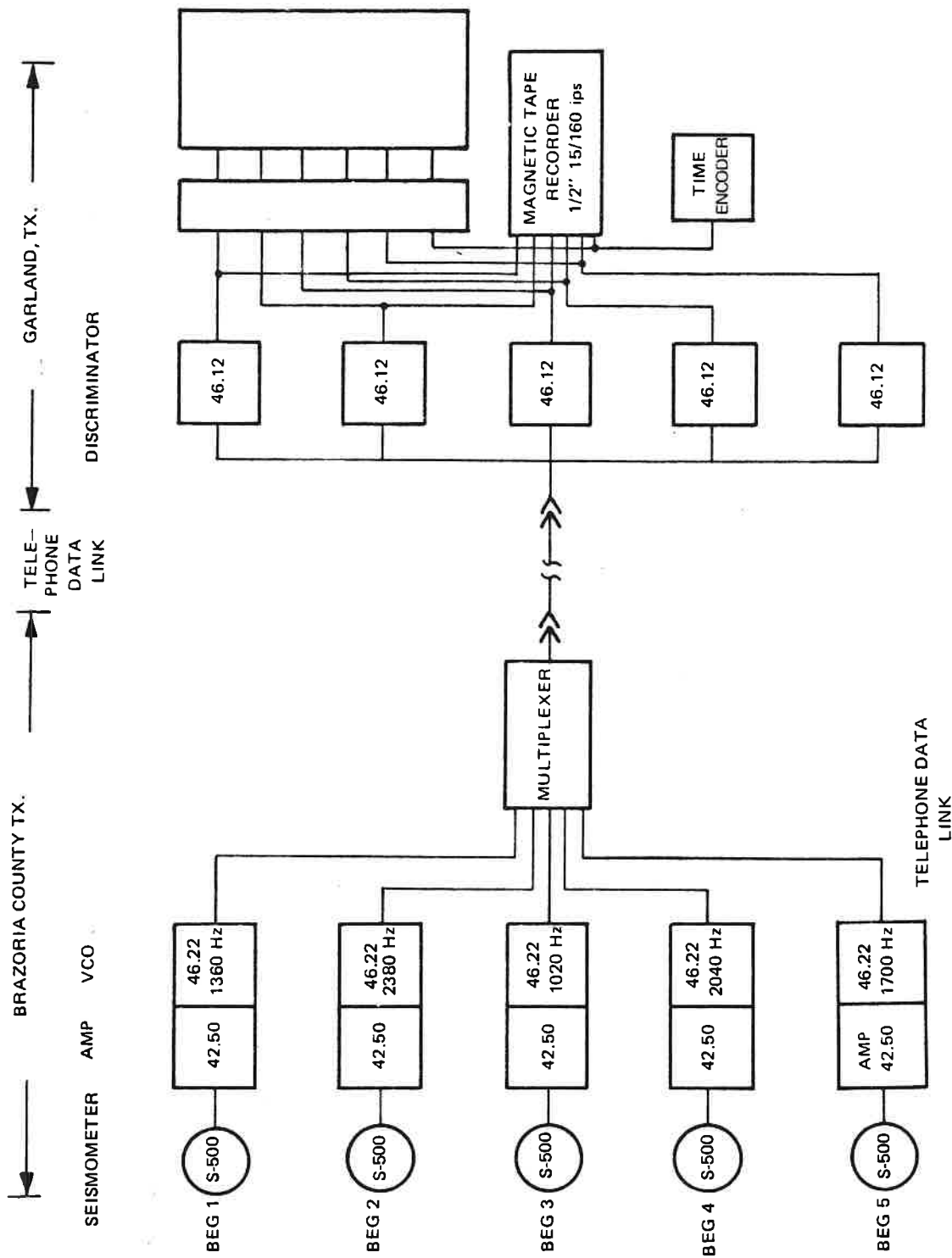
FIGURE 2. BLOCK DIAGRAM OF BRAZORIA COUNTY SEISMIC ARRAY

G 11908

-6-
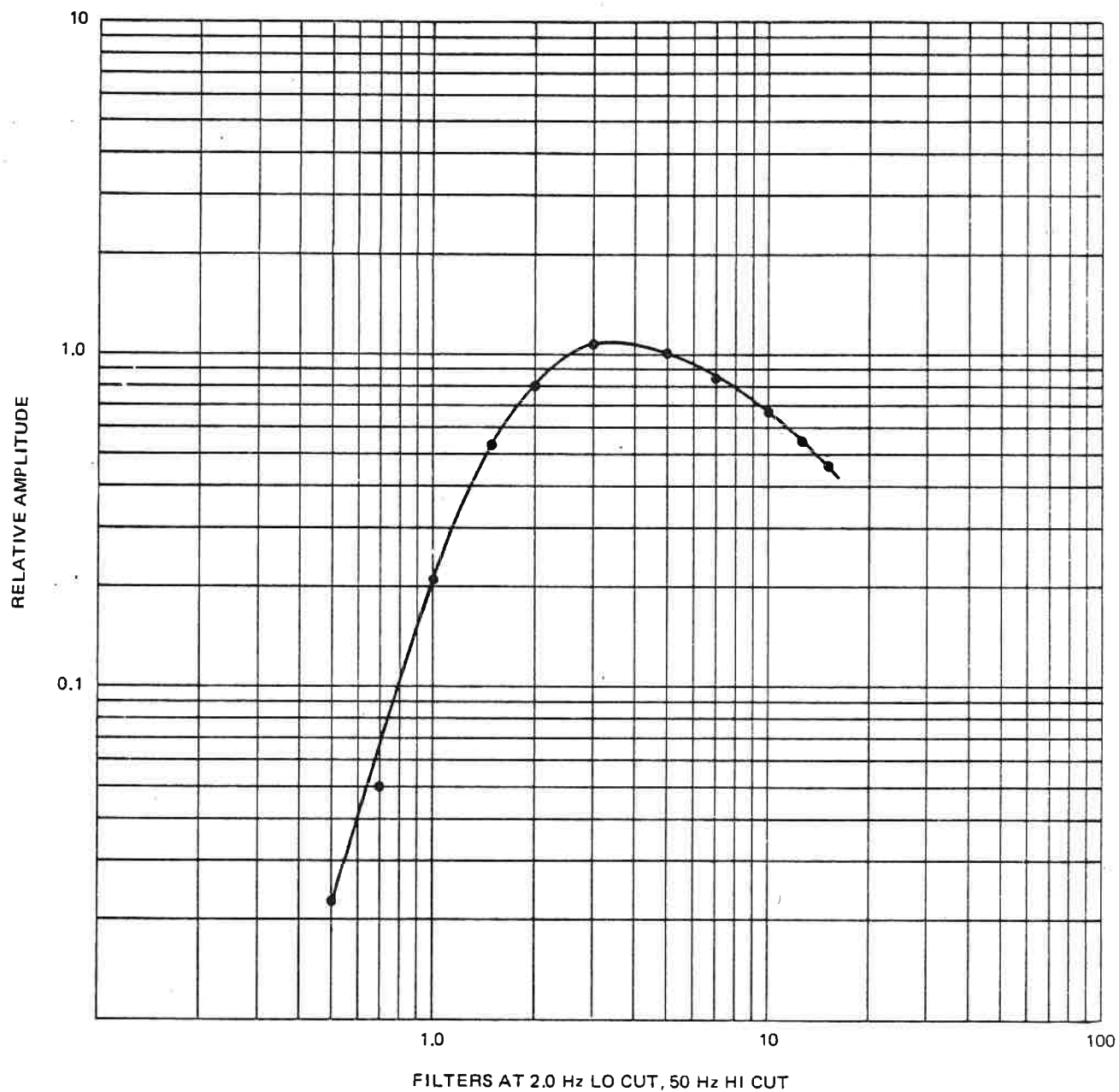
FIGURE 3. SYSTEM VELOCITY RESPONSE AT BRAZORIA

Y-axis: RELATIVE AMPLITUDE

X-axis: FILTERS AT 2.0 Hz LO CUT, 50 Hz HI CUT

G 11147C

-7-
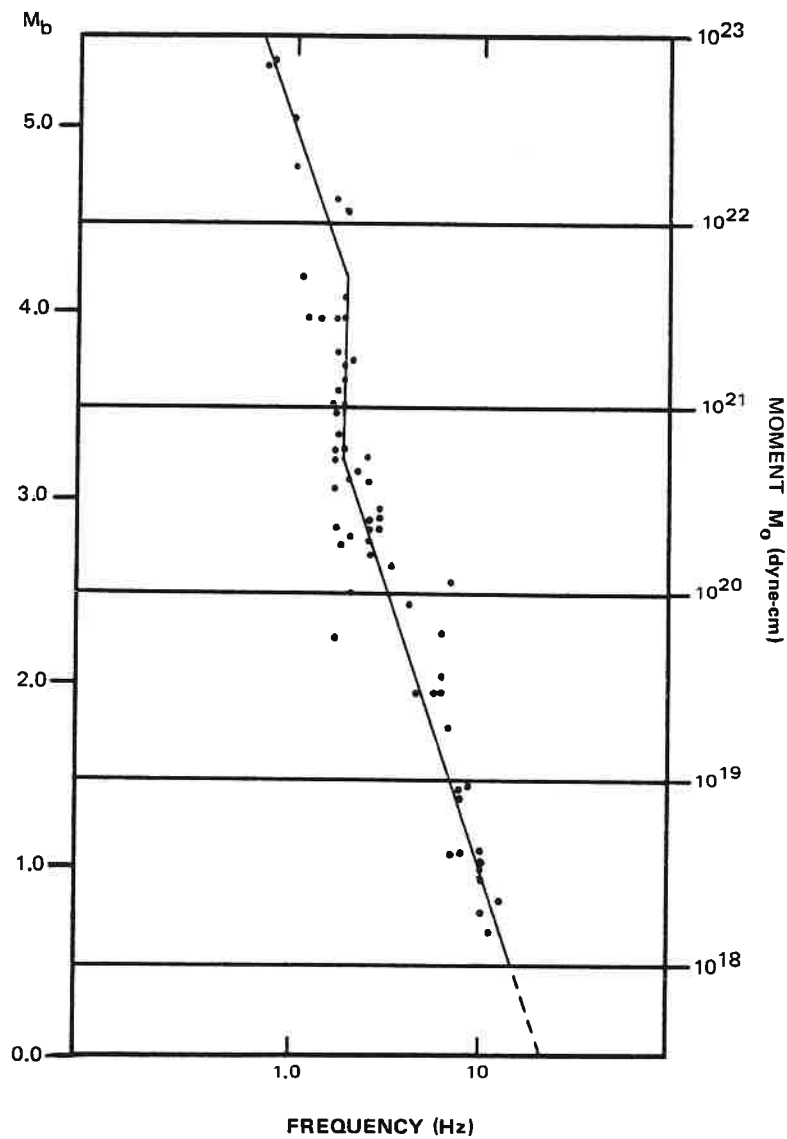
FIGURE 4. CORNER FREQUENCY VERSUS SEISMIC MOMENT FOR CENTRAL UNITED STATES EARTHQUAKES (AFTER STREET, HERRMANN, AND NUTTLI, 1975)

G 12321

In addition to observational constraints determined by instrumentation and
ambient noise conditions, data utility constraints also are dependent upon
station operational performance. Since event location procedures require
data from three or more stations, individual station operational performances
can determine and dramatically affect event location capabilities and spatial
coverage. The monthly operational performance logs for the Brazoria array
during 1982 are included as appendix A. The percentages listed are based on
continuous operation twenty-four hours daily, seven days a week. The maximum
possible recording efficiency is 99% if recording disruptions are constrained
to routine record changing. If the seismic array is operated only Monday
through Friday, the maximum possible recording efficiency is 73%. The array
was recorded continuously from January through September; however, field-
services manpower shortages required curtailment of weekend recording from
October through December. The percentages listed in Appendix A do not
reflect inability to use the data because of excessive cultural and/or
natural noise. Trains in the Chocolate Bayou area create excessive noise
amplitudes for durations of approximately ten minutes six times daily. This
noise source reduces the percentage of useable data by four percent per
month.

DATA ANALYSIS PROCEDURES

Body Wave Data

The data generated by the Brazoria seismic array are analyzed using standard procedures to yield basic information about origin times, locations and magnitudes of observed events. The 16-mm film seismograms are reviewed carefully to detect any microseismic events that may have occurred. When an event is detected, the analyst measures the amplitude, period, and arrival times of the P (compressional), S (shear), and L_R (surface) wave of the event. The desired accuracy of the arrival time estimates is ± 0.01 second for P waves and ± 0.05 second for S waves. If this degree of accuracy cannot be achieved utilizing the film records, the analyst may request a filtered version of the signal recorded on magnetic tape. Filter options include variable high-pass, low-pass, and band-pass operators. The amplitude, period and arrival time data are stored for subsequent input into a computer code (MEHYPO) which estimates the origin times, source coordinates and local magnitudes of the observed events. The estimation algorithm is similar to that described by Lee and Lahr (1972) in that it finds the origin time and set of source coordinates which minimizes the mean square difference between observed and predicted arrival times at the various sensor locations. The code also provides various location uncertainty estimates which are based upon the assumption that the arrival time errors are normally distributed and that the seismic velocity structure is known without error. The sensor frequency response data, the P-wave amplitude and period data are used to compute the local magnitudes of the observed events.

A generalized P-wave velocity structure for the Gulf Coast is illustrated in figure 5. The actual velocity structures used in the event location procedure are listed in tables 2a and 2b. Two different velocity structures are necessary because of sharp velocity inversions in shallow layers. These velocity inversion layers can be included in the location computational schemes for array-interior events because the wave incidence angles are sufficiently high to permit transmission of the waves through the layers. However, array exterior events can have wave incidence angles to the low velocity layers which do not permit theoretical transmission of the energy as a normal refracted wave and thus fail to converge to a location solution. Solutions exterior to the array can be obtained by smoothing these velocity inversions out of the structure as in table 2b. Comparisons of known and computed locations of explosions outside the array demonstrated that this smoothing procedure does not jeopardize the accuracy of the location. On the other hand, including the velocity inversion layers for array interior events improves both the precision and accuracy of the locations obtained.

The S-wave velocity structure was derived from the P-wave velocity structure using the formulation:

$$V_S = V_P / (1 + \overline{1 - 2\sigma})^{1/2}$$

-10-
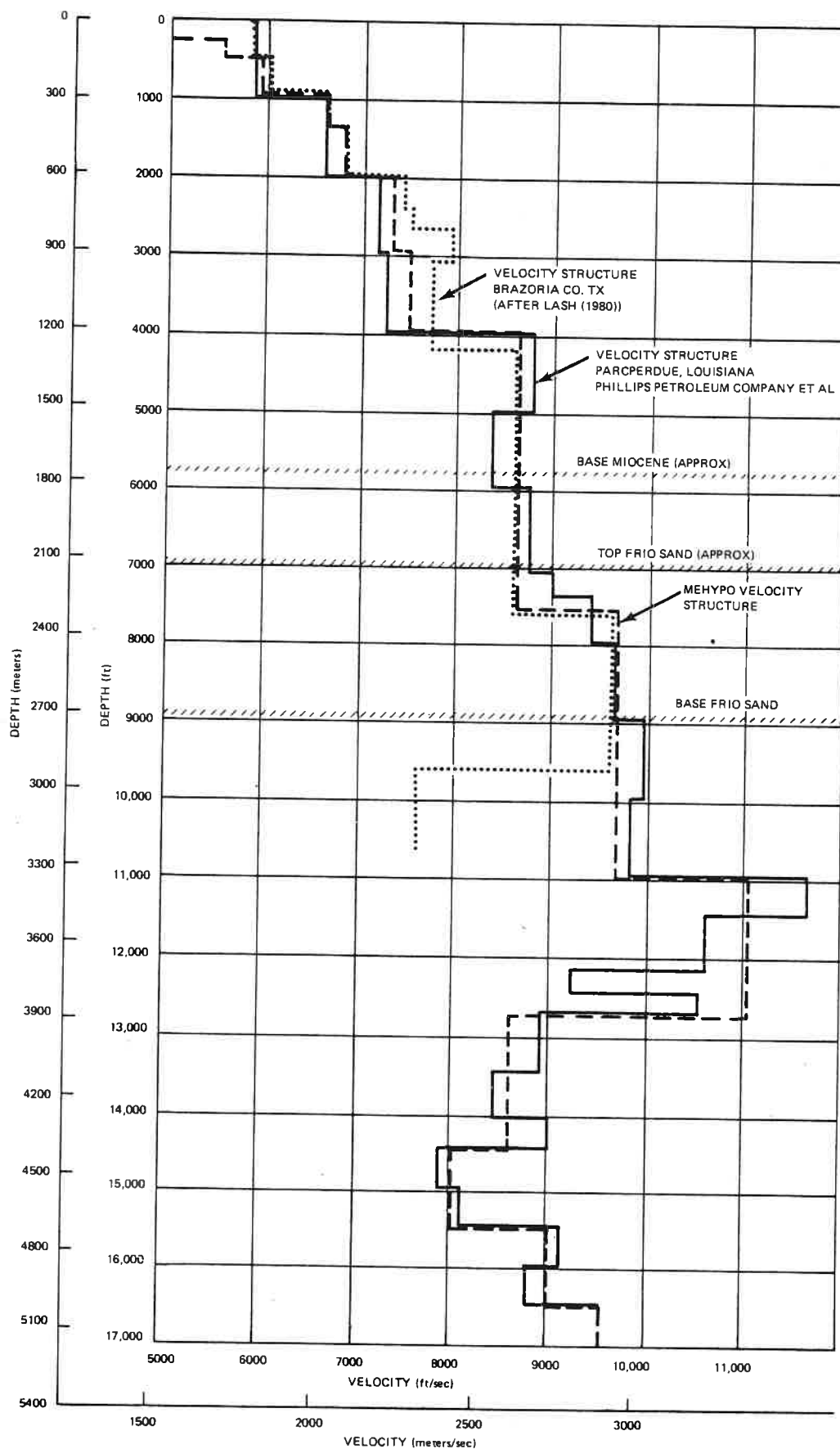
FIGURE 5. P-WAVE VELOCITY STRUCTURE

G 11746

TR 83-1

TABLE 2A.   VELOCITY STRUCTURE FOR EVENTS INSIDE THE ARRAY

Layer Parameters	P-Wave Vel. (Km/sec)	S-Wave Vel. (Km/sec)	Thickness (Km)
1	0.6100	.352	0.0091
2	1.7070	.986	0.1000
3	1.7500	1.010	0.0400
4	1.8000	1.039	0.1500
5	2.0120	1.162	0.1220
6	2.0730	1.197	0.2140
7	2.2550	1.302	0.2900
8	2.2860	1.320	0.3100
9	2.6210	1.513	1.036
10	2.9260	1.689	1.0500
11	3.3530	1.936	0.5500
12	2.6210	1.513	0.5200
13	2.4380	1.403	0.3100
14	2.7430	1.584	0.3100
15	2.9260	1.689	0.3000
16	3.1700	1.830	0.3000
17	3.5000	2.021	0.3000
18	3.8000	2.194	1000.0000

TABLE 2B.   VELOCITY STRUCTURE FOR EVENTS OUTSIDE THE ARRAY

Layer Parameters	P-Wave Vel. (Km/sec)	S-Wave Vel. (Km/sec)	Thickness (Km)
1	0.8000	0.4619	0.0600
2	1.1000	0.6351	0.0710
3	1.3910	0.8031	0.3270
4	2.2000	1.2702	0.2650
5	2.3500	1.3568	0.4500
6	3.5400	2.0439	1.6680
7	3.9600	2.2864	1.8140
8	4.2500	2.4538	0.6000
9	4.7000	2.7136	1.0000
10	4.9000	2.8291	5.0000
11	5.1000	2.9446	200.0000
12	5.3000	3.0600	1000.0000

where: V_S = Shear wave velocity
V_P = Compressional wave velocity
σ = Poisson ratio

Water has a Poisson ratio of 0.5, and most competent rock has a Poisson ratio of 0.25. Lash (1980) has determined the Poisson ratio for surficial Gulf Coast sediments to be greater than 0.45 with the ratio decreasing with increasing depth. To utilize S-waves for hypocenter location, we are using a fixed V_P/V_S ratio of 1.732 and treating them as pseudo P-wave arrivals. Epicenters are computed only for events observed at three or more stations because of possible ambiguities of solutions based on data from fewer stations.

Surface Wave Data

Signals consisting entirely of surface (Rayleigh) waves are recorded commonly by the Brazoria, Parcperdue, Sweet Lake, and Rockefeller Refuge seismic arrays. Hypocenters of events generating these signals cannot be determined using standard Geiger least-squares inversion procedures. It is possible to determine approximate epicenters of these events, however, if an appropriate wave velocity for the observed phase arrivals can be determined.

The excitation of surface waves, particularly in an environment characterized by significant variations in velocity in three dimensions, is more complex than excitation of primary body waves. Surface waves, unlike body waves, propagate not only as fundamental mode oscillations, but also as higher mode oscillations. These higher modes are analagous to overtones produced by musical instruments. Both the velocities and amplitudes of the Rayleigh modes excited are critically dependent on the body-wave (both P and S waves) velocity structure. Figure 6 illustrates the relative excitation of the first four vertically-oriented, two-hertz Rayleigh modes as a function of depth for a location near Apache, Oklahoma, (Douze, 1964). Also illsutrated are the density, P-wave, and S-wave profiles for the upper 3,000 meters of geological section. The relative amplitudes of the higher modes generally decline significantly as mode number increases when the velocity structure is free of low-velocity zone energy traps. If, on the other hand, the depth of a particular model maximum occurs in a low-velocity zone (LVZ), that mode will display an anomalous amplitude compared with that which would be excited if the LVZ were not present. The observed Rayleigh-wave energy at any particular frequency is dependent upon the depth of observation and the total energy integrated over all possible modes. Thus, for example, a seismogram from a location at a depth of 2,000 meters in the structure of figure 6 would display Rayleigh waves dominated by first, second and third higher mode arrivals with very little contribution by the fundamental mode.

The Gulf Coast sedimentary column is significantly more complex than the one illustrated in figure 6, and the relative importance of higher mode contributions, particularly at wave frequencies greater than two hertz, should not be underestimated. Figure 7 illustrates the computed and observed Rayleigh group velocities as a function of period for six Rayleigh modes in Gulf Coast sediments for Refugio County, Texas (Ebeniro, Wilson, and Dorman, 1983). Note that fundamental third-, fourth-, and fifth-order harmonics are

-13-
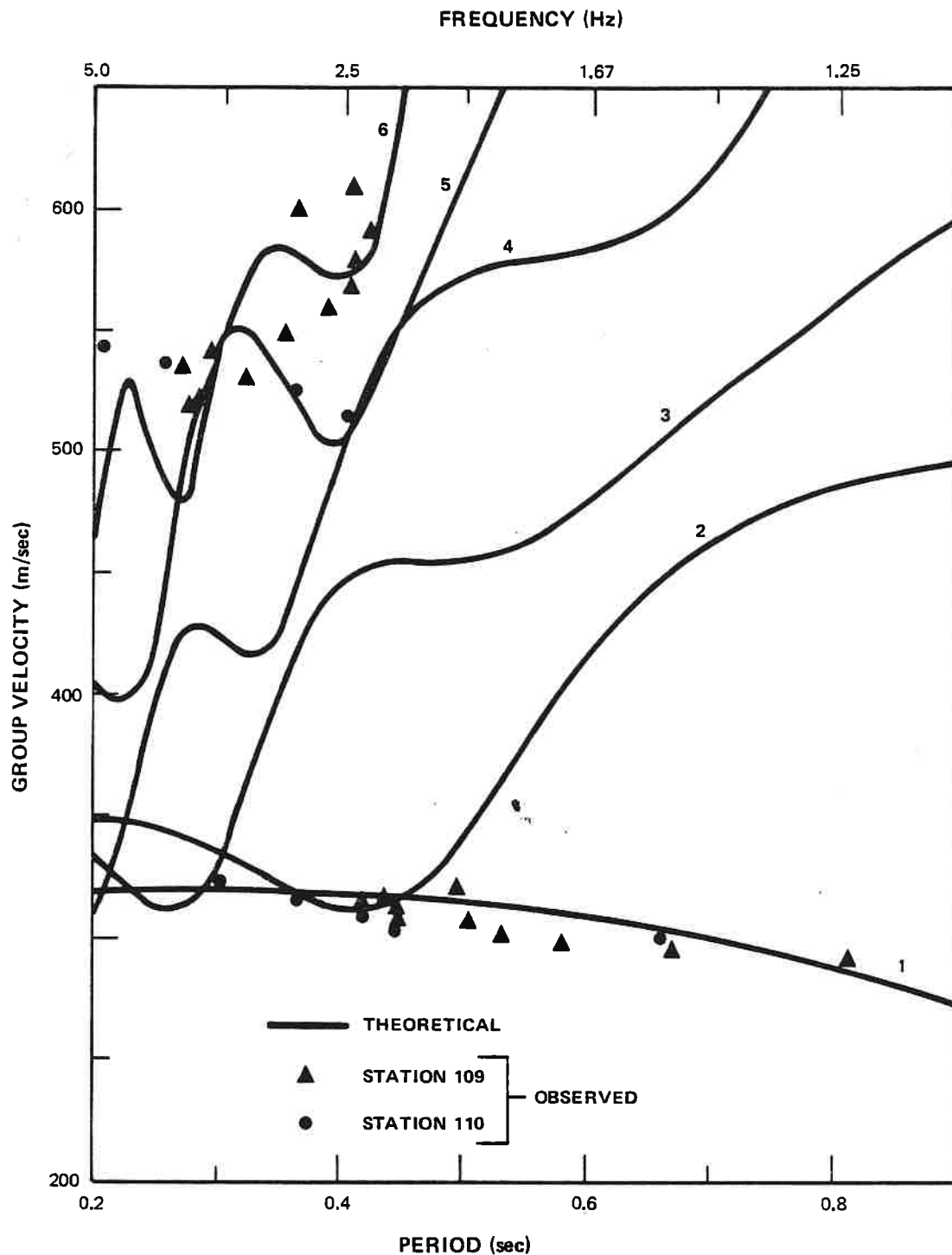
FIGURE 6. RAYLEIGH WAVE GROUP VELOCITY FOR SIX MODES IN TEXAS GULF COAST SEDIMENTS (AFTER EBENIRO,WILSON AND DORMAN, 1982)

G 13221
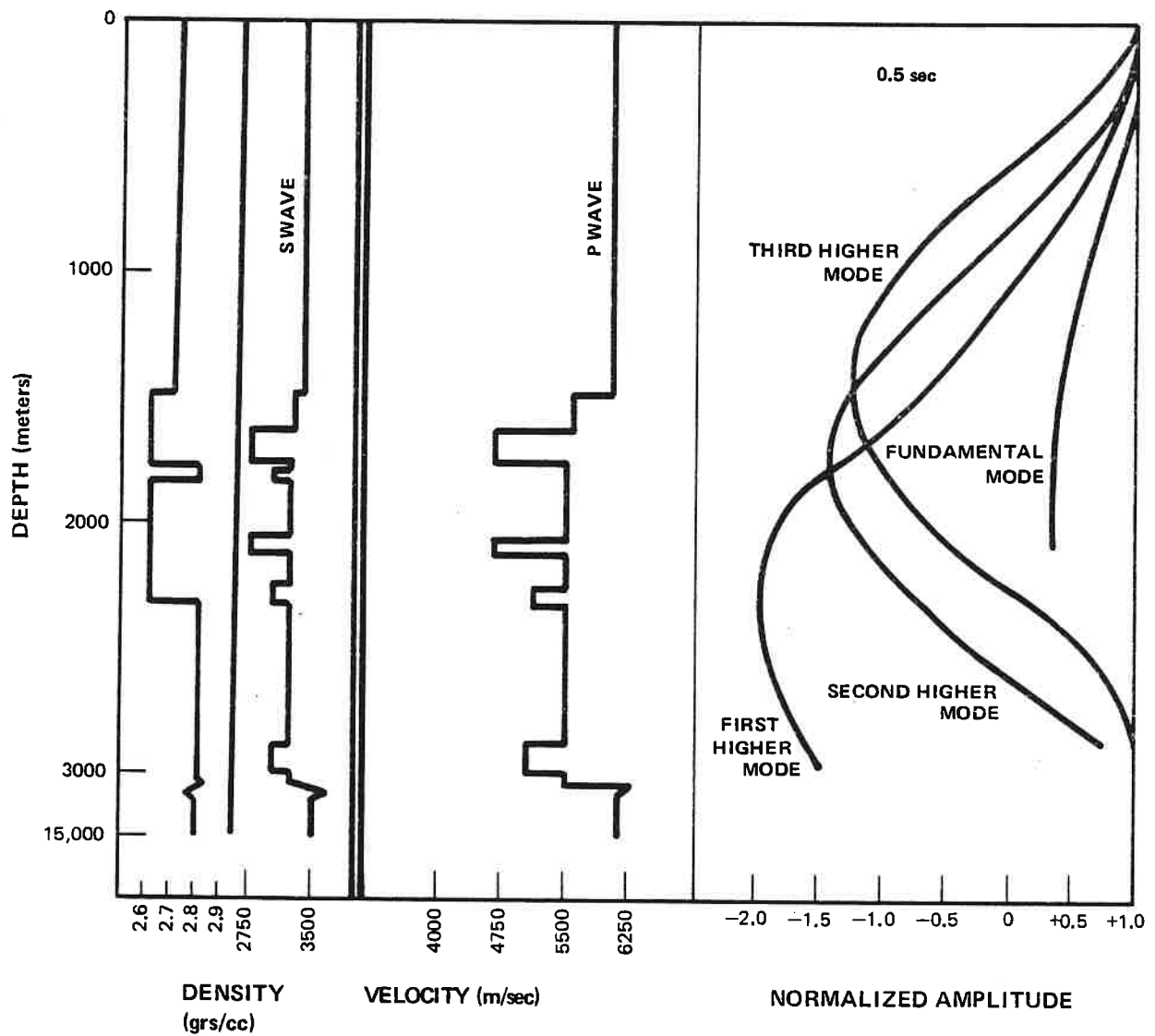
FIGURE 7. VELOCITIES, DENSITY, AND THEORETICAL RAYLEIGH WAVE AMPLITUDE—DEPTH CURVES AT 2.0 Hz, APACHE, OKLAHOMA (AFTER DOUZE, 1964)

observed, and that first and second higher modes are not. The higher modes are strongly, normally dispersed (i.e., phase and group velocities are inversely related to wave frequency). The fundamental mode, on the other hand, is relatively non-dispersed, or slightly inversely dispersed, in the frequency range from one to five hertz. This accounts for why the Rayleigh wave train frequently appears as an impulsive arrival in the time domain. Since the density, bulk and shear moduli are all low for Gulf Coast sediments, the fundamental mode Rayleigh wave velocities are also low, ranging from 290 m/sec to 350 m/sec. Unfortunately, this is the velocity range also occupied by acoustical transmissions through air, and significant coupling of atmospheric acoustic and earth Rayleigh waves is highly probable. Thus, it is very important to determine if observed impulsive Rayleigh waves are of atmospheric or earth origin. This discrimination is not necessarily obvious as will be shown in a later section.

Because of these complexities in Gulf Coast Rayleigh wave excitation and propagation, event epicenters computed from Rayleigh wave velocities must be regarded with a greater caution than more complete body wave solutions. The procedure we follow to locate these events is to solve iteratively for the least-squares error associated with both the location and wave velocity simultaneously. The functional relationship between epicentral area uncertainty and half-space velocity typically assumes approximately hyperbolic shape (see figure 8).

We assume that the hyperbolic vertex corresponds with the best half-space velocity and that the computed location using this velocity is the best approximation of the eipcenter. Depth is unconstrained in these solutions.

TR 83-1
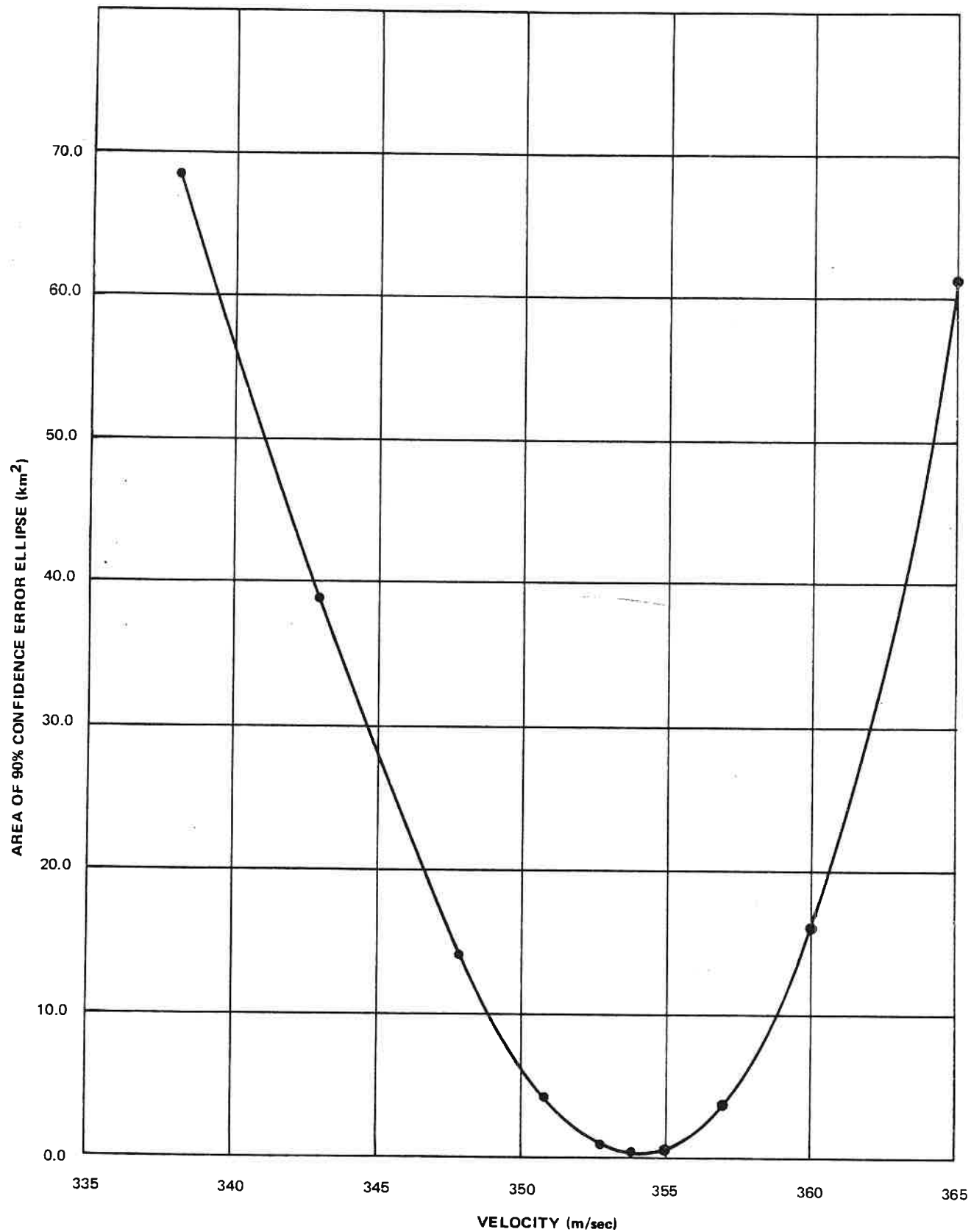
FIGURE 8. VELOCITY ANALYSIS OF IMPULSIVE RAYLEIGH EVENT
22 AUGUST 1982 AT 18:52:28.7 UCT TIME

G 13007

TR 83-1

Local seismic magnitudes are based upon maximum surface wave amplitude and are calculated as:

$$M_L = \log_{10} (A/2) - 1.15 + 0.8 \log_{10} (X)^2$$

where M_L is the local magnitude

where   A is the peak-to-peak surface wave amplitude in nanometers (10^{-9} meters)

where $X = [(\text{epicentral distance})^2 + (\text{hypocentral depth})^2]^{1/2}$
         (in kilometers)   (in kilometers)

and $X \geq 1.0$

The constant -1.15 in the magnitude equation assumes a surface wave to P-wave amplitude ratio of 10. Thus, a magnitude 0 event at 1 km distance would generate surface waves with a peak-to-peak amplitude of 28.3 nm and P waves with an amplitude of about 2.8 nm.

Magnitudes may be calculated alternatively using duration as

$$M_D = -2.22 + 1.18 \log (D)$$

where   D is duration in seconds from onset of P to return of coda to ambient noise level. It has been shown by Aki and Chouet (1975), Chouet, Aki, and Tsujiura (1978) and Aki (1981) that the duration of seismic coda is dependent on the number and distribution of potential backscattering sources. For this reason, coda duration magnitude formulations must be tailored specifically for each region where they were used. The duration magnitude formula we use is one for the Mississippi Embayment determined by the Tennessee Earthquake Information Center. Since a magnitude scale has not been developed for the Gulf Coast, it is possible that all quoted magnitudes are in error. The magnitudes quoted should agree approximately with normal Richter magnitudes.

The Event Catalogs

Each month, an event catalog is produced and event locations computed using the MEHYPO algorithm. Three types of events may be included in the catalog, explosions, natural events which have identifiable compressional and/or shear wave and surface/acoustic wave events, the origin of which are unknown but suspected to be natural. Acoustic signals related to atmospheric events such as thunder will not be included.

Explosions such as exploration shots will be entered as follows: the best recorded shot of the sequence will be timed and located using MEHYPO. No magnitudes will be calculated, and the remainder of the shot sequence will be identified by time of occurrence only. The one identified shot location can be taken as a general location for the sequence.

-18-

Natural events for which P and/or S phases are identified will be thoroughly
identified. The arrival times and amplitudes of significant phases will be
cataloged, and the hypocenter parameters determined. If the events are
prominent, photo duplicates of the records are included. Since the months of
November and December have not been reported previously, their data are
listed separately in this annual report.

An annual event catalog is compiled from the monthly event catalogs. Only
events which are significant to the geopressured/geothermal well program are
included in this catalog. The annual catalog of events is tabulated in the
Seismic Activity During 1982 section.

TR 83-1

DISCUSSION OF OBSERVED ACTIVITY FOR NOVEMBER AND DECEMBER, 1982

During the months of November and December, 1982, three events of interest were recorded by the Brazoria seismic array. The phase arrival data of these events are given in Table 3. All of these events are explosion shot series originating from outside the array.

Entries for the monthly data log utilize the following notation conventions:

Station Identification

BEG1, BEG2, BEG3, BEG4, BEG5

Phase Identification

    P - compressional wave

    S - shear wave

   LR - Rayleigh surface wave

    i - impulsive first motion

    e - emergent first motion

    c - compressional first motion

    d - dilatational first motion

    ? - ambiguity of designation

   pP - P-wave reflected at the crust near the epicenter

   sS - S-wave converted to P-wave at reflection like pP

Airy - Airy phase (minimum group velocity) of Rayleigh wave.

Phase Timing

Times are designated in Universal Coordinated Time (UTC) which is equivalent to Central Standard Time + six hours. Explosions in a sequence may be designated by hour and minute only.

Phase Amplitude and Period

A_m = maximum 0-peak amplitude of the phase in mm observed on develocorder review (20 x magnification)

A = sustained 0-P amplitude in mm observed on develocorder review (20 x magnification) of a train of waves.

TR 83-1

T = period of the wave in seconds.

D = duration of signal in seconds from onset of P to code = ambient noise.

C = number of cycles in a wave train.

Example Data Entry

BEG1   iPC   04:24:15.1, T = 0.5, A_m = 20.0, A = 13.0;
          eS   04:24:20.3, T = 1.0, D = 35

Station BEG1 recorded an impulsive-compressional P-wave at 04:24:15.1 UCT.
The sustained amplitude was 13 mm zero to peak, the maximum amplitude was 20
mm, the period of the wave was 0.5 seconds. An emergent S wave was recorded
at 04:24:20.3 UCT with a period of 1.0 seconds. The total event duration was
35 seconds.

TABLE 3. BRAZORIA COUNTY DATA LOG FOR NOVEMBER AND DECEMBER, 1982

1. 82-11-03
   16:41:08
   Explosion shot series

   Additional events:

       82-11-03: 16:46:55, 16:52:45, 16:57:20
       82-11-05: 16:01:26, 18:30:42

2. 82-11-12
   16:30:00
   Explosion shot series

   Additional events:

       82-11-12: 16:38:10, 16:54:00, 17:10:00, 17:19:00, 17:24:45,
                  17:35:40, 17:42:55

3. 82-12-16
   16:33:03
   Explosion shot series

   Additional events:

       82-12-16: 17:45:02, 17:56:30, 18:01:10, 18:08:27, 18:17:42,
                  18:22:15, 18:29:55, 18:33:52, 18:40:15, 18:43:20,
                  18:43:50, 18:49:00, 18:52:41, 18:55:40, 19:03:30,
                  19:16:12, 19:36:53, 19:41:40, 19:47:22, 19:50:01,
                  19:54:10, 19:58:37, 20:10:52, 20:14:01, 20:20:37,
                  20:26:30, 20:32:20, 20:38:52, 20:43:12, 20:48:20,
                  21:07:02, 21:31:28, 21:34:00, 21:37:19, 21:41:07
       82-12-17: 19:36:24, 19:41:36, 19:45:30, 20:48:33
       82-12-20: 19:09:35, 19:11:21, 19:12:33, 19:21:37, 19:22:53,
                  19:24:20, 19:25:40, 19:26:47, 19:28:18, 19:30:20,
                  19:32:00, 19:35:12, 19:39:56, 19:44:02, 21:41:20,
                  21:43:10, 21:45:30, 21:47:15, 21:48:20, 21:49:41,
                  21:54:50

SEISMIC ACTIVITY DURING 1982

If the seismic activity originating near the chemical complex east of the geopressured/geothermal well is excluded from consideration, remarkably little seismic activity occurred in the vicinity of the Pleasant Bayou design well during 1982. Table 4 lists by group all events which occurred in 1982, excluding exploration shot series. Only one microearthquake which had identifiable body phases occurred in 1982. A copy of this microearthquake is included as figure 9. Six events identified as impulsive Rayleigh Events occurred in 1982. Seismograms of two of these events are included in figures 10 and 11. Finally, there were four occurrences of rumble-type events and five episodes of harmonic tremor.

TABLE 4.   SEISMIC EVENTS AT BRAZORIA DURING 1982

Type I.   Microearthquakes

1.   82-01-23/G13213
     14:10:51.4 UCT
     29 17 30.2 N
     95 16 14.1 W
     H = 0.92 Kilometers
     90% confidence error ellipse Az=51 , a=1.6 km, b=1.3 km

BEG1	iP	16:31:27.30;
BEG2	eP	16:31:27.45;
BEG3	iP	16:31:27.10;
BEG4	P	16:31:24.50;
BEG5	eP	16:31:24.75

Type II.   Impulsive Rayleigh events

1.   82-01-09/G13220
     10:37:07.6 UCT
     29 29 26.7 N
     95 09 16.7 W
     Velocity=339 meters/second
     90% confidence error ellipse Az=30 , a=4.4 km, b=0.1 km

BEG1	iLR	10:38:33.10;
BEG2	iLR	10:38:25.30;
BEG3	iLR	10:38:31.85;
BEG4	iLR	10:38:35.40;
BEG5	iLR	10:38:38.60

2.   82-06-08
     00:49:29 UCT
     No epicenter determined

BEG1	LR	00:49:41.30;
BEG2	iLR	00:49:32.20;
BEG3	eLR	00:49:33.92;
BEG4	iLR	00:49:29.15;
BEG5	eLR	00:49:37.50

3.   82-07-16
     17:52:59 UCT
     No epicenter determined

BEG1	iLR	17:53:01.00;
BEG2	iLR	17:52:53.70;
BEG3	Inoperative	
BEG4	iLR	17:52:59.40;
BEG5	iLR	17:53:05.45

-24-

TR 83-1

TABLE 4. SEISMIC EVENTS AT BRAZORIA DURING 1982 (continued)

4. 82-08-21
    13:42:40 UCT
    No epicenter determined

BEG1	eLR	13:43:44.90;
BEG2	iLR	13:43:45.10;
BEG3	Inoperative	
BEG4	iLR	13:43:40.40;
BEG5	iLR	13:43:46.70

5. 82-09-14/G13219
    16:03:37.7 UCT
    29 17 57.4 N
    95 15 33.2 W
    Velocity=300 meters/second
    90% confidence error ellipse Az=174 , a=0.6 km, b=0.3 km

BEG1	iLR	10:38:33.10;
BEG2	iLR	10:38:25.30;
BEG3	iLR	10:38:31.85;
BEG4	iLR	10:38:35.40;
BEG5	iLR	10:38:38.60

Type III. Rumble events and Harmonic Tremors

1. 82-02-12
    15:00:15 UCT
    Harmonic Tremor, D=65 Min, Ap-p=15 mm

2. 82-03-05
    13:39:00 UCT
    Harmonic Tremor, D=60 Min, Ap-p=22 mm

3. 82-03-07
    15:11:20 UCT
    Rumble event

    Additional Events on 82-03-07:

    15:20:28 (D=40 Sec), 18:26:22 (D=15 Sec), 21:17:30 (D=50 Sec),
    21:19:04 (D=15 Sec)

4. 82-04-18
    01:47:00 UCT
    Harmonic Tremor, D=46 Min

    Additional Events on 82-04-18:

    02:40:40 (D=30 Sec), 02:42:40 (D=30 Sec), 02:46:20 (D=30 Sec),
    02:55:00 (D=30 Sec), 02:56:50 (D=30 Sec), 03:08:00 (D=180 Sec),
    03:19:20 (D=140 Sec)

TABLE 4. SEISMIC EVENTS AT BRAZORIA DURING 1982 (continued)

5. 82-04-19
   03:15:00 UCT
   Harmonic Tremor, D=180 Sec

6. 82-04-19
   03:48.00 UCT
   Rumble Event, D=11 Min

7. 82-04-21
   06:53:00 UCT
   Harmonic Tremor, D=10 Min

8. 82-08-01
   22:21:00 UCT
   Rumble Event, D=3 Min

9. 82-10-05
   01:37:00 UCT
   Rumble Event, D=150 Min

TR 83-1

FIGURE 9. EARTHQUAKE 6.5 KILOMETERS NORTHWEST OF THE GEOTHERMAL TEST WELL SITE,
OT = 14:10:51.4 UCT ON 23 JANUARY 1982, H = 0.92 KILOMETERS.

G 13213

-27-

FIGURE 10. EMERGENT RAYLEIGH EVENT, OT = 10:37:07.6 UCT ON 09 JANUARY 1982,
VELOCITY = 339 METERS/SECOND

10:38:40 UCT (UNCORRECTED)

39

10 SEC

BCD TIME

BEG 1 (120K)

BEG 2 (110K)

BEG 3 (106 K)

BEG 4 (104K)

BEG 5 (100K)

-28-

LSU 1 (92K)

LSU 2 (86K)

LSU 3 (96K)

LSU 4 (94K)

LSU 5 (92K)

G 13220

TR 83-1

16:04:00 UCT (UNCORRECTED)

10 SEC

16 04

BEG 1 (120K)

BEG 2 (110K)

BEG 3 (DEAD)

BEG 4 (104 K)

BEG 5 (100K)

BCD TIME

LSU 1 (92K)

LSU 2 (86K)

LSU 3 (96K)

LSU 4 (94K)

LSU 5 (DEAD)
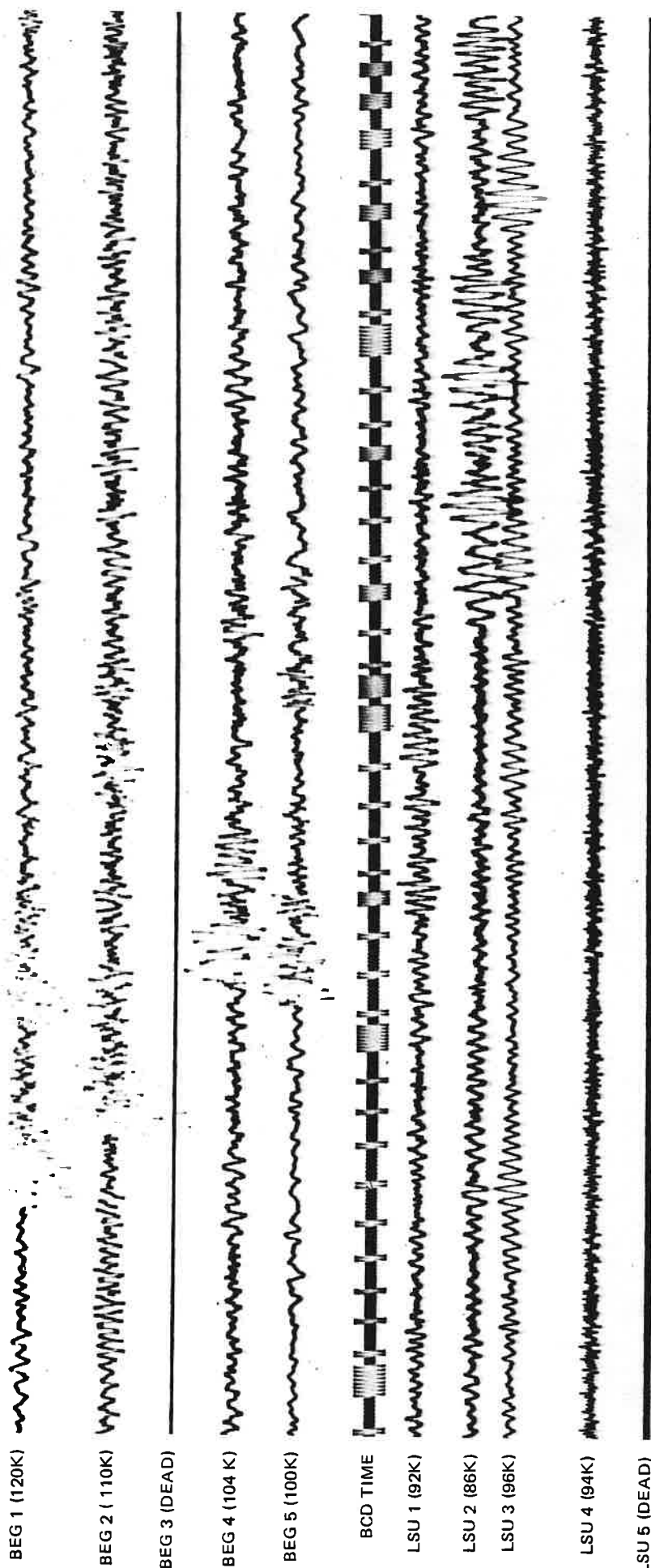
G 13219

FIGURE 11. IMPULSIVE RAYLEIGH EVENT, OT = 16:03:37.7 UCT ON 14 SEPTEMBER 1982, VELOCITY - 300 METERS/SECOND.

-29-

TR 83-1

SEISMICITY ORIGINATING NEAR THE CHEMICAL PLANT EAST OF THE GEOPRESSURED/GEOTHERMAL ENERGY WELL

Nine complex episodes of seismicity were recorded by the Brazoria seismic array between 6 December 1981 and 25 September 1982. All episodes included impulsive Rayleigh events varying in number from a few to several hundred. Many episodes exhibited periods of pronounced rumble, and a few exhibited periods of high-amplitude harmonic tremor with durations up to several hours. Detailed descriptions of each episode of seismic activity are given in table 5. In addition, portions of the seismic records for each of the nine episodes are included as figures 12 through 26. The computed origins for an impulsive Rayleigh event in each of the seismicity episodes are illustrated on the 1:24,000 U.S.G.S. topographic map of figure 29 as inverted triangles. The location of the Pleasant Bayou geopressured/geothermal energy wells is illustrated by the hatchured square on figure 29.

Unquestionably, these seismicity episodes are the most intense signals we have observed throughout the operatonal history of the Brazoria array. Since there is no evidence which would substantiate correlating these intense seismicity episodes with any activity at the geopressured/geothermal energy well, we choose to address them as a group in this special section of the technical report and separate them completely from other seismicity observed to date.

These seismicity episodes are both extremely interesting and enigmatic to interpret. In the collective seismic monitoring histories at all of the geopressured/geothermal energy design wells, these nine seismicity episodes are unique. Furthermore, no known natural sequences of similar character are known to the authors. We conclude, therefore, that these seismicity episodes are induced. Because of the proximity of the computed epicenters and the chemical plant illustrated in figure 29, it is reasonable to assume that some activity associated with the chemical complex has resulted in the ground vibrations observed.

There are many activities at industrial complexes which result in seismic signals observable at distances of many miles. In general, these signals exhibit spectral and temporal properties which distinguish them as man-made sources. The signals observed in these nine eipsodes of activity are complex, exhibiting several characteristic types of behavior; i.e., impulsive Rayleigh events, rumble sequences and harmonic tremor periods. Although the mechanisms to produce these different signals may be independent, the contemporaneous onset and disappearance of the different signals in nine separate episodes would argue strongly for a mutually interdependent mode of origin.

Before presenting two alternative models which may account for the signals observed, it is useful to summarize some of the salient aspects of the seismicity episodes which require rational explanation. (1) The times of occurrence of the event or event sequences is an important consideration. No similar episodes of activity were recorded prior to 6 December 1981. Considering the longevity of chemical plant operation, and without knowledge to the contrary, we must assume operational continuity. An operational change

TABLE 5. SEISMICITY EPISODES LOCATED NEAR THE CHEMICAL COMPLEX
EAST OF THE GEOPRESSURED/GEOTHERMAL WELL

1. 81-12-06/G13214
    08:49:48.72
    Impulsive Rayleigh event and rumble event sequence

    BEG1   iLR   08:50:09.65;
    BEG2   iLR   08:50:00.65;
    BEG3   iLR   08:50:02.27;
    BEG5   iLR   08:50:04.00

Description of event series on 05 December 1981:

   22:57:00 - High-frequency rumble event begins and continues until 08:47:30
              on 06 December 1981

Description of event series on 06 December 1981:

   00:01:00 - A very slight harmonic tremor was recorded at this time with a
              duration of approximately 8 minutes

   08:47:30 - The high-frequency rumble event subsides to the normal noise
              level for this site

   08:49:28 - Low-amplitude Impulsive Rayleigh event listed above

   08:50:00 - Low-level rumble activity begins and intermittently occurs
              during the times listed below:

                    08:50:00 - 09:43:10
                    09:46:37 - 09:43:10
                    09:48:10 - 09:47:20
                    09:49:33 - 09:50:10
                    09:51:00 - 09:51:30
                    09:52:12 - 09:53:00
                    09:53:40 - 09:54:15
                    09:54:55 - 09:55:40
                    09:56:15 - 09:57:00
                    09:57:35 - 09:58:10
                    09:58:50 - 09:59:30
                    10:00:10 - 10:00:50
                    10:01:32 - 10:02:20
                    10:02:50 - 10:03:22
                    10:04:10 - 10:04:50
                    10:05:30 - 10:06:10
                    10:07:00 - 10:07:40
                    10:09:50 - 16:00:00

-31-

09:46:25.32 - Impulsive Rayleigh event/G13216

        BEG1   iLR   09:46:46.55;
        BEG2   iLR   09:46:37.50;
        BEG3   iLR   09:46:39.08;
        BEG5   iLR   09:46:40.80

2. 82-01-05/G12842
    09:49:16.9
    Impulsive Rayleigh event

        BEG1   iLR   09:49:39.08, A=5, D=4;
        BEG2   iLR   09:49:29.70, A=4, D=4;
        BEG3   iLR   09:49:31.18, A=3, D=4;
        BEG4   iLR   09:49:26.40, A=8, D=5;
        BEG5   iLR   09:49:32.93, A=4, D=4

Description of event series on 05 January 1982:

  04:50:13 - A series of eleven impulsive Rayleigh arrivals (figure 14) ending
             at 04:51:36, followed by a slight rumbling.

  04:51:40 - A high-amplitude rumble begins (A=8mm) which decreases to normal
             ambient noise levels at 05:04:07.

  05:04:17 - A weak set of impulsive Rayleigh arrivals.

  05:05:20 - More high-amplitude rumbling occurs (A=8mm), which remains a
             constant 8-10 hertz rumble with higher frequencies of noise
             present. This rumble persists with very few harmonic episodes
             until 09:49:00, when an emergent ending occurs in the same order
             in which the impulsive Rayleigh waves arrive.

  09:49:27 - A very prominent impulsive Rayleigh event occurs, which
             apparently indicates a shutting down of some type, and is the
             last sign of any activity from the area southeast of the array
             for this date.

3. 82-01-10/G12843
    07:20:17.3
    Impulsive Rayleigh event

        BEG1   iLR   07:20:39.10;
        BEG2   iLR   07:20:29.70;
        BEG3   iLR   07:20:31.50;
        BEG4   iLR   07:20:26.50;
        BEG5   iLR   07:20:33.35

TABLE 5. SEISMICITY EPISODES LOCATED NEAR THE CHEMICAL COMPLEX
EAST OF THE GEOPRESSURED/GEOTHERMAL WELL
(continued)

Description of event series on 10 January 1982:

00:02:20 - An emergent, high-amplitude rumble with a five-second duration.

00:03:25 - A harmonic tremor occurs and sustains a constant amplitude on A=8 for approximately 20 minutes. The amplitude is nearly half (A=4) for the next 60 minutes and even lesser for the next 6 hours, although the tremor is still noticeable.

02:02:40 - An impulsive Rayleigh arrival with a different type of sinuous coda forming the tail of the event.

06:07:00 - The harmonic tremor mentioned above ends in a rumble type of ending which is emergent in nature.

06:13:01 - An impulsive Rayleigh arrival which precedes another rumble episode which lasts for 90 seconds.

06:17:05 - An impulsive Rayleigh arrival precedes another rumble episode of numerous high frequencies which has an emergent ending at 07:09:30.

07:20:25 - An impulsive Rayleigh arrival (see figure 15) precedes a harmonic tremor episode which lasts until 08:11:25, where a rumble type of ending occurs.

08:14:37 - An impulsive Rayleigh arrival occurs with another sinuous coda tailing the arrival. These tails are 4-8 seconds in duration and are closely followed by a rumble episode at 08:16:05 which lasts for 30 seconds.

08:17:10 - An impulsive Rayleigh arrival with the same type of rumble activity following until 08:33:30, when the rumble activity ceases with a surge of rumble activity.

08:33:40 - An impulsive Rayleigh arrival precedes more rumble activity which diminishes at 08:39:10, and progressively builds up to a peak in rumble activity at 09:17:40. The rumble continues with few noticeable harmonic episodes until a severe rumble episode occurs at 10:43:23 which lasts for over 2 minutes and ends abruptly in the same order of arrival as the impulsive Rayleigh events.

10:46:48 - An impulsive Rayleigh arrival followed by a low-level rumble episode with slight harmonics noted.

11:27:00 - A high-frequency rumble episode occurs which lasts to 11:45:00 where a 10-second, noise-free interval exists. The rumble epi-

-33-

sode continues until another noise-free interval of 7 seconds is
present at 12:00:00.

12:00:07 – A very small, impulsive Rayleigh arrival precedes another high-
frequency rumble episode which remains at a very low amplitude
and contains increasingly more harmonics over the next 10 hours.

19:56:30 – The amplitude of the harmonic tremor nearly quadruples for the
next few minutes. The harmonic tremor continues until indis-
tinguishable from the ambient noise nearly 17 hours later.

4.   82-04-18/G12844
     03:25:38.5
     Impulsive Rayleigh event

BEG1	iLR	03:26:01.05;
BEG2	iLR	03:25:53.00;
BEG3	iLR	03:25:53.68;
BEG4	iLR	03:25:48.20;
BEG5	iLR	03:25:54.40

Description of event series on 18 April 1982:

01:47:00 – A harmonic tremor begins which lasts until 02:33:00.

02:40:40 – The harmonic tremor begins approximately 30-second bursts at
02:42:40, 02:46:20, 02:55:00, 02:56:50, and another 3-minute
burst at 03:08:00.

02:58:53 – A series of six impulsive Rayleigh events ending at 03:00:08.

03:18:03 – A large amplitude harmonic tremor begins, and ends at 03:21:40
with a series of approximately ten impulsive Rayleigh events
(see figure 16). The ground motion in nanometers for this
event has been calculated to be as follows: BEG 1-83 nm, BEG
2-103 nm, BEG 3-140 nm, BEG 4-144 nm, BEG 5-83 nm. This clearly
shows that BEG 2,3 and 4 are the closest stations to the source
of the event. The decrease in ground motion at BEG 5 can be
explained by interference from a major growth fault situated
near the station.

03:25:53 – A series of four impulsive Rayleigh events ending at 03:27:20.

03:40:49 – Two impulsive Rayleigh events which are followed by a rumble
event with very few harmonics noted. The rumble activity con-
tinues to diminish steadily over the next six hours.

TR 83-1

10:04:31 - A single impulsive Rayleigh event.

11:10:18 - The beginning of a series of at least twenty impulsive Rayleigh events which last periodically up until 12:24:18.

Description of additional events on 19 April 1982:

03:15:00 - A harmonic tremor begins which lasts approximately 3 minutes.

03:48:00 - A high-frequency rumble event occurs which lasts for 11.5 minutes.

5. 82-05-03/G12845
   05:00:36.0
   Impulsive Rayleigh event

BEG2	iLR	05:00:49.87;
BEG3	iLR	05:00:50.60;
BEG4	iLR	05:00:45.24;
BEG5	iLR	05:00:51.49

Description of event series on 03 May 1982:

04:03:23 - A rumble episode begins which lasts until 04:04:42. This rumble episode contains a slight harmonic tremor from 04:04:10 to 04:04:24.

04:53:00 - A series of multiple impulsive Rayleigh arrivals begins which precedes a high-frequency rumble episode which is nearly three times the amplitude of the normal ambient noise. This rumble episode lasts until 05:00:38, when an emergent ending occurs in the same order of arrival as the impulsive Rayleigh events (see figure 17).

05:00:45 - An impulsive Rayleigh event (see figure 17) precedes another high-frequency rumble episode which is also much higher in amplitude than the normal ambient noise character of the record. This rumble episode contains few harmonics and has an emergent ending at 05:25:00.

05:28:00 - A high-frequency rumble episode begins emergently and continues until 09:25:15. A noted peak in activity was recorded from 07:38:00 to 07:50:00.

Additional Harmonic tremor episodes on 03 May 1982:

17:12:00, D=20 minutes
17:42:00, D=13

Additional Harmonic tremor episodes on 04 May 1982:

  01:25:00, D=15 minutes
  01:46:00, D=5
  02:37:00, D=7
  03:34:00, D=67
  05:54:00, D=26
  08:35:00, D=11
  11:21:00, D=8
  11:40:00, D=2

6. 82-05-18/G13215
   00:35:35.3
   Impulsive Rayleigh event

BEG1	iLR	00:35:58.10;
BEG2	iLR	00:35:48.77;
BEG3	iLR	00:35:50.71;
BEG4	iLR	00:35:45.47;
BEG5	iLR	00:35:52.27

7. 82-06-12/G13280
   11:35:49.0
   Impulsive Rayleigh event and rumble event sequence

BEG1	iLR	11:36:10.00;
BEG2	iLR	11:36:01.90;
BEG3	iLR	11:36:02.63;
BEG4	iLR	11:35:57.30;
BEG5	iLR	11:36:03.70

Additional activity on 12 June 1982:

  08:26:00 - Emergent beginning of a rumble event

  08:51:00 - Decrease in amplitude until 09:02:00

  09:26:00 - Increase in amplitude to 40 millimeters peak-to-peak which
                 lasts until 10:28:00

  10:28:00 - Rumble continues with slightly noticeable harmonics

  11:33:00 - Rumble event ends emergently

  11:35:58 - Impulsive Rayleigh event listed above

  11:37:52 - Impulsive Rayleigh event listed below

TABLE 5. SEISMICITY EPISODES LOCATED NEAR THE CHEMICAL COMPLEX EAST OF THE GEOPRESSURED/GEOTHERMAL WELL (continued)

BEG1	iLR	11:38:05.40;
BEG2	iLR	11:37:57.38;
BEG3	iLR	11:37:58.38;
BEG4	iLR	11:37:52.78;
BEG5	iLR	11:37:59.30

13:16:00 - Small rumble event lasting until 13:18:30

8. 82-08-22/G13009, G13010, G13011, G13012, G13013
   18:52:28.7
   Impulsive Rayleigh event and rumble sequence

BEG1	iLR	18:52:51.25;
BEG2	iLR	18:52:43.14;
BEG4	iLR	18:52:38.71;
BEG5	iLR	18:52:44.79

Additional events on 82-08-22

GROUP I - 18:52:38 to 19:21:52

21 impulsive Rayleigh events followed by a rumble episode containing no events (D=22 mins.)

18:52:42, 18:53:34, 18:54:30, 18:54:32, 18:54:39, 18:55:53, 18:56:46,
18:56:49, 18:56:52, 18:57:32, 18:57:35, 18:57:36, 18:57:40, 18:57:42,
18:57:45, 18:57:48, 18:57:52, 18:58:10, 18:58:16, 18:59:00, 18:59:04,
18:59:06, 18:59:21, 18:59:25, 18:59:38, 18:59:56

GROUP II - 19:21:52 to 20:20:10

An uncounted number of impulsive Rayleigh events occurring almost continually during this period. Separation between most events is less than one second.

GROUP III - 20:20:10 to 20:34:42

Harmonic tremor (D=9 mins) begins at 20:20:10, with a series of 23 impulsive Rayleigh events beginning 7 minutes later. These 23 events are followed by 5 minutes of no recorded seismic activity.

20:27:10, 20:27:44, 20:27:58, 20:28:04, 20:29:06, 20:29:11, 20:29:36,
20:30:02, 20:30:26, 20:30:48, 20:31:00, 20:31:17, 20:31:24, 20:31:40,
20:32:11, 20:32:18, 20:32:20, 20:32:32, 20:33:38, 20:33:45, 20:33:53,
20:34:37, 20:34:42

GROUP IV - 20:40:37 to 20:46:10

Harmonic tremor (D=6 mins.) begins with an impulsive Rayleigh
event at 20:40:37. Three other similar events occur during this
tremor at 20:41:13, 20:41:30 and 20:41:51.

GROUP V - 20:54:03 to 20:59:20

Another harmonic tremor (D=5 mins.) begins with an impulsive
Rayleigh event at 20:54:03. Approximately 35 other impulsive
Rayleigh events were recorded during this short-duration tremor.

GROUP VI - 22:13:27 to 22:13:42

Three smaller impulsive Rayleigh events were recorded during
this fifteen-second period at 22:13:27, 22:13:34 and 22:13:42.

9. 82-09-25/G13140, G13141
    00:47:38.2
    Impulsive Rayleigh event and rumble event sequence

BEG1	iLR	00:47:59.56;
BEG2	iLR	00:47:51.60;
BEG3		Inoperative
BEG4	iLR	00:47:47.02;
BEG5	iLR	00:47:53.20

00:44:00 - Emergent beginning of the rumble event. Amplitude and frequency
begin to increase steadily from approximately 5 hertz to
approximately 7 hertz

00:47:40 - Amplitude diminishes to 4 millimeters peak-to-peak on BEG 4

00:47:47 - Impulsive Rayleigh event occurs which is listed above. The
high-frequency portion of the wave is of duration approximately
2 seconds

00:48:30 - Seismic traces return to the normal ambient noise level

FIGURE 12. IMPULSIVE RAYLEIGH EVENT SEQUENCE NO. 1 ORIGINATING NEAR THE CHEMICAL PLANT EAST OF THE GEOTHERMAL TEST WELL SITE. OT=08:49:48.7 UCT ON 6 DECEMBER 1981, VELOCITY = 350 METERS/SECOND.

FIGURE 13. IMPULSIVE RAYLEIGH EVENT SEQUENCE NO. 1 ORIGINATING NEAR THE CHEMICAL PLANT EAST OF THE GEOTHERMAL TEST WELL SITE. OT = 09:46:25.32 UCT ON 6 DECEMBER 1981, VELOCITY = 350 METERS/SECOND

G 13216

-40-

04:50:00 UCT (UNCORRECTED)

10 SEC

BCD TIME

BEG 1 (144K)

BEG 2 (131K)

BEG 3 (141K)

BEG 4 (137K)

BEG 5 (145K)

FIGURE 14. IMPULSIVE RAYLEIGH EVENT SEQUENCE
NO. 2 ORIGINATING NEAR THE CHEMICAL PLANT EAST
OF THE GEOTHERMAL TEST WELL SITE. OT = 09:49:16.9
UCT ON 5 JANUARY 1982, VELOCITY = 338 METERS/
SECOND.

−41/42−   G 12842

TR 83-1

FIGURE 15. IMPULSIVE RAYLEIGH EVENT SEQUENCE NO. 3 ORIGINATING NEAR THE CHEMICAL PLANT EAST OF THE GEOTHERMAL TEST WELL SITE. OT = 07:20:17.3 UCT ON 10 JANUARY 1982, VELOCITY = 338 METERS/SECOND.

G. 12843

-43/44-

TR 83-1

FIGURE 16. IMPULSIVE RAYLEIGH EVENT SEQUENCE NO. 4 ORIGINATING NEAR THE CHEMICAL PLANT EAST OF THE GEOTHERMAL TEST WELL SITE. OT = 03:25:38.5 UCT ON 18 APRIL 1982, VELOCITY = 347 METERS/SECOND. ASSOCIATED HARMONIC TREMOR ACTIVITY IS APPROXIMATELY 1.35 Hz.

G 12844

-45/46-

TR 83-1
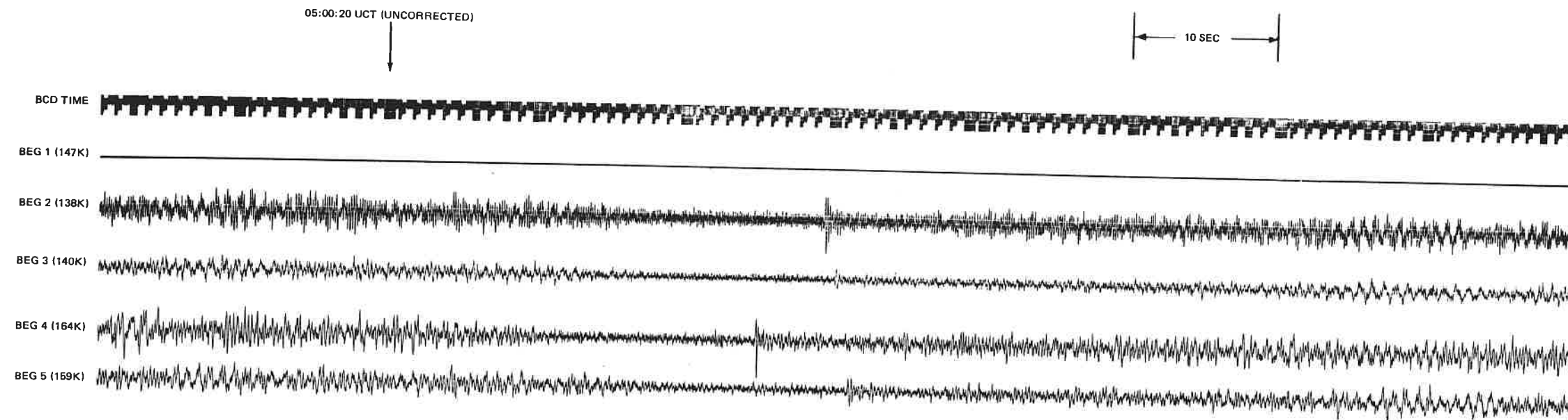
FIGURE 17. IMPULSIVE RAYLEIGH EVENT SEQUENCE NO. 5 ORIGINATING NEAR THE CHEMICAL PLANT EAST OF THE GEOTHERMAL TEST WELL SITE. OT = 05:00:36.0 UCT ON 3 MAY 1982, VELOCITY = 348 METERS/SECOND. NOTE ASSOCIATED HIGH FREQUENCY RUMBLE ACTIVITY TEN SECONDS BEFORE AND IMMEDIATELY FOLLOWING THE IMPULSIVE RAYLEIGH EVENT.

G 12846

-47/48-

TR 83-1
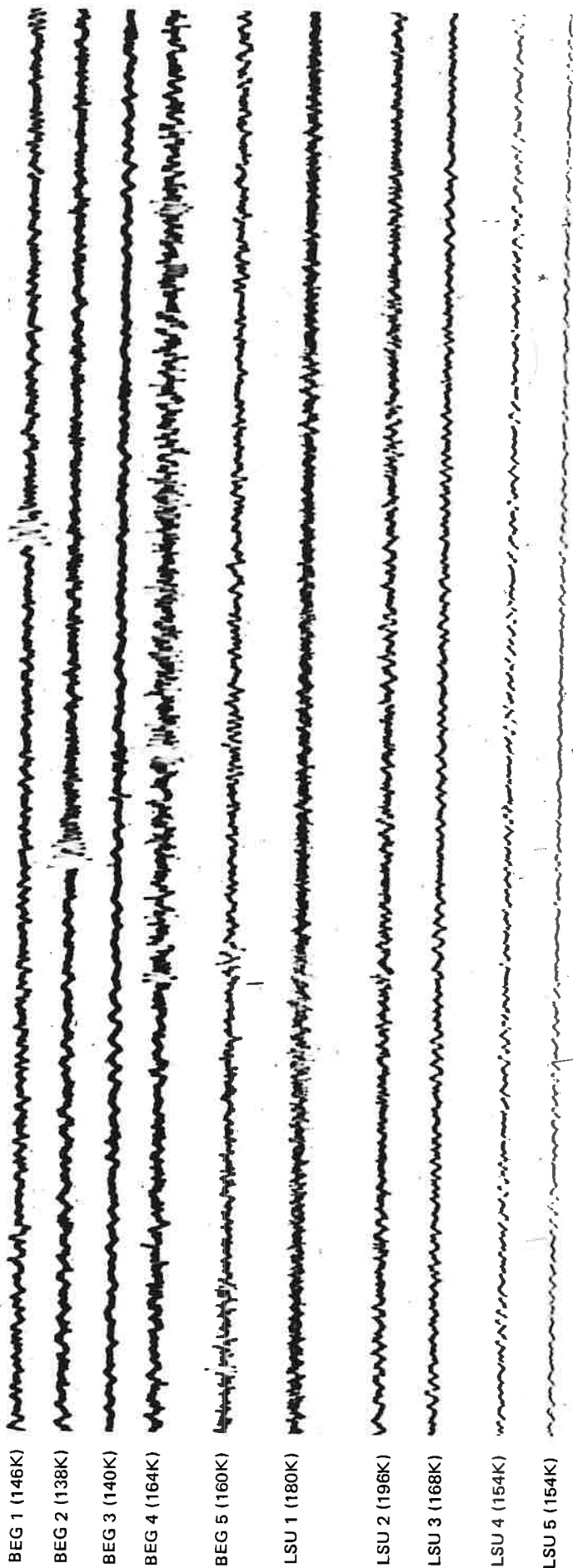
FIGURE 18. IMPULSIVE RAYLEIGH EVENT NO. 6 ORIGINATING NEAR THE CHEMICAL PLANT EAST OF THE GEOTHERMAL TEST WELL SITE. OT = 00.35:35.3 UCT ON 18 MAY 1982, VELOCITY = 340 METERS/SECOND

00:36:00 UCT (UNCORRECTED)

10 SEC

BEG 1 (146K)
BEG 2 (138K)
BEG 3 (140K)
BEG 4 (164K)
BEG 5 (160K)
LSU 1 (180K)
LSU 2 (196K)
LSU 3 (168K)
LSU 4 (154K)
LSU 5 (154K)

G 13215

-49-

TR 83-1
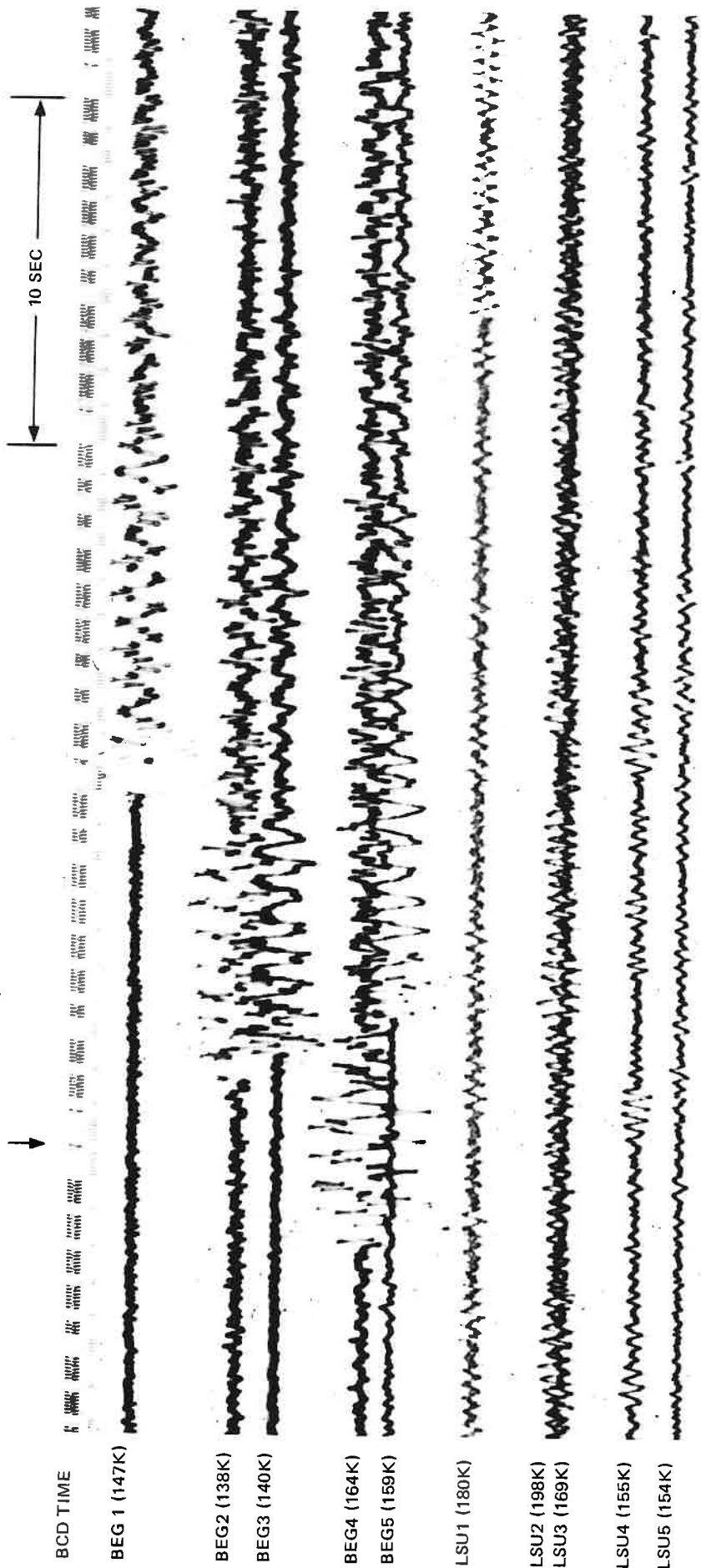
FIGURE 19. IMPULSIVE RAYLEIGH EVENT SEQUENCE NO. 7 ORIGINATING NEAR THE CHEMICAL PLANT EAST OF THE GEOTHERMAL TEST WELL SITE. OT = 11:35:49.0 UCT ON 12 JUNE 1982, VELOCITY = 348 METERS/ SECOND.

G 13280

BCD TIME

BEG 1 (147K)

BEG2 (138K)
BEG3 (140K)

BEG4 (164K)
BEG5 (159K)

LSU1 (180K)

LSU2 (198K)
LSU3 (169K)

LSU4 (155K)
LSU5 (154K)

11:36:00 UCT (UNCORRECTED)

10 SEC

18:53:00 UCT (UNCORRECTED)

18 53

10 SEC

BEG 1 (147K)

BEG 2 (138K)

BEG 3 (DEAD)

BEG 4 (164K)

BEG 5 (159K)

BCD TIME

LSU 1 (180K)

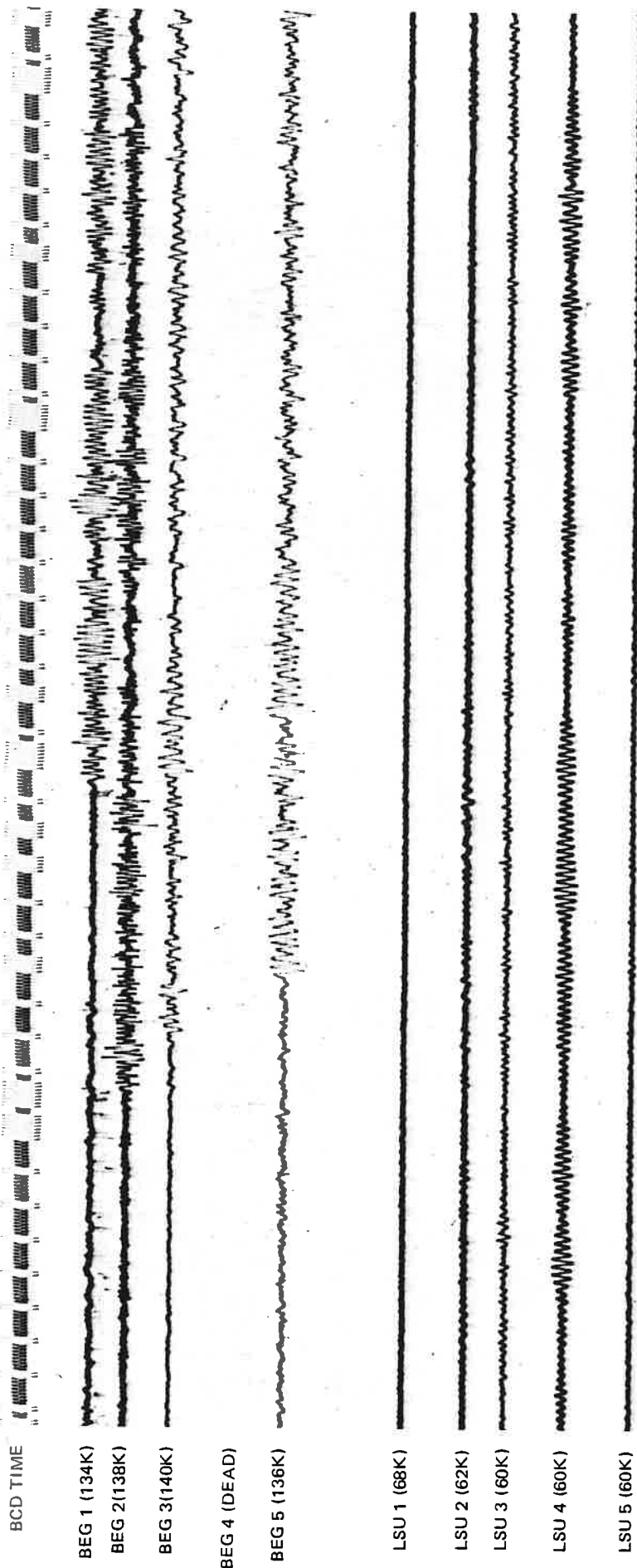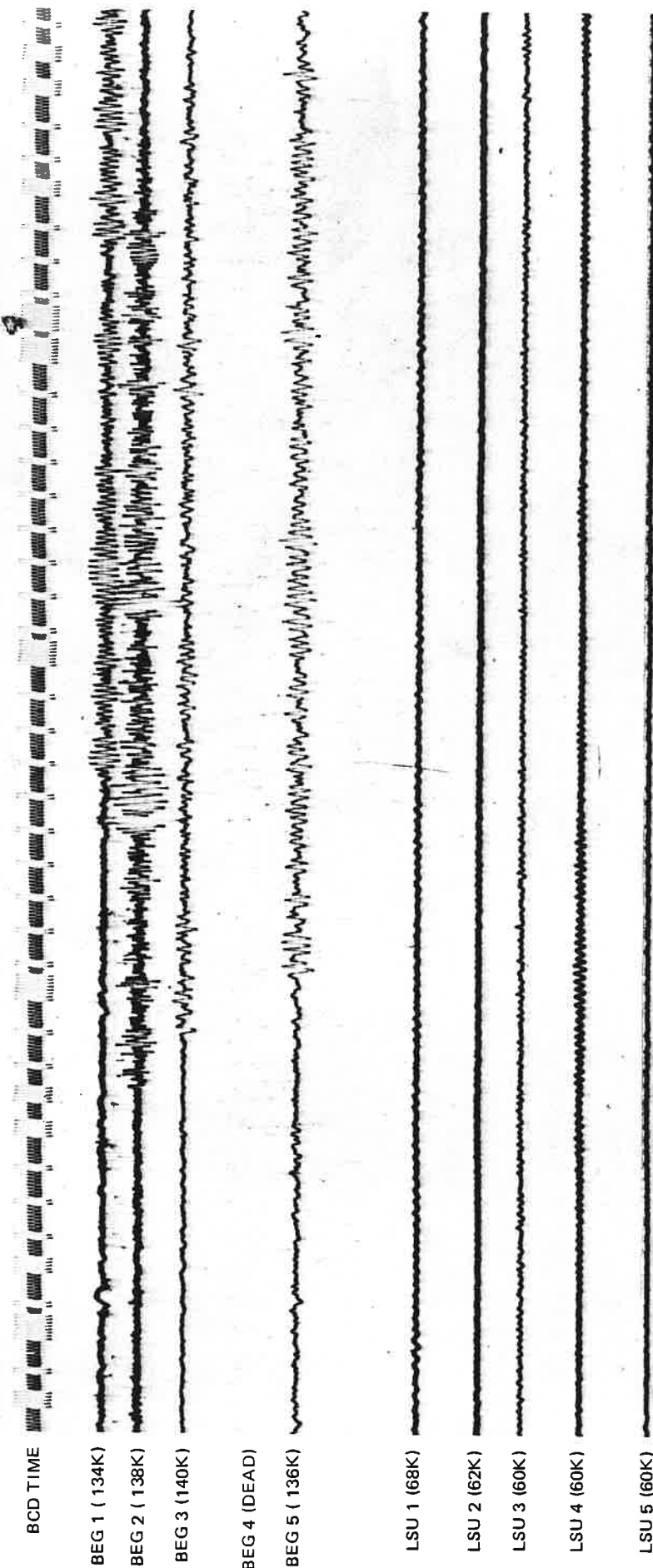LSU 2 (198K)

LSU 3 (169K)

LSU 4 (155K)

LSU 5 (154K)
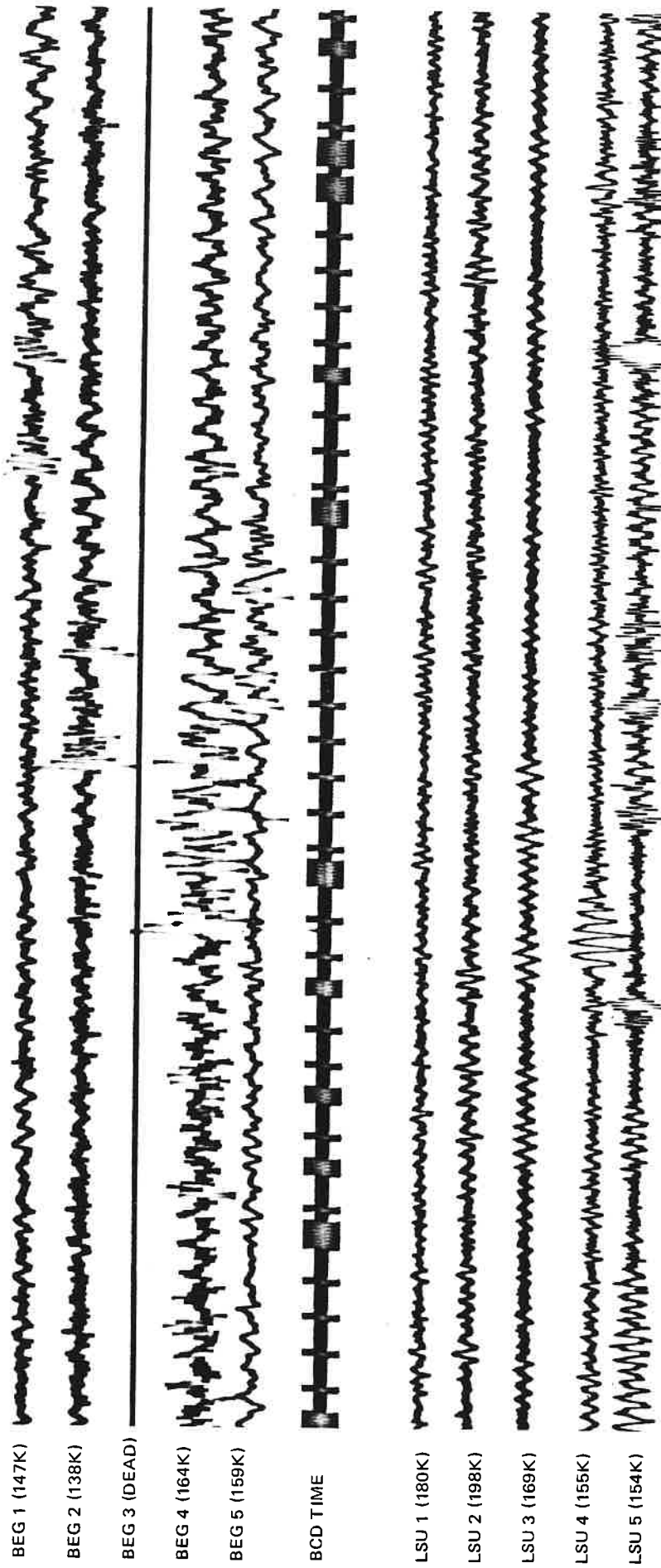
FIGURE 20. IMPULSIVE RAYLEIGH EVENT SEQUENCE NO. 8 ORIGINATING NEAR THE CHEMICAL PLANT EAST OF THE GEOTHERMAL TEST WELL SITE. OT = 18:52:28.7 UCT ON 22 AUGUST 1982, VELOCITY = 354 METERS/SECOND.

G 13009

-51-

TR 83-1
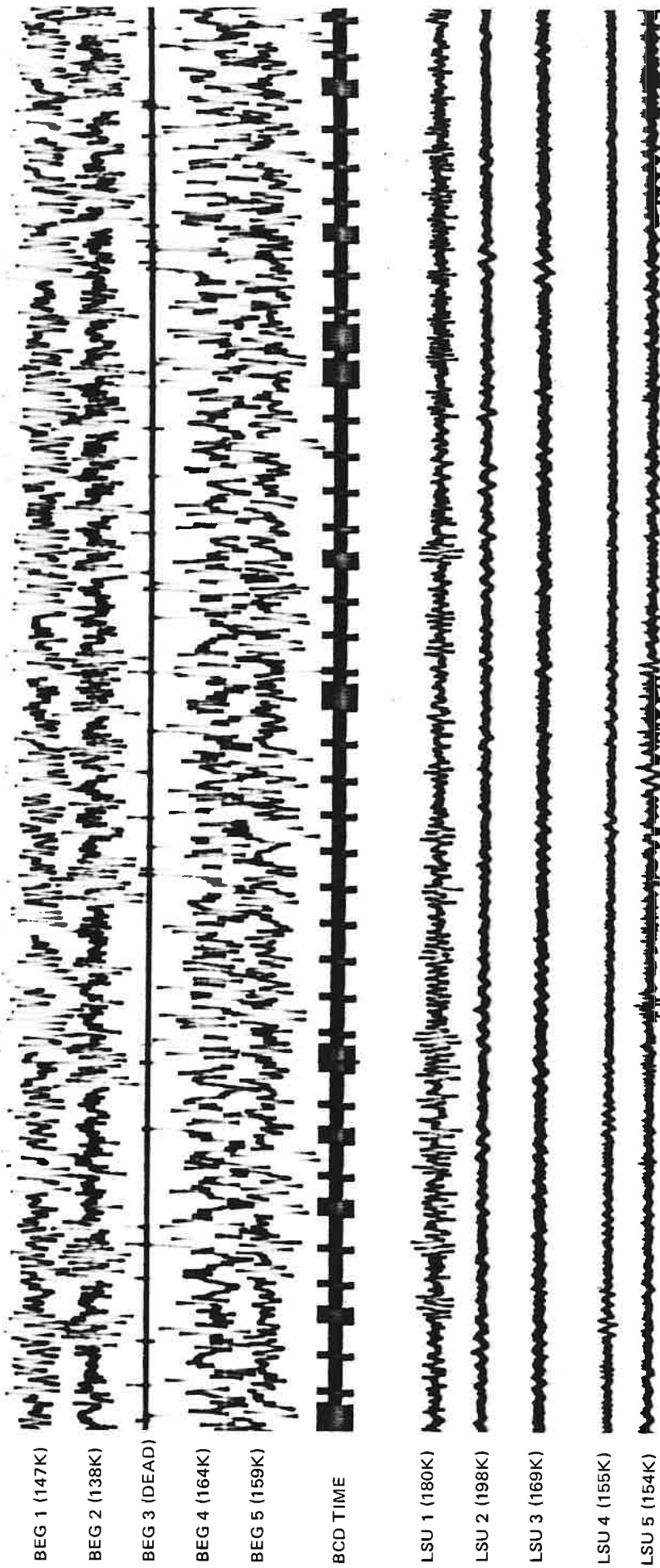
FIGURE 21. SEQUENCE OF MULTIPLE IMPULSIVE RAYLEIGH EVENTS SPACED 1 TO 2 SECONDS APART. FROM IMPULSIVE RAYLEIGH EVENT SEQUENCE ON 22 AUGUST 1982 AT 19:26:00 UCT.

TR 83-1
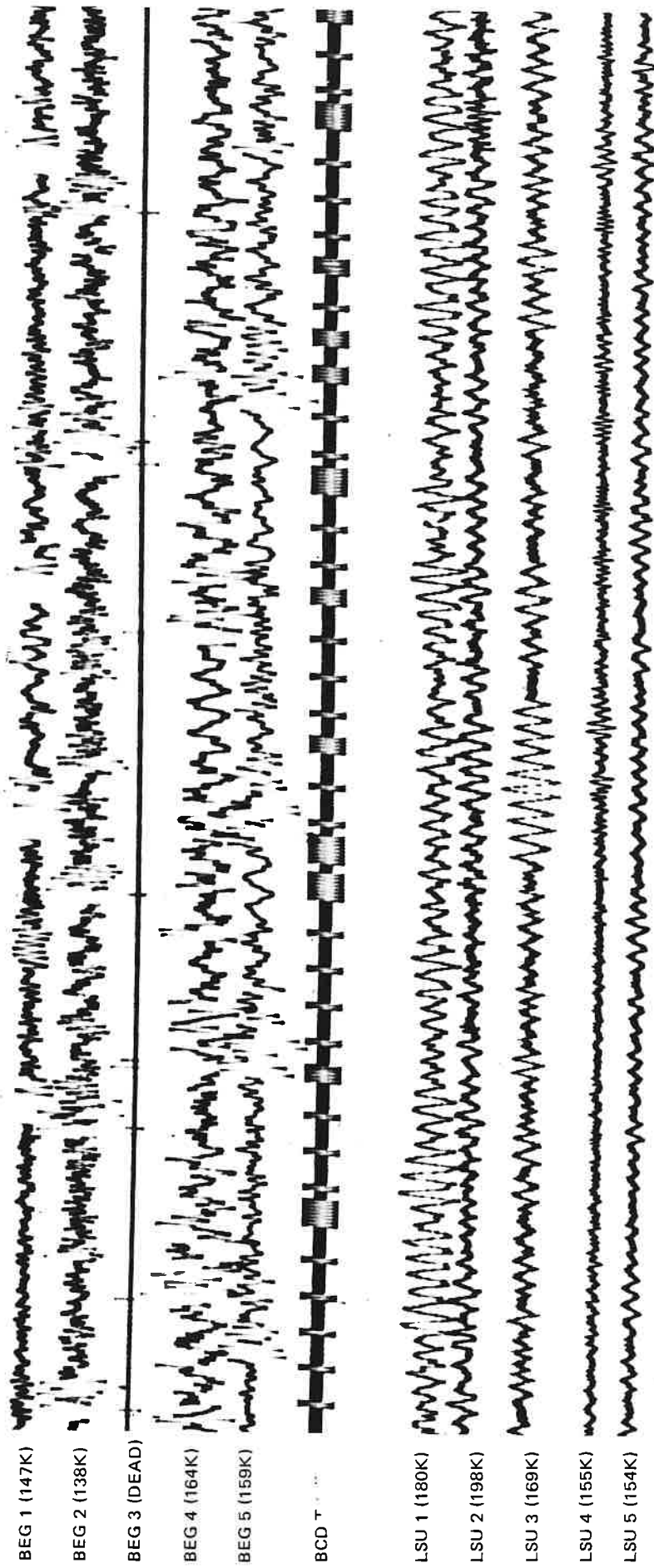
FIGURE 22. SEQUENCE OF MULTIPLE IMPULSIVE RAYLEIGH EVENTS IRREGULARLY SPACED 3 TO 10 SECONDS APART FROM IMPULSIVE RAYLEIGH EVENT SEQUENCE NO. 8 ON 22 AUGUST 1982 AT 20:12:00 UCT.

TR 83-1
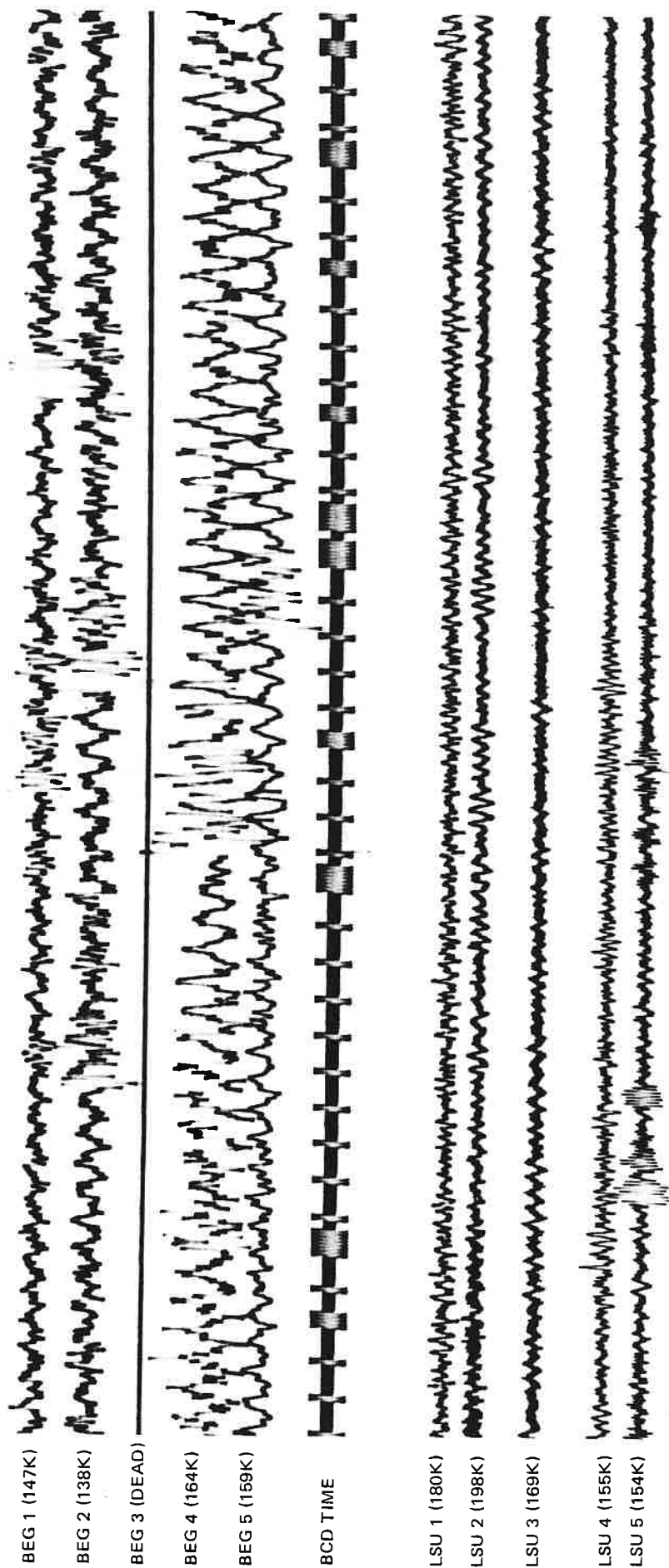
FIGURE 23. TWO IMPULSIVE RAYLEIGH EVENTS FROM IMPULSIVE RAYLEIGH EVENT SEQUENCE NO. 8, RECORDED DURING A LOW AMPLITUDE HARMONIC TREMOR ON 22 AUGUST 1982 AT 20:42:00 UCT.

-54-
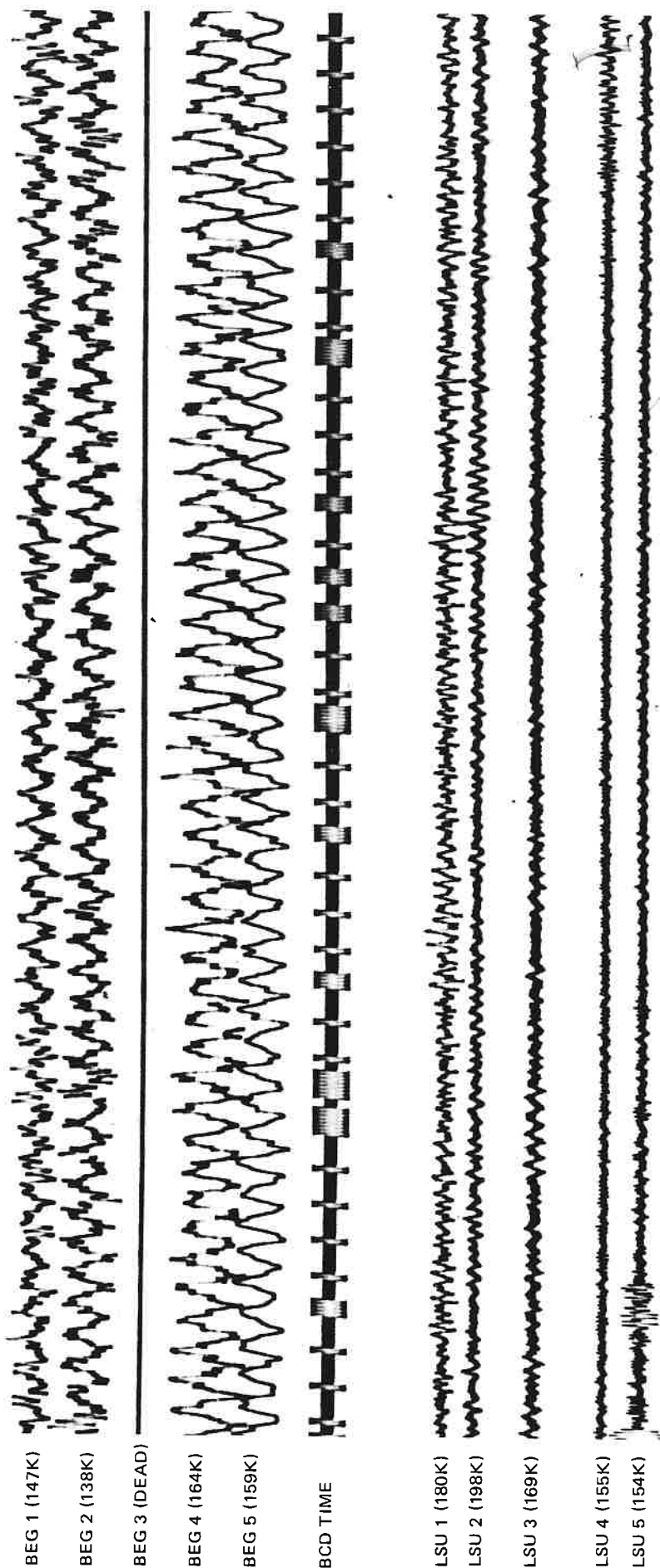
FIGURE 24. HARMONIC TREMOR AT MAXIMUM AMPLITUDE, FREQUENCY = 1.4 HERTZ, FROM IMPULSIVE RAYLEIGH EVENT SEQUENCE NO. 8, 22 AUGUST 1982 AT 20:44:00 UCT.
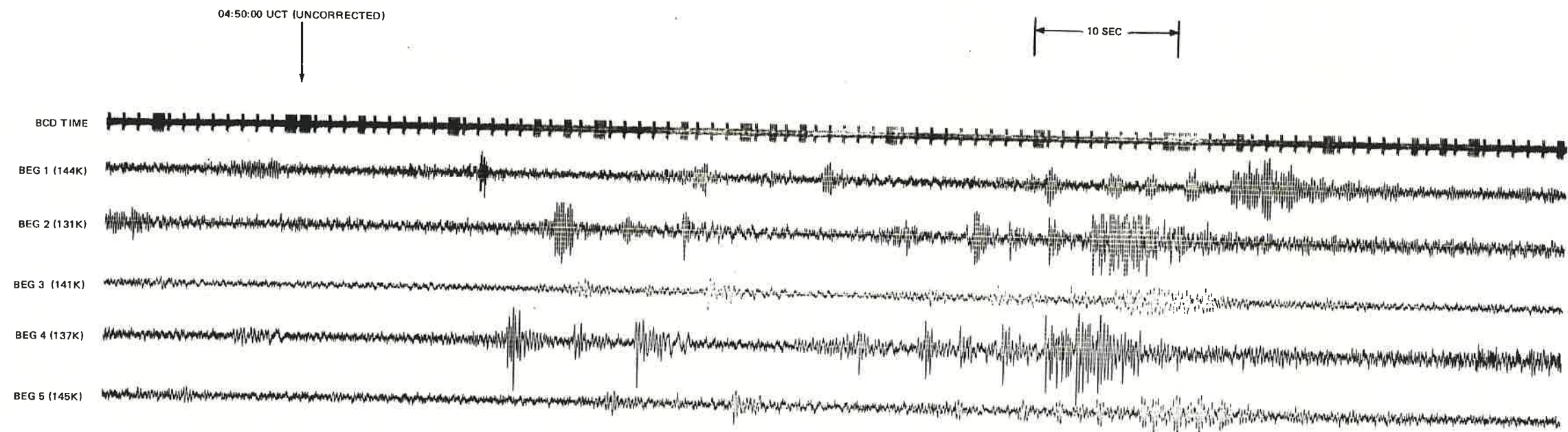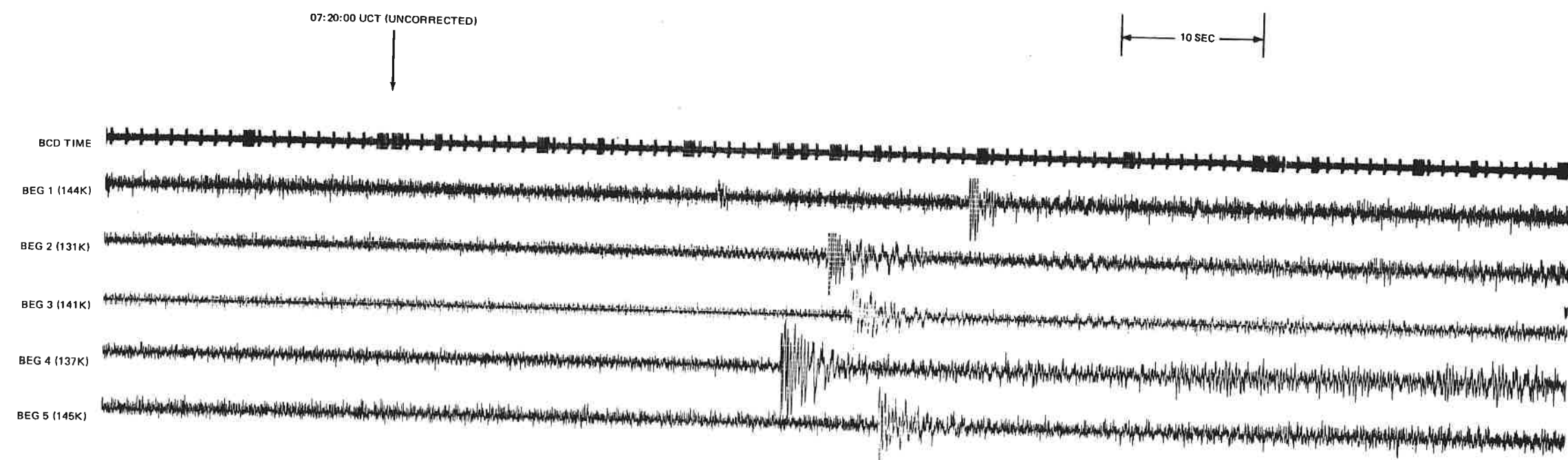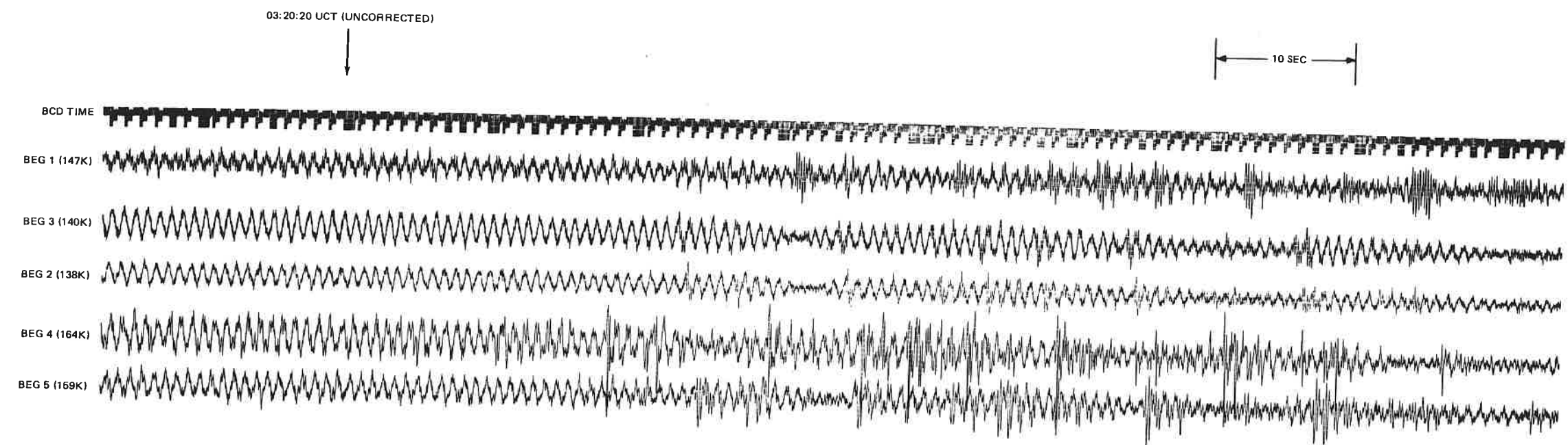
G 13013

TR 83-1
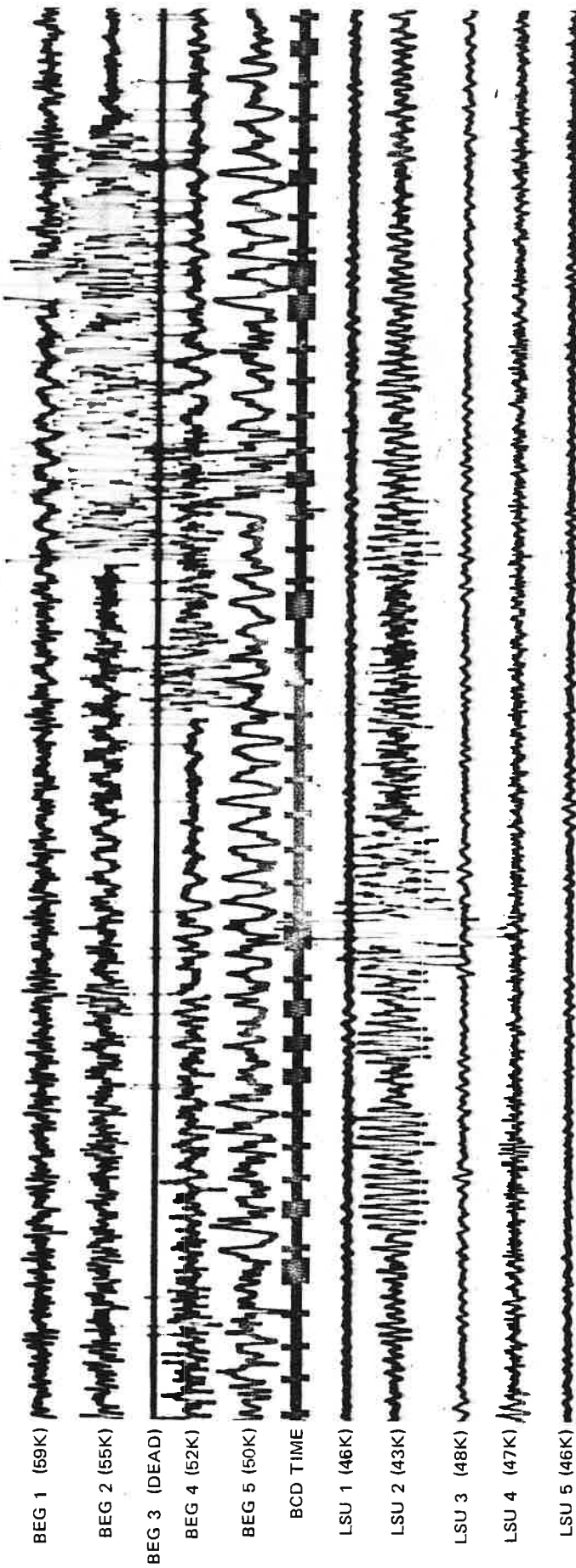
FIGURE 25. IMPULSIVE RAYLEIGH EVENT SEQUENCE NO. 9 ORIGINATING NEAR THE CHEMICAL PLANT EAST OF THE GEOTHERMAL TEST WELL SITE. OT = 00:47:38.2 UCT ON 25 SEPTEMBER 1982.
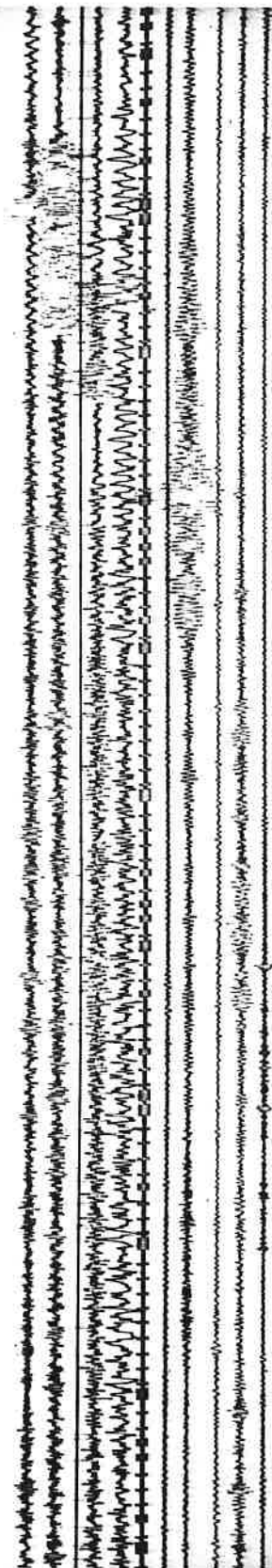
TR 83-1

FIGURE 26. HIGH FREQUENCY RUMBLE EPISODE DIRECTLY PRECEDING THE IMPULSIVE RAYLEIGH EVENT SEQUENCE NO. 9 OF FIGURE 25. OT = 00:47:38.2 UCT ON 25 SEPTEMBER 1982.
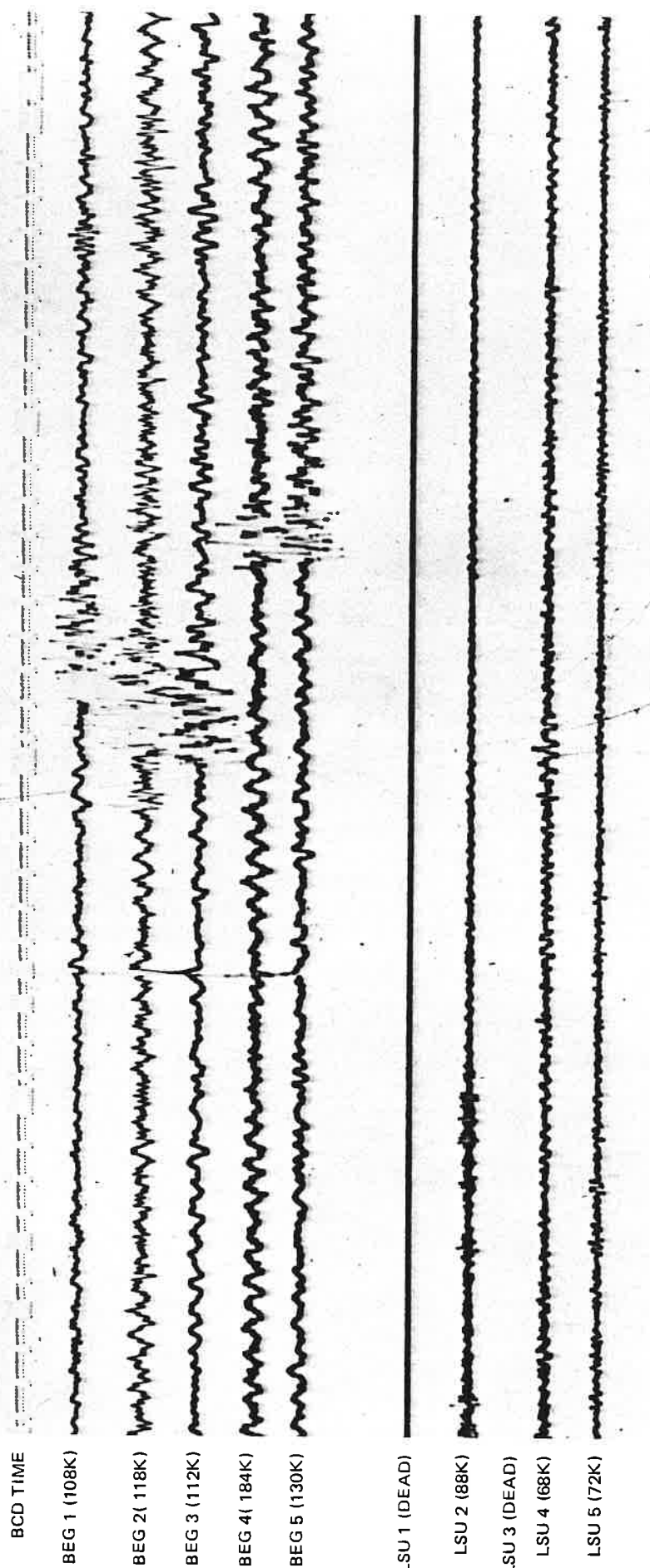
-57-

FIGURE 27. IMPULSIVE RAYLEIGH EVENT FROM 6 KILOMETERS NNW OF THE GEOTHERMAL TEST WELL SITE. OT = 14:30:32.0 UCT ON 3 MAY 1981, VELOCITY = 325 METERS/SECOND.
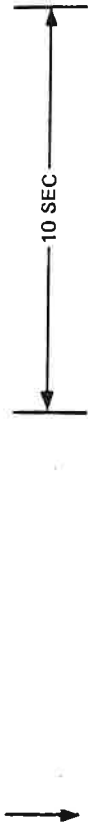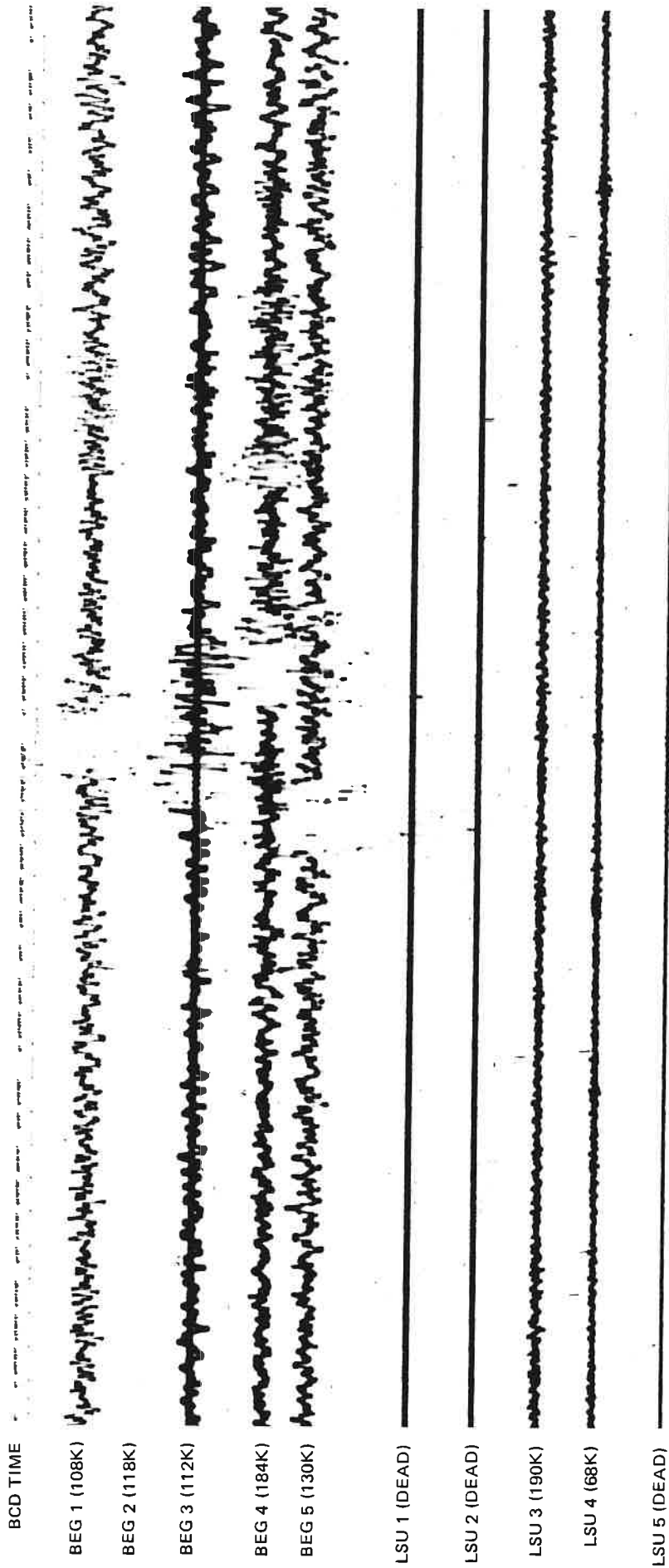
FIGURE 28. IMPULSIVE RAYLEIGH EVENT FROM 5 KILOMETERS NORTHWEST OF THE GEOTHERMAL TEST WELL SITE. OT = 00:27:13.2 UCT ON 10 MAY 1981, VELOCITY = 350 METERS/SECOND

TR 83-1

SCALE 1:24000
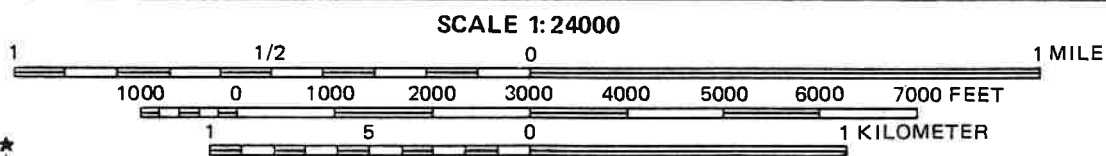
CONTOUR INTERVAL 5 FEET
DATUM IS MEAN SEA LEVEL

2010'/INCH
80'/mm

Ø INJECTION WELL

PLEASANT BAYOU
NO. 2 TEST WELL

IMPULSIVE
RAYLEIGH EVENT

GEOPRESSURED/GEOTHERMAL
TEST WELL SITE

TEXAS

QUADRANGLE
LOCATION

FIGURE 29. IMPULSIVE RAYLEIGH EVENTS ORIGINATING EAST OF THE GEOPRESSURED/
GEOTHERMAL TEST WELL SITE.

G 13188

–60–

TR 83-1

immediately prior to 6 December 1981 should be suspect for generation of the observed signals. (2) The complexity of the signals observed in the episodes is a second important consideration. Some of the episodes, e.g., 18 May 1982 (episode 6), and 6 December, 1981 (episode 1), are very simple, consisting of one or two impulsive Rayleigh events with associated rumble. Others, like 22 August, 1981 (episode 8), are extremely complex with periods characterized by hundreds of impulsive Rayleigh events or harmonic tremor lasting many hours. (3) All of the signals observed are surface waves. In the data analysis section, it was shown that Rayleigh wave velocities and atmospheric acoustic velocities are nearly the same in the Texas Gulf Coast. Coupling of atmospheric acoustic waves and earth Rayleigh waves is therefore extremely likely. For this reason, sources of Rayleigh wave signals could be of atmospheric or earth origin. (4) Separate impulsive Rayliegh events in any given sequence have nearly identical phase arrival order at the array sites indicating a single location of origin. In addition, the events in any sequence display an approximate power law distribution of amplitudes not a single, constant amplitude.

To illustrate the approximate size of these events, we have computed the amplitudes of the ground displacements, velocities and accelerations for two of the impulsive Rayleigh events at station BEG 4. The signal at 04:50:15 UCT on figure 14 yielded the following: maximum amplitude signal frequency 5.18 hertz, maximum (peak-trough) displacement amplitude corrected for instrument response 2.22×10^{-7} m, maximum velocity of the signal 7.32×10^{-6} m/sec, maximum acceleration 2.35×10^{-4} m/sec^2 or 2.4×10^{-5} g. The signal on figure 14 yielded the following: maximum displacement amplitude 2.42×10^{-7} m, maximum velocity 5.78×10^{-6} m/sec, and maximum acceleration 1.38×10^{-4} m/sec^2 or 1.4×10^{-5} g. Using the duration magnitude formula for the 10 January event yields an approximate magnitude of -0.5. Interestingly, if the peak velocity is compared with the empirical formulations of Nuttli (1979) for central U.S. earthquakes, it also indicates the event to be approximately magnitude -0.5. Thus, the largest magnitude for these events is probably 0.0, and the smallest observable magnitude is -2.0. Furthermore, the temporal distribution of individual events in a sequence is aperiodic. (5) The spatial distribution of event episodes suggest two subparallel trends approximately N42°W (see figure 29). (6) Monotonic harmonic tremor is associated with some, but not all, seismic episodes. It is particularly prominent with episodes 18 April, 1982 (figure 15) and 22 August, 1982 (figure 23).

The amplitudes of the displacements, velocities, and accelerations at station BEG 4 associated with the harmonic tremor on 18 April 1982 have been computed. The frequency of the harmonic tremor is 1.27 hertz, the (peak-trough) displacement amplitude corrected for instrument response is 2.1×10^{-7} m, the corresponding ground velocity and acceleration are respectively 1.68×10^{-6} m/sec and 1.34×10^{-5} m/sec^2 (1.37×10^{-6} g).

Two forms of effluent disposal from industrial complexes potentially can result in the types of seismic signals observed. These are high-pressure effluent flares and high-volume subsurface injections. Both of these disposal methods are known to be practiced by the chemical plant where the seismic episodes appear to originate.

Model I Hypothesis: <u>The observed seismic episodes are related to unusual flare conditions at one or more industrial stacks.</u>

Under normal circumstances, the flaring of industrial gasses should not result in noticeable seismic signals at moderate distances. If the ignition of the flare was erratic, however, it could result in repeated ignitions and extinctions which might generate acoustic signals. The amplitude and dominant period of the acoustic signals would correlate with fireball dimensions, and the temporal separation would relate to the time between reignitions. The seismometers in the far-field would record these signals as impulsive, acoustic-coupled Rayleigh waves with variable amplitude and spacing, and each episode would appear to originate from a single source. Due to changing atmospheric conditions, different episodes might appear to originate from different sources because of variations in acoustic velocity and atmospheric refractive conditions. In addition, the lesser constrained axis of the 90% location confidence ellipse is oriented at approximately N45°W; thus, the apparent linear trends might be an artifact of location precision and atmospheric conditions. The occurrences of rumble-type events could correspond with episodic turbulent flow from the stack which might result in additional acoustic signals. The harmonic tremor possibly might be the result of "organ pipe" resonance of the stacks under high-volume flow conditions or, alternatively, a pipe hammer induced in a valved feed pipe. Essentially, this hypothetical model could rationalize all of the seismic phenomena observed. Flare stacks are known to be located near the impulsive Rayleigh episode clusters 1, 2, 3 and 5, 9 and 7. Convincing demonstration that hypothetical Model I is the rational explanation of the observed seismic activity requires additional, detailed information about activities at the chemical plant and observational data which are unavailable at this time.

Model II Hypothesis: <u>The observed seismic episodes are related to subsurface waste injection at one or more disposal wells.</u>

There are many documented cases where subsurface injection of fluids resulted in induced microearthquakes. Perhaps the best documented case is that of injections at the Rocky Mountain Arsenal Well and the Denver earthquakes (Hollister and Weimer, 1968). It is possible to interpret the ensemble of seismic event characteristics exhibited by the complex episodes from 6 December 1981 and 25 September 1982 by a hypothetical model which involves intermittent flow of injected fluids controlled by stress-sensitive asperities along a system of formational discontinuities. This hypothesis would require the impulsive Rayleigh events to be of earth rather than atmospheric origin. Since body waves are not observed for these events, a mechanism to justify their absence is required (see Data Analysis Procedures Surface Wave Data section). The fact that events of this type, i.e., impulsive Rayleigh events, have been recorded previously at all geopressured/geothermal design well sites and that a suite of such events at the Brazoria site appears to collocate with microearthquakes located using body phases (see figures 27 and 28) would support the theory that these are also microearthquakes. This hypothesis would suggest that the orientation and spatial distribution of the impulsive Rayleigh events comprising the episodes are significant and not an artifact of mislocation and changing atmospheric conditions. Because the epicentral precision of the swarms of events is extremely good at the 90% confidence level, and,

-62-

collectively, the swarms define two distinct linear trends separated by approximately six hundred meters within which no events have bee located, it is necessary to rationalize geologically why these trends could exist. The mean orientation of these two seismic trends is N47°W. Zoback and Zoback, (1980) have shown that the regional orientation of the horizontal least-compressive stress for Brazoria County, Texas, is approximately N25°W. Assuming that this regional trend is correct, the actual stress field in the vicinity of the chemical plant would be the result of this regional stress field plus the perturbations superposed by local geological features such as salt domes and faults. The most-significant perturbation to the regional stress field in the Chocolate Bayou area would be the injection of the Danbury Dome and Hoskins Mound salt domes. Although the absolute stress effect of these intrusions is not known, the relative effect on the uniform stress field produced by this type of perturbation has been shown by Jaeger, (1969, p. 188). Given the relative position of the two salt domes with respect to the chemical plant, the combined effect would be to rotate the regional stress trajectories counterclockwise from the unperturbed orientations. Whether or not these intrusions could cause a 20° rotation of the stress field is not known. The sense of the rotation is correct, and we suggest that the linear trends of the observed seismic swarms may be aligned with the local horizontal least-compressive stress direction. Further, since specific locations appear to be the sites of repeated activity, e.g., site of episodes 1, 2 and 3, episodes 4 and 8, episodes 5 and 9, these locations may constitute asperities along a formational discontinuity as defined by Das and Scholz (1981). This would explain also why the events in any one swarm episode were so spatially restricted. Extending this hypothetical model further, comparing the general character of the seismic episodes defining each asperity suggests that the asperity tends to behave in a repeatedly consistent manner. Events 1, 2 and 3 are characterized by sequences of impulsive, high-frequency, Rayleigh-mode events which are temporally distinct. The seismic records between events during these episodes is comprised of high-frequency noise with amplitudes two to three times that of the normal ambient conditions. In comparison, event episodes 5 and 9 are characterized by seismic records between events with high-frequency noise similar to that described and, in addition, transitory appearances of a 1.38 hertz resonance. In contrast, event episodes 4 and 8 are characterized by high-frequency Rayleigh-mode events which are superimposed on a very prominent 1.38 hertz, nearly monotone wave train of remarkable amplitude. In a previous report, Mauk (1982) suggested that the origin of this harmonic tremor may be explained by the resonance of a fluid-driven crack as proposed by Aki, Fehler, and Das (1977) and Chouet (1981) or Ferrick, Quamar, and St. Lawrence (1982). Essentially, this hypothetical model could also rationalize all of the seismic phenomena observed; but, without additional information and data, it too cannot be convincingly demonstrated to be the correct interpretation.

In conclusion, nine episodes of complex seismicity were recorded by the Brazoria seismic array between 6 December, 1981 and 25 September, 1982. Two alternative models have been presented which could rationalize the data equally well. Model I associates the seismicity with effluent from industrial flare stacks. Model II associates the seismicity with effluent fluids injected into a geological formation. Other models not presented also

may account for the observations, and it should not be assumed that either model presented is necessarily the correct solution. This enigmatic seismicity will require additional information, data and analyses if a solution is to be found.

THE PHASE II LONG-TERM FLOW TEST

The Phase II, long-term flow test of the Pleasant Bayou No. 2 geopressured/geothermal design well was reinitiated approximately 27 September 1982 following a shut-in of over fourteen months. In anticipation that some aspect of the production history may display a causality relationship with induced seismicity, we maintain a computer log of wellhead tubing pressure and approximate withdrawal rate from the Pleasant Bayou No. 2 well and the wellhead injection pressure for the Pleasant Bayou No. 1 well. Data for this computer log are provided by Gruy Federal Corp. Data are entered at hourly increments from 1 October through 23 October 1982. All subsequent data are entered at daily increments because more detailed logs were no longer provided to us by Gruy Federal. Graphs of the production wellhead tubing pressure and approximate brine withdrawal rate and the wellhead brine injection pressure as a function of time for the period from 1 October through 31 December, 1982 are illustrated in figure 30. Specific times when flow rate has been altered are indicated by the alphabetic markers at the bottom of figure 30. The explanations for the identified flow rate alterations of figure 30 are given in table 6. Except for seven shut-ins, all other entries indicate times when choke adjustments were made. Although alteration of choke settings and shut-ins result in some short-term perturbations of the production and disposal histories, the production pressure curve generally displays a long-term exponential pressure decline typically observed for confined aquafers. Similarly, the injection pressure curve displays a long-term logarithmic increment in injection pressure as a function of time commonly observed at other injection wells. No seismological effects attributable to this long-term flow test have been observed in 1982. It is anticipated that seismicity related to this flow test will initiate in the first six months of 1983.

PRODUCTION INTERVAL
14,647' – 14,707'

INJECTION INTERVAL
6,226' – 6,538'
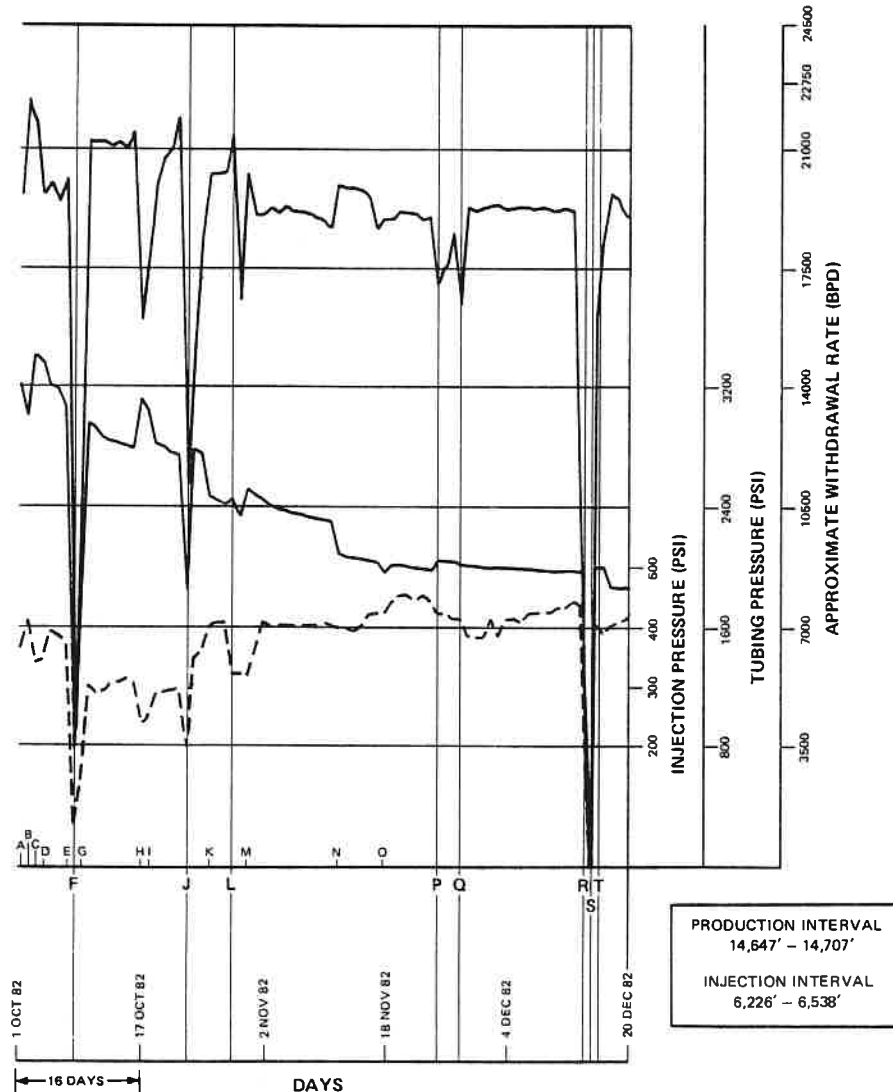
TABLE 6. BRAZORIA EVENT LOG FOR PHASE II TESTING

EVENT	DATE	TIME	EXPLANATION (DURATION)	CHOKE SIZE
A	1 OCT 82	07:00	OPEN TEST WELL	48/64"
B	2 OCT 82		CHOKE ADJUSTMENT	52/64" – 58/64"
C	3 OCT 82		CHOKE ADJUSTMENT	40/64" – 52/64"
D	4 OCT 82		CHOKE ADJUSTMENT	56/64"
E	7 OCT 82		CHOKE ADJUSTMENT	56/64"
F	8 OCT 82	12:30	SHUT-IN REPAIRS (27.5 HRS)	48/64" – 84/64"
G	9 OCT 82		CHOKE ADJUSTMENT	24/64" – 56/64"
H	17 OCT 82		CHOKE ADJUSTMENT	40/64" – 50/64"
I	18 OCT 82		CHOKE ADJUSTMENT	56/64"
J	23 OCT 82	13:30	SHUT-IN LEAK (4.5 HRS)	S/I
K	26 OCT 82		CHOKE ADJUSTMENT	60/64"
L	29 OCT 82	14:00	SHUT-IN MAINTAINANCE (1.75 HRS)	32/64" – 60/64"
M	31 OCT 82		CHOKE ADJUSTMENT	56/64"
N	12 NOV 82		CHOKE ADJUSTMENT	60/64"
O	18 NOV 82		CHOKE ADJUSTMENT	62/64"
P	25 NOV 82	13:40	SHUT-IN REPAIRS (2.33 HRS)	48/64" – 62/64"
Q	28 NOV 82	13:30	SHUT-IN POWER FAILURE (3 HRS)	S/I
R	14 DEC 82	12:00	SHUT-IN MAINT & CALS (23 HRS)	S/I
S	15 DEC 82		CHOKE ADJUSTMENT	24/64"
T	16 DEC 82	06:00	SHUT-IN POWER FAILURE (20 HRS)	62/64"
U	18 DEC 82		CHOKE ADJUSTMENT	64/64"

FIGURE 30.   INJECTION PRESSURE, TUBING PRESSURE AND FLOW RATE HISTORY OF THE PHASE II TESTING OF THE PLEASANT BAYOU NO. 2, GEOPRESSURED/GEOTHERMAL TEST WELL FROM 1 OCTOBER TO 20 DECEMBER 1982

G 13279

-66-

SEISMICITY AND THE PLEASANT BAYOU DESIGN WELL TESTS

The primary objective of the Brazoria seismic monitoring program has been to assess if high-volume brine production and/or disposal induces and/or enhances seismic activity in the vicinity of the Pleasant Bayou design well. A review of the design well production history and the data produced by the Brazoria seismic array from 1979 through 1982 suggests a possible causality relationship between high-volume brine production and increased seismic activity in the vicinity of the Pleasant Bayou test well program. The evidence for, and limitations of, this interpretation are discussed below.

Since the inception of the Brazoria seismic monitoring program, there have been four periods during which brines were produced from the Pleasant Bayou design well. These periods of production have been detailed elsewhere (Hartsock, 1981; Garg, Riney, Fou, 1981; Mauk, 1982) and are briefly summarized in table 7. An implicit assumption to the argument that the observed local seismicity correlates with brine production from the Pleasant Bayou design wells is that all activity at other regional wells constitutes an insignificant perturbation to the local stress field in comparison. The validity of this assumption is not known but is certainly suspect considering that volumes of fluid equivalent to those produced by the Pleasant Bayou No. 2 well are injected daily by the Chemical Plant into wells within one mile of the Pleasant Bayou No. 1 well.

Excluding the sequences of observed seismic activity in 1982 which locate near the chemical complex east of the geopressured/geothermal well, the nature, spatial and temporal characteristics of all other seismicity observed since 1979 constitute an interesting set of observations. Basically, there are three distinct types of signals which have been recorded by the Brazoria seismic array throughout the operational period: (1) events with distinguishable P and/or S phases (type I), (2) events with indistinguishable body phase arrivals, but with impulsive Rayleigh wave signatures (type II), and (3) events with indistinguishable body or surface wave arrivals which are identifiable as high-amplitude "noise" bursts traversing the array (type III).

The events with identifiable P and/or S phase arrivals which are either unquestionably or suspected to be microearthquakes and not explosions have many common characteristics. P and S waves from these events are rich in frequencies greater than five hertz, and the seismogram coda tails display typical exponential amplitude decay similar to those of microearthquakes observed at other locations.

Determination of P-wave first motions is not unambiguous but appears to be predominantly dilitational (downward) on most seismograms when discrimination is possible. This is a characteristic consistent with a downward local geological block movement. All of type I events yield hypocentral solutions which suggest a depth of origin generally between two and five kilometers. No events have been observed which locate deeper than five kilometers. Epicenters of the type I events cluster within a kilometer of the projected 15,000-feet deep locations of growth faults on the west and northwest edge of

TABLE 7. PLEASANT BAYOU PRODUCTION HISTORY

Test No.	Flow Test Identification	Flow Initiation	Flow Cessation	Volume Produced (* 10^5 bbl)	Average Rate bbl/d
1	Pre Phase I	15 November 1979	3 December 1979	2.74	15,222
2	Phase I (Short Term)	16 September 1980	31 October 1980	5.37	Variable 6,600–19,200
3	Phase II (Long Term) Aborted	2 July 1981	18 July 1981	2.21	Variable 14,000–28,000
4	Phase II (Long Term)	27 September 1982	Continuing	—	19,000

TR 83-1

the reservoir (see figure 31, locations indicated by large asterisks). Although a few events appear to associate with the northeast trending fault near Liverpool and Chocloate Springs, the majority of the epicenters appear to associate with a north-south trending growth fault which passes near seismograph stations BEG 5 and BEG 3, and terminates near Chocloate Springs. Furthermore, the majority of epicenters since 1979 which have computed locations near this proposed fault are on the east (up-dip) side of the fault. Since the location precision of most of these events is poor and the location accuracy of the growth fault and the epicenters is unknown, little significance can be placed on the relative position of the epicenters to the growth fault, however. The magnitudes of type I events are all small, between 0.0 and 1.5, and there is no obvious functional relationship between the frequency of occurrence and the magnitude of these events. In fact, the occurrence of this type of event is relatively rare. The largest annual number, 10, occurred in 1981, while possibly one was recorded in 1982.

Excluding the type II events in 1982 which locate near the chemical complex, the impulsive Rayleigh events display a similar temporal distribution to that of the type I microearthquakes. Furthermore, the epicentral distribution of the type II events is indistinguishable from that of the type I microearthquakes (see figure 31, locations indicated by small asterisks), given the location method discussed earlier. Depths of the impulsive Rayleigh events are indeterminant, however. The only characteristic distinguishing the type I and type II events is the absence of identifiable body phase arrivals for the latter group.

There are three reasonable explanations for this peculiar phenomenon. The body phases for the type II events may be very high frequency, (i.e., > 50 hertz), highly attenuated by the sediments, and outside the principal magnification band of the instruments being used to monitor the region. This explanation is attractive from the point of view that the body phases exist but are not observed because of poor transmission properties of the earth and/or poor spectral resolution of the recording system. If this is the correct explanation for why the body phases of type II events are absent, then the differences in spectral content of the body and surface waves for these events differ by over an order of magnitude. The similarity of body and surface wave spectra for type I microearthquakes, however, would argue against this explanation.

A second explanation for the absence of body phases for type II events is that the events occur at a particular depth below a low-velocity layer which acts as a waveguide trapping the body-wave energy. Sonic logs from all local boreholes which were examined indicate the presence of several shallow, low-velocity layers which could potentially act as leaky waveguides. If this mechanism for eliminating the body phases of type II events is correct, then the depth of origin is the parameter distinguishing type I and type II events. Since body waves are also observed for exploration shots buried to a depth of thirty meters, this would argue that the depth of the type II events and the low-velocity layer or layers is between thirty meters and two kilometers. Events at depths greater than five kilometers cannot be considered because of the relative excitation of the surface Rayleigh waves. Although this explanation for the absence of body phases of type II events is

SCALE 1:62500

1	0	1	2	3	4 MILES
3000	0	3000 6000 9000 12000 15000 18000			21000 FEET
1 .5	0	1 2 3 4			5 KILOMETERS

✳ EARTHQUAKE LOCATION	✳ RAYLEIGH EVENT LOCATION
⊕ TEST WELLS	▲ SEISMOGRAPH STATIONS

▬▬ GROWTH FAULTS NEAR 16,000 FT. DEPTH
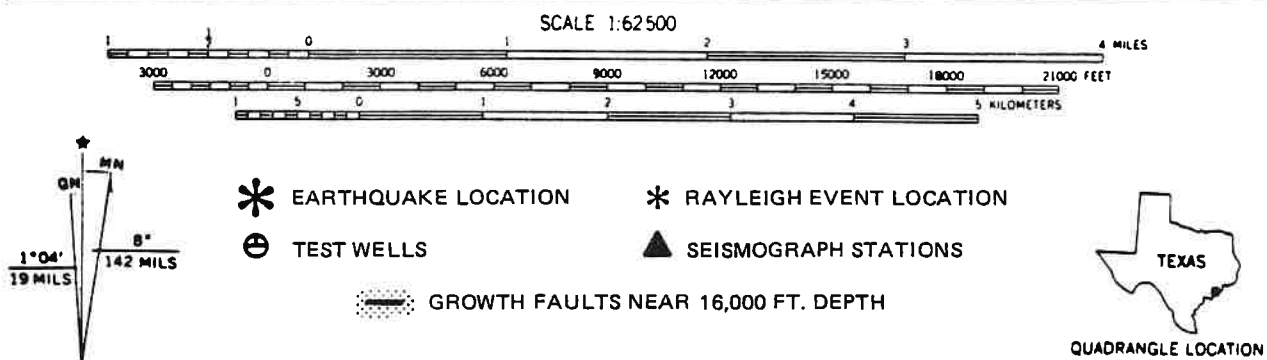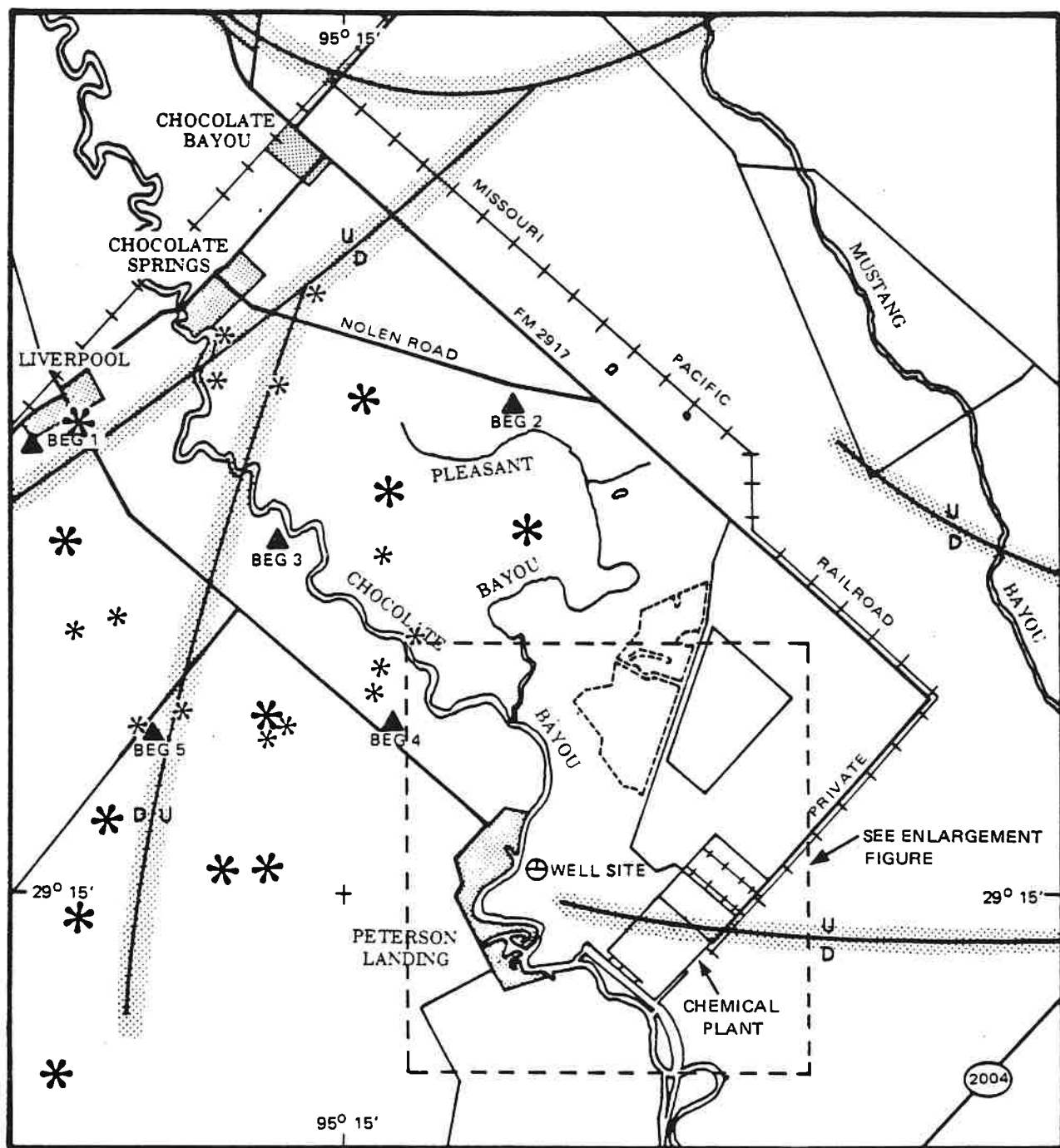
FIGURE 31. 1981 AND 1982 SEISMIC EVENT EPICENTERS

TEXAS

QUADRANGLE LOCATION

G 12657A

-70-

TR 83-1

favored currently, and can be tested with computer modeling, such tests have yet to be performed. If this explanation is correct, the coincidence of the type I and type II event populations is fortuitous and possibly not related.

A third possible explanation for the absence of body phases for the type II events is that they are not generated. If these signals are atmospheric in origin, they are transmitted to the stations as acoustic-coupled Rayleigh waves, and there are not body phases to observe. If this explanation is correct, these events have nothing to do with the release of earth stresses and are not relevant to the monitoring problem. Although this explanation cannot be discounted totally, the coincidence spatially and temporally of the type I and type II events would argue against this possibility.

Although any of these mechanisms could account for the missing body phases of type II events, it seems likely that either, or possibly both, of the first two explanations are most satisfactory. The population of impulsive Rayleigh events therefore is an extension of the microearthquake population.

Type III events, unlike type I and type II events, are unable to be located. These events, comprised of two members, rumble and harmonic tremor, have emergent arrival onsets, generally have variable amplitudes and durations, and have no identifiable body or surface arrivals. Harmonic tremor signals are distinguished from rumble signals because they are very monotonic. It is quite unlikely that the origins of these two signals are the same, and they are classified together because of the inability to locate them. Interestingly, rumble signals display a temporal distribution similar to type I and type II events; i.e., during years when type I and type II events are more numerous, so are type III. It seems likely that rumble events are an extension of the microearthquake population and that harmonic tremors are a different phenomenon completely.

Figure 32 illustrates the temporal distribution of all seismic events, types I, II and III, which have been recorded since the beginning of the Phase I short-term flow test in 1980. Type I and II events appear as solid bars on the histogram. Type III events appear as hatchured bars. In addition to the seismic event occurrences, the times of the Pleasant Bayou test productions are indicated by arrows. This illustration clearly demonstrates the correlation of rumble type activity with events which can be located. In addition, the temporal distribution of all observed events is obviously peaked in the latter half of 1981. Although it is not possible to relate the seismicity to particular aspects of the Phase I short-term flow test and/or the aborted Phase II long-term flow test, the seismic activity is unquestionably higher following the Pleasant Bayou well production periods. If the strain diffusion rate (14 m/d) mentioned in the supplement to the 1981 annual progress report is correct, then we should expect to see a reactivation of the growth fault seismic activity associated with the new Phase II long-term flow test, which began approximately 1 October 1982, in May to June 1983.

In conclusion, a review of the data produced by the Brazoria seismic array from September 1979 through December 1982 and the subsequent analyses of that data suggest the likelihood of a causality relationship between high-volume brine production from the Pleasant Bayou design well and enhanced local

-71-
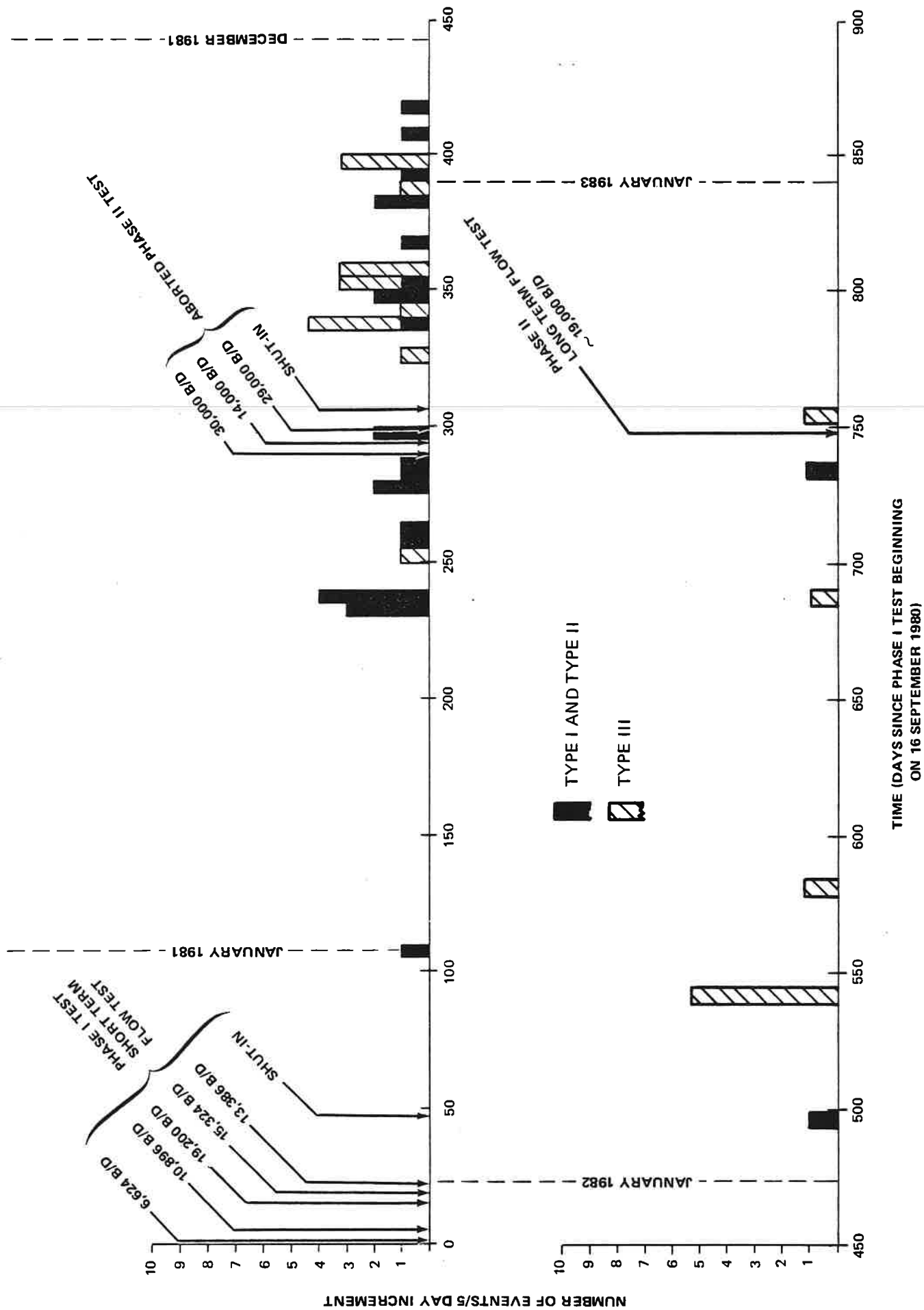
FIGURE 32. TEMPORAL DISTRIBUTION OF SEISMICITY AT PLEASANT BAYOU DURING 1981 AND 1982

G 13030 A

-72-

seismicity. At this time, it remains unknown how the seismicity is related to the design well test program. It is unknown whether the seismicity is related to withdrawal or injection of the brines produced, or whether the induction of seismicity is total volume or volume-rate dependent. Emphasis in further research should concentrate on the answers to these questions.

REFERENCES

Aki, K., Fehler, M. and Das, S., (1977), Source Mechanism of Volcanic Tremor: fluid driven crack models and their application to the 1963 Kilauea eruption, Jour. Volcanol. Geotherm. Res., 2, pp. 259-287.

Aki, K., and Chouet, B., (1975), Origin and Coda Waves: Source Attenuation and Scattering Effects, Jour. Geophys. Res., 80, pp 3322-3342.

Aki, K., (1981), Source and Scattering Effects on the Spectra of Small Local Earthquakes, Bull. Seis. Soc. Amer., 71, pp 1687-1701.

Chouet, B., Aki, K., and Tsujiura, M., (1978), Regional Variation of the Scaling Law of Earthquake Source Spectra, Bull. Seis. Soc. Amer., 68, pp 49-79.

Chouet, B., (1981), Ground motion in the near field of a fluid driven crack and its interpretation in the study of shallow volcanic tremor, Jour. Geophys. Res., 86, pp. 5985-6016.

Das, S., and Scholz, Ch. H., (1981), Theory of Time Dependent Rupture in the Earth, Jour. Geophys. Res., 86, 6039-6051.

Douze, E. J., (1964), Rayleigh Waves in Short Period Seismic Noise, Bull. Seis. Soc. Amer., 54, pp. 1197-1212.

Ebeniro, J., Wilson, C. R., and Dorman, J., (1983), Propagation of Dispersed Compressional and Rayleigh Waves on the Texas Coastal Plain, Geophys., 48, pp. 27-35.

Ferrick, N. G.N., Qamar, A., and St. Lawrence, W. F., (1982), Source mechanism of volcanic tremor, Jour. Geophys. Res., 87, pp. 8675-8683.

Garg, S. K., T. D. Riney, and J. M. Fwu, (1981), 'Analysis of Phase I Flow Data from Pleasant Bayou No. 2 Geopressured Well', in Proceedings of the Fifth Conference Geopressured-Geothermal Energy: U.S. Gulf Coast, Edited by D. G. Bebout and A. L. Bachman, Louisiana State University, Baton Rouge, Louisiana, pp. 97-100.

Hartsock, J. H., (1981), 'Test Prognosis and Actual Test Performance of the Pleasant Bayou No. 2 Well', in Proceedings of the Fifth Conference Geopressured-Geothermal Energy: U.S. Gulf Coast, Edited by D. G. Bebout and A. L. Bachman, Louisiana State University, Baton Rouge, Louisiana pp. 91-95.

Hollister, J. C., and Weimer, R. J., (1968), Denver Earthquakes and the Arsenal Well, Quarterly of the Colorado School of Mines, Vol. 63, No. 1, January 1968, 251 p.s

Jaeger, J. C., (1969), Elasticity, Fracture and Flow, Methuen's Monographs on Physical Subjects, Barnes and Noble Publishers, 268 p.

REFERENCES (continued)

Lash, C. C., (1980), Shear waves, multiple reflections, and converted waves found by a deep vertical wave test (vertical seismic profiling), Geophys. 45, pp 1373-1411.

Mauk, F., (1982), Microseismic Monitoring of Chocolate Bayou, Texas, the Pleasant Bayou No. 2 Geopressured/Geothermal Energy Test Well Program 1981 Annual Progress Report, Teledyne Geotech Technical Report No. 82-2, 74 p.

Mauk, F., (1982), Microseismic Monitoring of Chocolate Bayou, Texas, the Pleasant Bayou No. 2 Geopressured/Geothermal Energy Test Well Program 1981 Annual Progress Report, Teledyne Geotech Technical Report No. 82-2, 74 p.

Nuttli, O., (1979), The relation of sustained maximum ground acceleration and velocity to earthquake intensity and magnitude, State-of-the-Art for Assessing Earthquake Hazards in the United States Report 16, U.S. Army Corps of Engineers Miscellaneous Papers S-73-I, 74 p.

Zoback, M. L., and Zoback, M., (1980), State of Stress in the Conterminous United, Jour. Geophys. Res., 85, pp. 6113-6156.

TR 83-1

APPENDIX A

Monthly Performance Logs for the Brazoria Array

January through December 1982

Brazoria County, Texas Seismic Array Monthly
Develocorder Record Performance Log - January, 1982

	BEG1	BEG2	BEG3	BEG4	BEG5
Operational efficiency	81%	82%	82%	82%	82%
Total operational hours	744	744	744	744	744
Total hours of down time	138	131	131	131	131
Down time due to routine changing procedures	13	13	13	13	13
Down time due to recording system failure	27	20	20	20	20
Down time due to telemetry failure	6	6	6	6	6
Down time due to station failure	0	0	0	0	0
Other * See explanation	92	92	92	92	92

* Explanation

Holidays January 1-4 (86 hours)
Develocorder maintenance (6 hours)

Brazoria County, Texas Seismic Array Monthly
Develocorder Record Performance Log – February, 1982

	BEG1	BEG2	BEG3	BEG4	BEG5
Operational efficiency	97%	97%	97%	97%	97%
Total operational hours	654	654	654	654	654
Total hours of down time	18	18	18	18	18
Down time due to routine changing procedures	8	8	8	8	8
Down time due to recording system failure	10	10	10	10	10
Down time due to telemetry failure	0	0	0	0	0
Down time due to station failure	0	0	0	0	0
Other	0	0	0	0	0

A-3

Brazoria County, Texas Seismic Array Monthly
Develocorder Record Performance Log - March, 1982

	BEG1	BEG2	BEG3	BEG4	BEG5
Operational efficiency	98%	97%	52%	98%	98%
Total operational hours	732	721	385	732	732
Total hours of down time	12	23	359	12	12
Down time due to routine changing procedures	12	12	12	12	12
Down time due to recording system failure	0	0	0	0	0
Down time due to telemetry failure	0	0	0	0	0
Down time due to station failure	0	11	347	0	0
Other	0	0	0	0	0

Brazoria County, Texas Seismic Array Monthly
Develocorder Record Performance Log - April, 1982

	BEG1	BEG2	BEG3	BEG4	BEG5
Operational efficiency	91%	52%	54%	58%	91%
Total operational hours	656	377	389	416	654
Total hours of down time	64	343	331	304	66
Down time due to routine changing procedures	12	12	12	12	12
Down time due to recording system failure	52	52	52	52	52
Down time due to telemetry failure	0	0	0	0	0
Down time due to station failure	0	279	267	240	0
Other	0	0	0	0	2

* Explanation

  Battery charging

Brazoria County, Texas Seismic Array Monthly
Develocorder Record Performance Log - May, 1982

	BEG1	BEG2	BEG3	BEG4	BEG5
Operational efficiency	92%	92%	92%	92%	92%
Total operational hours	683.5	683.5	683.5	683.5	683.5
Total hours of down time	60.5	60.5	60.5	60.5	60.5
Down time due to routine changing procedures	13.5	13.5	13.5	13.5	13.5
Down time due to recording system failure	11.0	11.0	11.0	11.0	11.0
Down time due to telemetry failure	36.0	36.0	36.0	36.0	36.0
Down time due to station failure	0.0	0.0	0.0	0.0	0.0
Other	0.0	0.0	0.0	0.0	0.0

Brazoria County, Texas Seismic Array Monthly
Develocorder Record Performance Log – June, 1982

	BEG1	BEG2	BEG3	BEG4	BEG5
Operational efficiency	91%	91%	43%	70%	91%
Total operational hours	651.8	652.3	312.8	504.3	652.3
Total hours of down time	68.2	67.7	407.2	215.7	67.7
Down time due to routine changing procedures	8.2	8.2	8.2	8.2	8.2
Down time due to recording system failure	58.0	58.0	58.0	58.0	58.0
Down time due to telemetry failure	2.0	1.5	2.0	1.5	1.5
Down time due to station failure	0.0	0.0	339.0	148.0	0.0
Other	0.0	0.0	0.0	0.0	0.0

Brazoria County, Texas Seismic Array Monthly
Develocorder Record Performance Log – June, 1982

	BEG1	BEG2	BEG3	BEG4	BEG5
Operational efficiency	81%	80%	0%	52%	82%
Total operational hours	604	596	0	384	610
Total hours of down time	140	148	744	360	134
Down time due to routine changing procedures	7	7	7	7	7
Down time due to recording system failure	36	36	36	36	36
Down time due to telemetry failure	0	0	0	0	0
Down time due to station failure	0	7	610	219	0
Other - *See explanation	97	98	91	98	91

* Explanation

Shutdown for 4th of July holiday weekend; battery charging

Brazoria County, Texas Seismic Array Monthly
Develocorder Record Performance Log – August, 1982

	BEG1	BEG2	BEG3	BEG4	BEG5
Operational efficiency	65%	65%	0%	65%	65%
Total operational hours	480	480	0	480	480
Total hours of down time	264	264	744	264	264
Down time due to routine changing procedures	5	5	0	5	5
Down time due to recording system failure	53	53	0	53	53
Down time due to telemetry failure	0	0	0	0	0
Down time due to station failure	0	0	744	0	0
Other - *See explanation	206	206	0	206	206

* Explanation

* Develocorder yearly maintenance and parts replacement.

Brazoria County, Texas Seismic Array Monthly
Develocorder Record Performance Log – September, 1982

	BEG1	BEG2	BEG3	BEG4	BEG5
Operational efficiency	67%	68%	0%	68%	68%
Total operational hours	483	486	0	486	486
Total hours of down time	237	234	720	234	234
Down time due to routine changing procedures	5	5	0	5	5
Down time due to recording system failure	41	41	0	41	41
Down time due to telemetry failure	3	0	0	0	0
Down time due to station failure	0	0	700	0	0
Other – *See explanation	188	188	0	188	188

* Explanation

Develocorder shut down for preventive maintenance and repairs.

A-10

TR 83-1

Brazoria County, Texas Seismic Array Monthly
Develocorder Record Performance Log - October, 1982

	BEG1	BEG2	BEG3	BEG4	BEG5
Operational efficiency	52%	52%	0%	52%	52%
Total operational hours	390	390	0	390	390
Total hours of down time	354	354	744	354	354
Down time due to routine changing procedures	3	3	0	3	3
Down time due to recording system failure	101	101	0	101	101
Down time due to telemetry failure	0	0	0	0	0
Down time due to station failure	0	0	744	0	0
Other - *See explanation	250	250	0	250	250

* Explanation

Develocorder shutdown for weekends.

A-11

Brazoria County, Texas Seismic Array Monthly
Develocorder Record Performance Log – November, 1982

	BEG1	BEG2	BEG3	BEG4	BEG5
Operational efficiency	54%	54%	0%	54%	54%
Total operational hours	388	388	0	388	388
Total hours of down time	332	332	720	332	332
Down time due to routine changing procedures	2	2	0	2	2
Down time due to recording system failure	0	0	0	0	0
Down time due to telemetry failure	0	0	0	0	0
Down time due to station failure	0	0	720	0	0
Other - *See explanation	330	330	0	330	330

* Explanation

Shut down for Thanksgiving Holiday (November 24-29)

A-12

TR 83-1

Brazoria County, Texas Seismic Array Monthly
Developorder Record Performance Log - December, 1982

	BEG1	BEG2	BEG3	BEG4	BEG5
Operational efficiency	18%	11%	6%	14%	18%
Total operational hours	134	79	48	102	134
Total hours of down time	610	665	696	642	610
Down time due to routine changing procedures	2	2	0	2	2
Down time due to recording system failure	0	0	0	0	0
Down time due to telemetry failure	0	0	0	0	0
Down time due to station failure	0	55	86	32	0
Other - *See explanation	608	608	608	608	608

* Explanation

Renovation of Developorder building

Shut down for Christmas Holiday (December 23-31)

APPENDIX B

Seismological Effects of
Geopressured/Geothermal Reservoir Production

Introduction

Geopressured (pressure gradients more nearly lithostatic than hydrostatic) geothermal (temperatures exceeding 125°C) brines are contained in Cretaceous and Tertiary aged high-permeability formations which underlie much of the Texas and Louisiana Gulf Coast. Early estimates of economically recoverable energy from these formations has been 3.17×10^{15} kjoules (300 quads) of thermomechanical energy and 8.44×10^{15} kjoules (800 quads) of methane (Weshusing, 1981). If the annual per capita energy use for the U.S. in 1971 (1.9×10^8 kjoules) is multiplied by the current Dallas-Ft. Worth metroplex population (2,974,878), the current annual energy use by the metroplex is 5.7 $\times 19^{14}$ kilojoules. Even considering the downward revision of the estimated recoverable methane from geothermal-geopressured formations, this alternative energy source could meet all of the energy requirements of the metroplex at its current population for as long as forty years. Thus, although this alternative energy reserve is not as extensive as lignite, for example, it remains worthy of consideration. The feasibility for economic development of these resources, however, necessitates both the production and subsurface disposal of these environmentally hazardous brines at volumetric rates for individual wells exceeding $3.2 \times 10^3 m^3$ (20,000 bbl) per day. Such high volumetric transfer rates can affect significantly the state of local geological stress and potentially result in ground surface subsidence and/or induced earthquakes, both of which may be environmentally and economically undesirable. Because the potential detrimental long-term environmental impact associated with the development of these resources may be as important as the short-term economic benefits, a variety of environmental monitoring programs has been initiated by the Texas Bureau of Economic Geology and the Louisiana Geological Survey in conjunction with the operation of design test wells by the Department of Energy. The locations of the primary design well prospects and the four design wells which are in various stages of completion are illustrated in Figure 1. Teledyne Geotech, with the authorization of the Texas Bureau of Economic Geology and the Louisiana Geological Survey, has conducted seismic monitoring programs in the vicinity of two of these design wells, the Pleasant Bayou No. 2 well in Brazoria County, Texas, (Figure 1, location A) and the DOW L. R. Sweezy No. 1 well in Vermillion Parish, Louisiana (Figure 1, location D). The purpose of these monitoring programs is to assess the effects of design well development on the state of local geological stress and the potential modes of strain release.

Before proceeding to a description of the monitoring system and results of the programs, it is worth examining possible displacement scenarios. Figure 2a illustrates a block diagram of the earth with a pre-existing zone of weakness. The arrows P_1 and P_2 indicate the ambient stress loading conditions on the block. With fluid withdrawal or injection, the equilibrium balance of the stresses P_1 and P_2 may be disturbed resulting in the slip displacement, S, on the zone of weakness as illustrated in Figure 2b. In this diagram, the dilatant opening of the zone of weakness orthogonal to the slip surface is assumed to be insignificant. Figure 2c illustrates several possible displacement time histories to accomplish the total observed displacement. If, for the sake of discussion, we assume that the total displacement is relatively large and occurs in one movement with a velocity approaching that of the shear wave velocity of the medium, then the movement
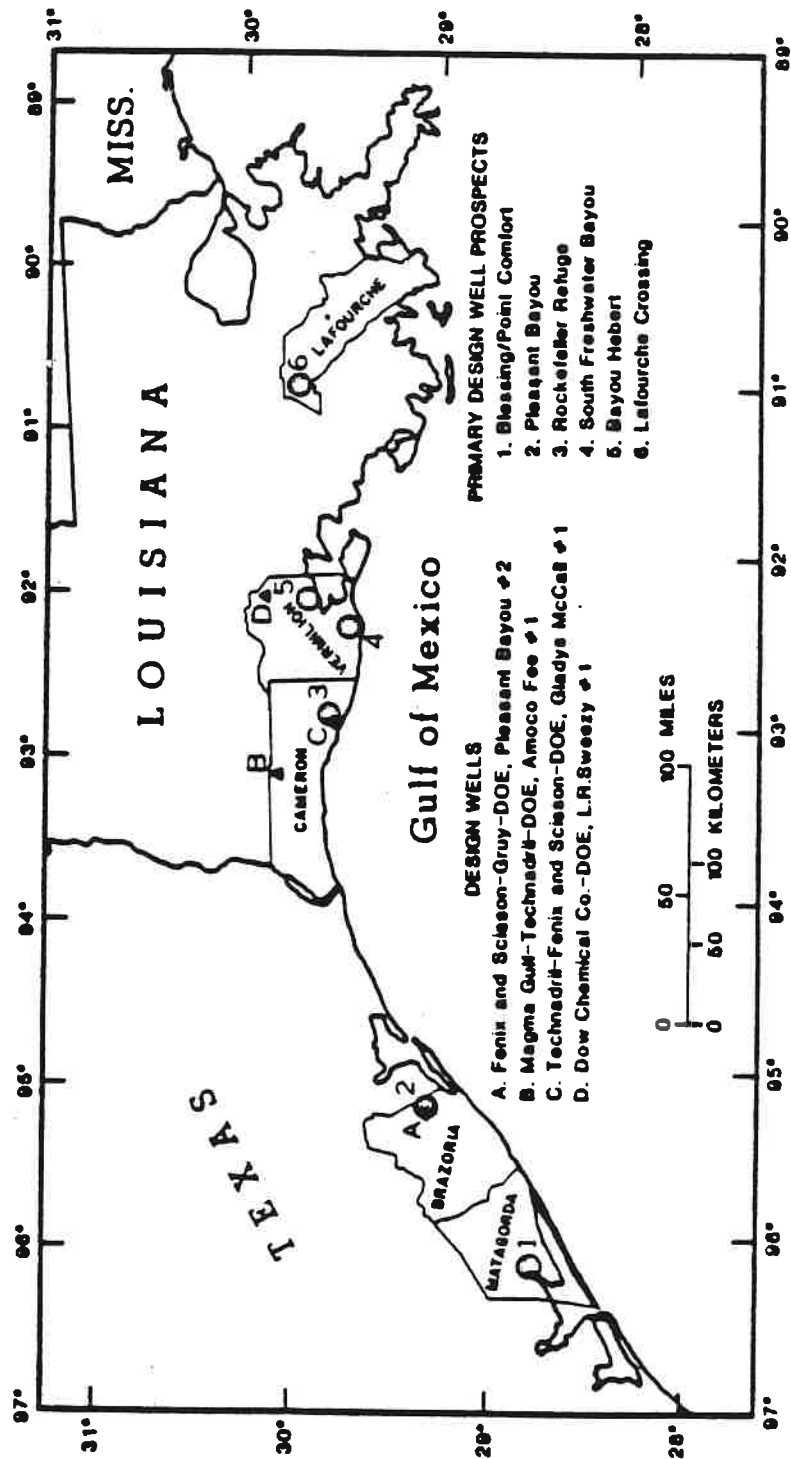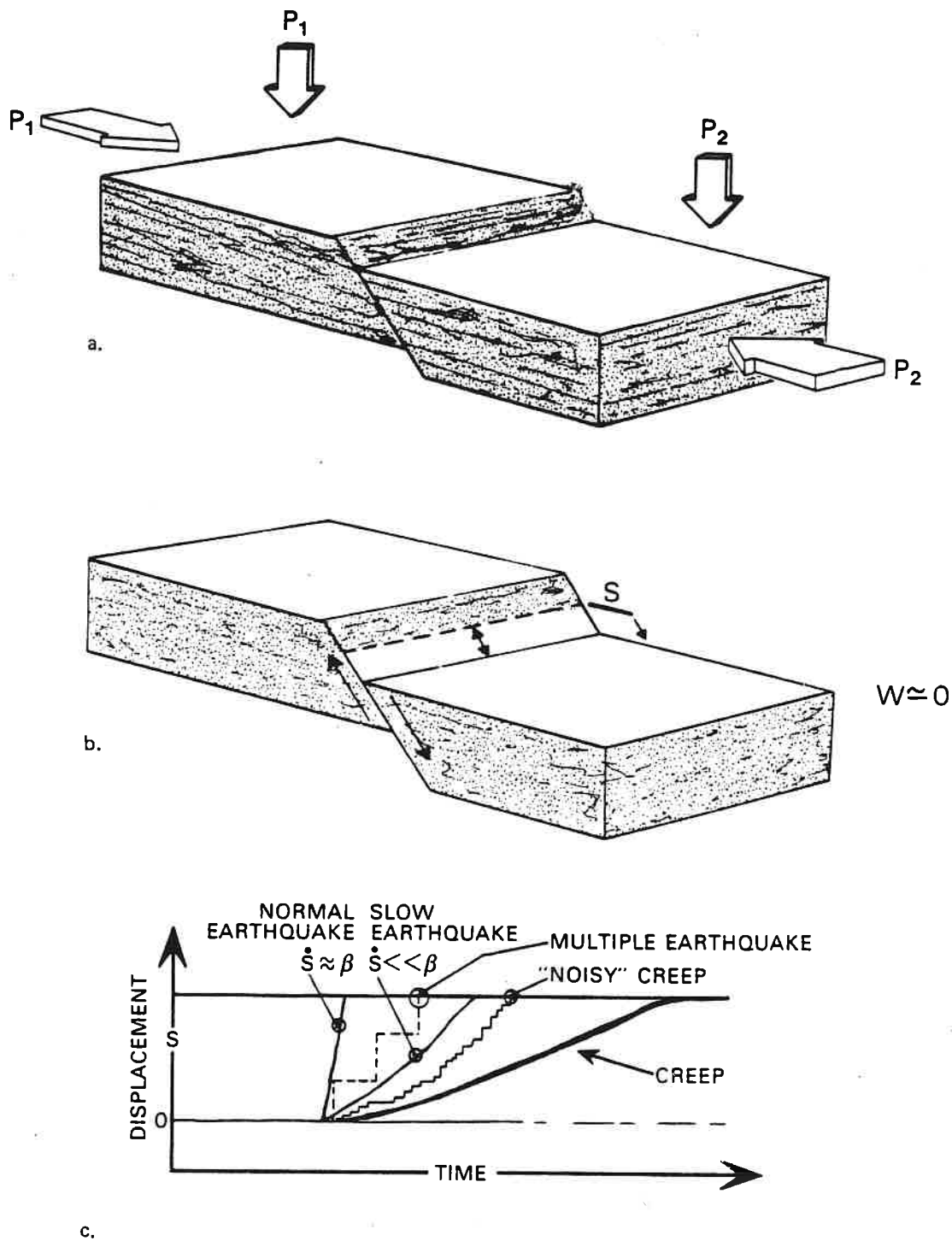
B-2

TR 83-1

FIGURE 1.

DESIGN WELLS
A. Fenix and Scisson–Gruy–DOE, Pleasant Bayou #2
B. Magma Gulf–Technadril–DOE, Amoco Fee #1
C. Technadril–Fenix and Scisson–DOE, Gladys McCall #1
D. Dow Chemical Co.–DOE, L.R.Sweezy #1

PRIMARY DESIGN WELL PROSPECTS
1. Blessing/Point Comfort
2. Pleasant Bayou
3. Rockefeller Refuge
4. South Freshwater Bayou
5. Bayou Hebert
6. Lafourche Crossing

TR 83-1

FIGURE 2. a. BLOCK DIAGRAM OF EARTH PRIOR TO SLIP DISPLACEMENT
          b. BLOCK DIAGRAM OF EARTH FOLLOWING SLIP DISPLACEMENT
              ASSUMING NO FRACTURE DILATANCE
   c. POSSIBLE DISPLACEMENT TIME HISTORIES TO PROCEED FROM a TO b.

G 12323

B-4

would be referred to as a normal earthquake of relatively moderate magnitude. If, on the other hand, the velocity of displacement was slow in comparison to the shear wave velocity of the medium, then the earthquake would be referred to as a slow earthquake. Alternatively, if the total displacement occurred in two or more discrete events in time, then the displacements would be referred to as a multiple earthquake sequence. Finally, if the displacement, S, occurs over a large length of time, it would be referred to as creep, possibly "noisy" seismically if some elastic energy were radiated in the process.

The growth faults in the Gulf Coast are characterized by large geological offsets, yet there have never been recorded any large-magnitude earthquakes. This evidence indicates that these displacements must be accommodated either by a series of smaller events or, possibly, by creep. In addition, because of the high density of faults in the Gulf Coast, and low yield strength of the rocks comprising the geological column, it appears that sufficient stress accumulation in a large volume of rock to result in a moderate-sized (magnitude greater than 5.5) earthquake is not very likely. For these reasons, monitoring of fault displacements in the Gulf Coast logically takes two forms: (1) microseismic monitoring for small magnitude displacements, and (2) some form of creep monitoring for aseismic displacement. The seismic monitoring programs at the Pleasant Bayou No. 2 and L. R. Sweezy No. 1 wells conducted by Teledyne Geotech are of the former type. Attempts by other investigators to ascertain if creep-type events also are occurring in the regions have been less definitive due to both instrumental difficulties and the short time period over which the observations have been made. Little information in this area will be included here.

Because the development of these geopressured reservoirs involves high volumetric fluid tranfer rates from and into naturally-faulted formations, an alternative fault behavior to shear displacement must also be considered. Fluid-driven dilatant opening of a fault is illustrated in Figure 3. The faulted reservoir of Figure 2a has been reproduced as Figure 3a. In this case, however, the fault can be thought to be a permeability barrier for communication of fluids between the two halves of the reservoir. Either rapid drawdown or injection of fluids on one side of the fault or the other can result in a significant stress differential along the fault plane between the two reservoir segments. Under the right stress conditions, the fault dilatantly opens as illustrated in Figure 3b which permits rapid fluid transfer between the reservoir segments. Aki, Fehler and Das (1977) estimate that this type of behavior can be initiated in transfer of magma in volcanoes at a depth of one kilometer with as little as 9.99 MPa (290 psi) stress normal to the fault, i.e., hydraulic head. The fault would remain in a dilated state until the critical normal stress was no longer exceeded, at which time the fault would return to a permeability barrier. This displacement history is schematically illustrated in Figure 3c. Repeated opening and closing of the fracture should be controlled by the permeability of the medium and the extent of the differential stress over or under pressuring. In summary, this type of harmonic behavior may be initiated by drawdown of the target reservoir or injection into the disposal reservoir. The spectral frequencies of the harmonic tremors observed at volcanoes and a few injection operations fall into the same spectral region covered by the microseismic monitoring systems; therefore, if this type of phenomenon occurs, it will be observable.

B-5
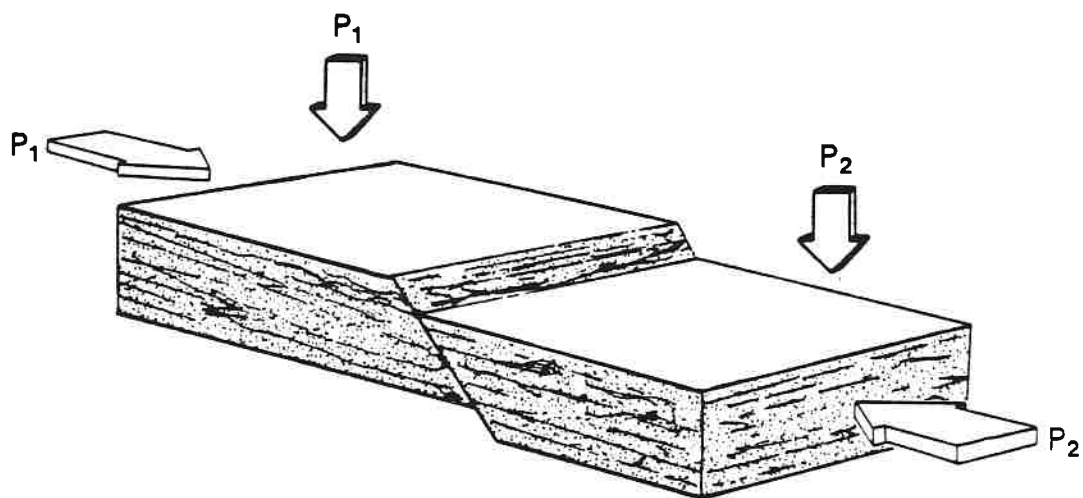
a. FAULTED RESERVOIR
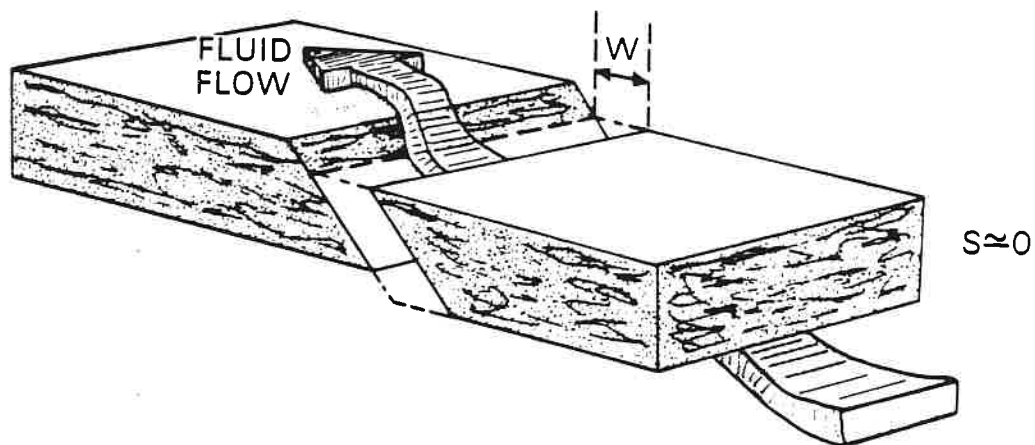
b. DILATANT FAULT BEHAVIOR PERMITTING
   FLUID FLOW
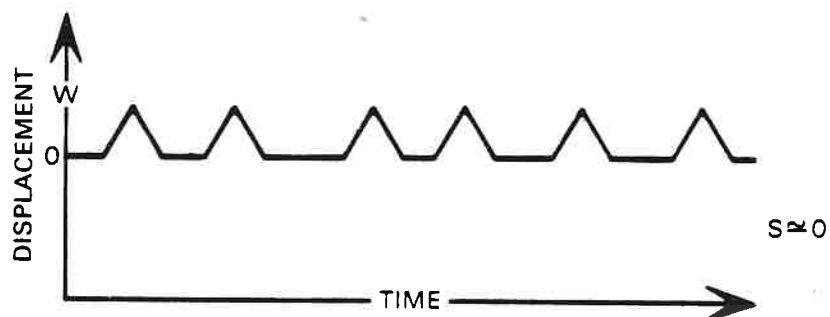
c. DILATANT DISPLACEMENT TIME HISTORY

FIGURE 3. HYPOTHETICAL DILATANT FAULT BEHAVIOR

G 12324

Microseismic Monitoring Arrays

The microseismic monitoring system used at both the Pleasant Bayou site (BEG) and the Dow L. R. Sweezy site (LSU) is schematically illustrated in Figure 4. Both arrays consist of five sensor locations, each of which is equipped with a Teledyne Geotech S-500 seismometer, Model 42-50 amplifier, and voltage-controlled oscillator (VC). The seismometers are mounted at the bottom of one-hundred feet deep boreholes. All associated electronics are at the surface. The signals from all of the sensors are multiplexed together and transmitted to the Teledyne Geotech Laboratory via continuous telephone telemetry circuits. At Garland, Texas, the signals are demultiplexed using Teledyne Geotech 46.12 discriminators. The individual continuous signals then are recorded simultaneously on the magnetic tape and 16-millimeter film. The film records are the only permanent data archive. Magnetic tapes are only used to reproduce events of interest.

The layout of the BEG and LSU arrays is illustrated in Figures 5 and 6 respectively. The seismograph sensor locations are illustrated in both figures as solid triangles. The locations of the test wells are illustrated as divided circles. The locations and sense of motion of local growth faults at a depth of approximately 4573 meters (15,000 feet) are illustrated as shaded lines on both maps. The seismograph system frequency response at both arrays is illustrated in Figure 7. This response is particularly suited for observing microearthquakes in the magnitude range 0 to 3. Magnification factors of the amplifiers permit recording (without distortion) of any earth movement within six kilometers of any station which has a displacement amplitude greater than 5×10^{-9} meters and less than 5×10^{-6} meters and vibration frequencies between one and twenty hertz.

Data generated by the monitoring systems are analyzed using standard microseismic data analysis techniques to yield basic information about the origin times, locations, and magnitudes of observed events. The 16-mm film seismograms are reviewed carefully to detect any microseismic event that may occur. When an event is detected, the analyst measures the amplitude, period of vibration and arrival times of the P (compressional), SV (vertical mode shear) and LR (surface Rayleigh) waves from the event. Desired accuracy of arrival time picks is less than $\pm$ 0.01 seconds. If this degree of accuracy is not attainable utilizing the film records, the analyst may choose to play back the analog tape of the event with selected filtration to enhance the signal-to-noise ratio or increase the recording speed to enhance time resolution. Since two of the three principal factors determining the precision of locating explosions or earthquakes are the quantity and quality of the arrival time data, it is very important that the time picks and phase identification be as accurate as possible.

The location procedure used is the Geiger least-squares error analysis technique in which a trial location and origin time are specified with a given velocity structure and arrival times for given station locations, and, through an iterative process, relocates the trial location and origin time to best fit the observed arrival times. The precision of the final solution is determined by the dimensions of the observed minus predicted arrival time errors and is translated into an error ellipse of specified semi-axes lengths at a
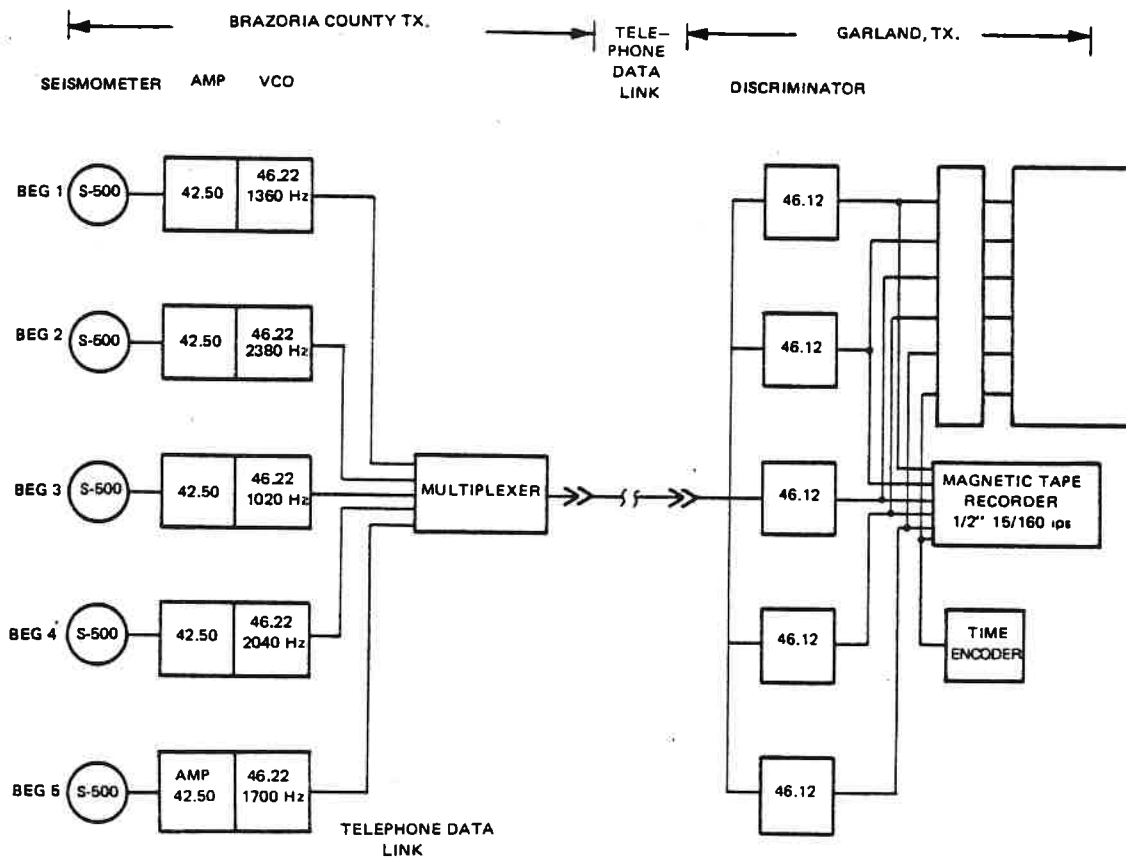
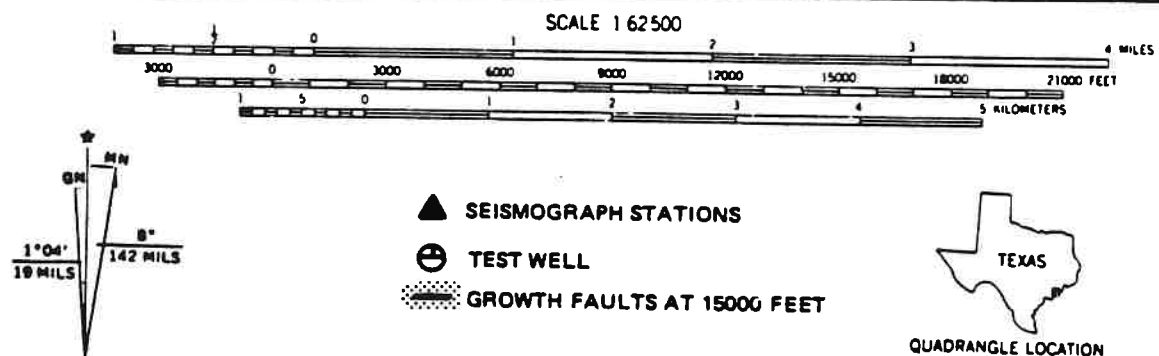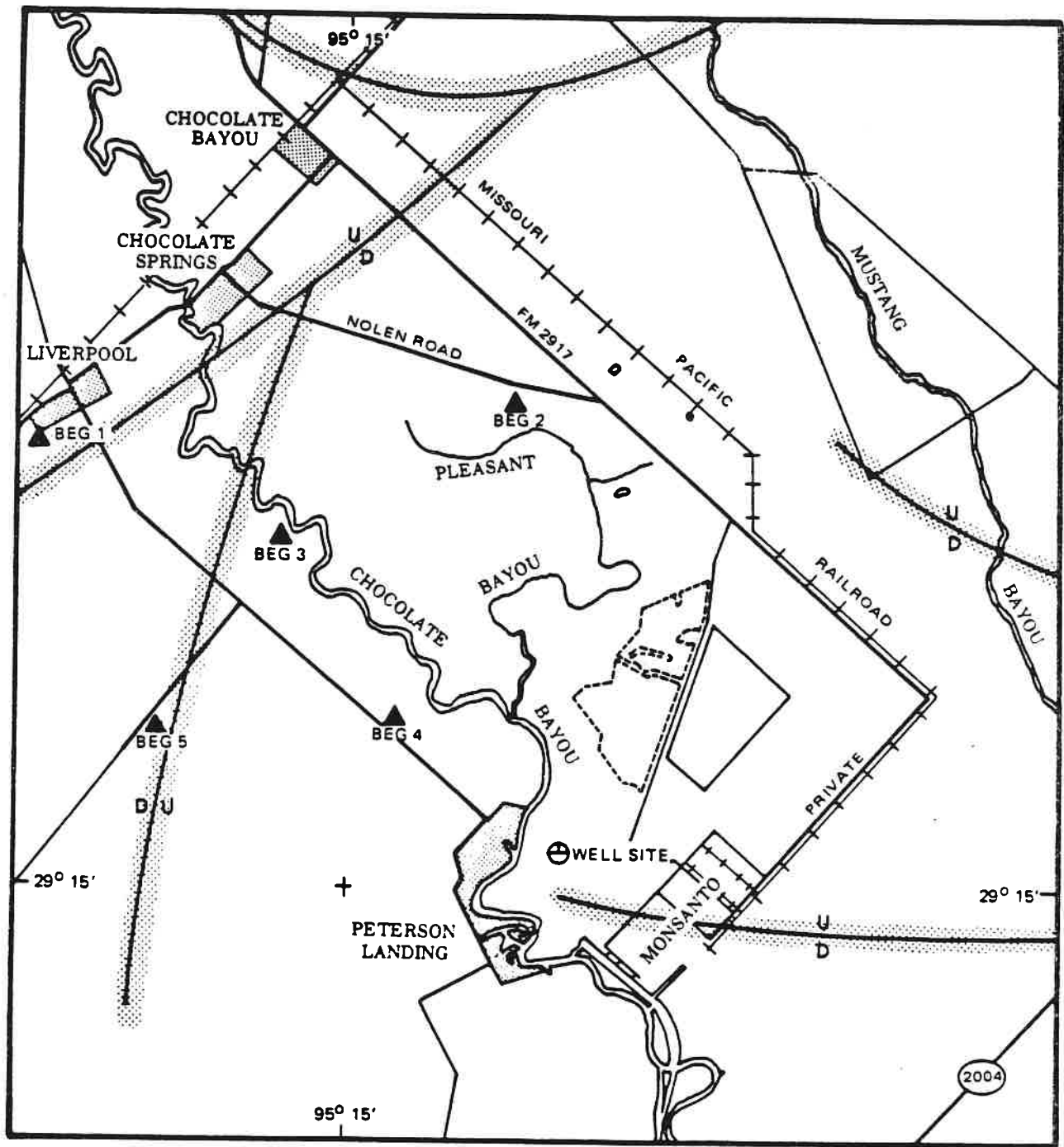FIGURE 4. BLOCK DIAGRAM OF BRAZORIA COUNTY SEISMIC ARRAY

G 11908

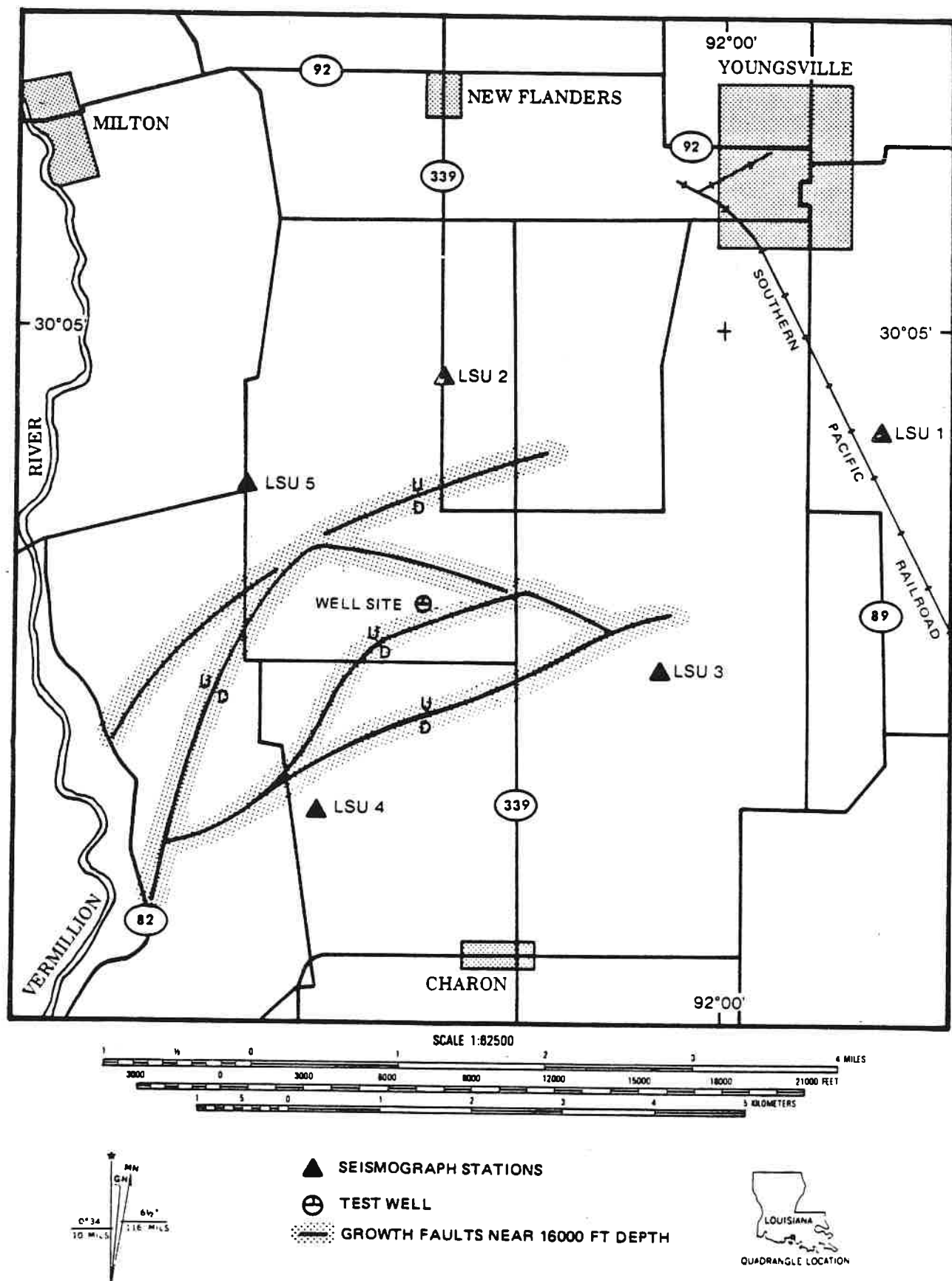FIGURE 5. BRAZORIA COUNTY TEXAS SEISMIC ARRAY

G 11907

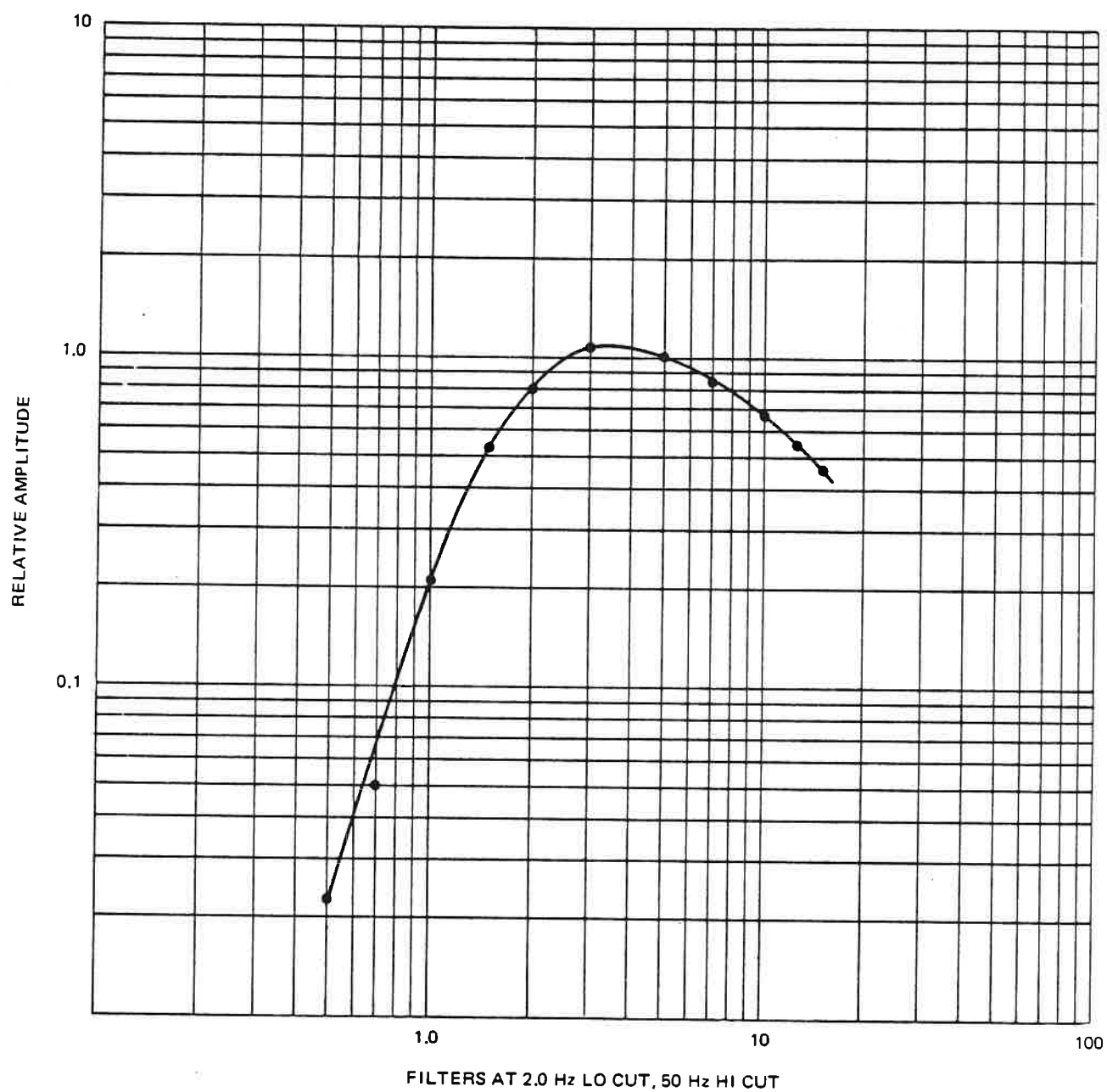FIGURE 6. PARCPERDUE LOUISIANA SEISMIC ARRAY

G 11905

B-10

FIGURE 7. SYSTEM VELOCITY RESPONSE AT BRAZORIA

G 11147C

TR 83-1

particular probability confidence level. We choose to set the confidence
level at 90%, although other investigators may use alternative limits. The
generalized P-wave velocity structure used in the location inversion proce-
dure is illustrated in Figure 8. The specific P-wave velocity structures for
the BEG and LSU projects are determined from sonic logs from local wells and
vary slightly from the illustrated, generalized structure. In general, com-
parable shear-wave velocity structure is not available, so S-waves are treated
as pseudo P-waves via the relationship:

$$V_S = V_P / (1 - \frac{1}{1-2\sigma})^{1/2}$$

where: V_S = Shear wave velocity

         V_P = Compressional wave velocity

         σ = Poisson ratio (0.25)

Frequently, the body phases (P and S) are indistinguishable from the ambient
noise; however, the Rayleigh wave arrivals are very prominant. Location of
these events is also possible using a modified Geiger inversion which simul-
taneously determines the appropriate half-space velocity and least-squares
error of location. Because this procedure is less constrained than the com-
parable body-wave technique, the source locations are less confidently
constrained. Source depth, for example, is nearly unconstrained in these
surface wave solutions.

Microseismicity Recorded During 1981

Although both the Brazoria and Parcperdue seismic arrays have been operational
for several years, for brevity, only the seismicity for 1981 will be
discussed. It is important to realize that neither geopressured/geothermal
test well had been produced at the volumetric rates porposed at the onset of
the program. The Brazoria test well had a few short-term tests and the
Parcperdue well was untested by the end of 1981. Thus, the seismicity
reported here can be considered to be more representative of ambient con-
ditions prior to withdrawal than under the conditions of full production.

In the introduction, several alternative mechanisms of fault behavior were
outlined. Many of these have been observed at both test wells and are
illustrated in the following figures. An example of a normal microearthquake
recorded at the Parcperdue array is illustrated in Figure 9. Note the high
frequency character of this event, the clear impulsive arrival of the P-wave
and the typical exponential decay of the coda. Three or four of these events
are recorded each year at both arrays. They always have location solutions
at the depths of a few kilometers and tend to occur near locations of mapped
growth faults. An example of a "slow" microearthquake, i.e., an earthquake
whose rupture velocity is significantly slower than shear-wave velocity, is
illustrated in Figure 10. This event, recorded at the Brazoria array, is the
only occurrence of this type of event which has been observed to date.
Comparing Figures 9 and 10 clearly illustrates the difference in character of
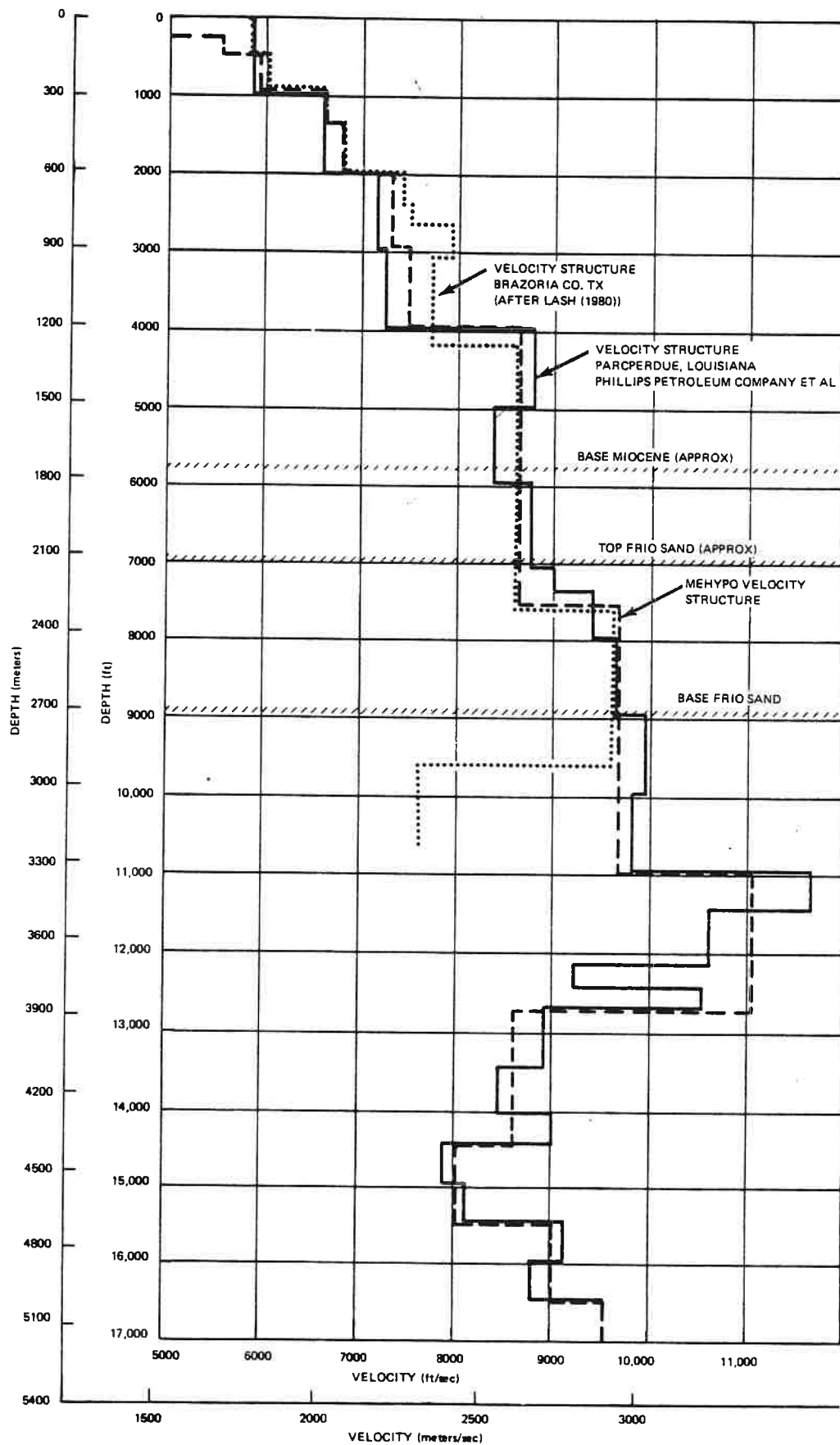
FIGURE 8. P-WAVE VELOCITY STRUCTURE

G 11746

B-13

TR 83-1

FIGURE 9. EVENT 1, 27 MARCH 1981, 17:48: 16:42 UCT (CST + 6 HRS), MAGNITUDE M_L = 1.3, M_D = 1.4

G 11919

FIGURE 10. EARTHQUAKE 1 JANUARY 1981, 03:32:29.3 UCT

TR 83-1

these types of earthquakes. The "slow" earthquake has a much lower frequency P-wave and S-wave than the comparable energy normal earthquake. The reason for the lower frequency phase arrivals is related to the much longer period of time over which the movement occurred. This event, like the normal earthquake, locates at depths near known growth faults.

Figure 11 illustrates a relatively common event recorded at both arrays. These events are classified as impulsive Rayleigh events because they lack any distinguishable body (P or S) phases and are located using Airy phase Rayleigh mode velocities. Depth discrimination of this type of event is very poor in normal Geiger solution schemes. During and post well production periods at the Brazoria, Parcperdue and Sweet Lake prospects (see Figure 1), there has been an increase in the number of these events which occur. Because of their character, however, additional studies must be performed to determine whether these events are related to the withdrawal or injection process. At this time, it cannot be specified with which process these events tend to be produced. Figures 9, 10, and 11 constitute the three event types recorded by the two test well monitoring networks which have arrival times capable of being inverted to an origin location. Before discussing the relationship of the recorded seismicity to known tectonic features, I would like to illustrate two additional frequently occurring event types which are nonlocatable.

One of these atypical microseismic events is illustrated in Figure 12. I refer to this event type as rumble. It characteristically has an emergent onset precluding normal hypocenter calculations, a duration which is variable but ranges from ten to eighty seconds, and incoherent phases across the array, although all stations will be affected by it. Since these events are atypical of normal seismic signals, I can only speculate as to their origin. I believe that the phase incoherence across the array is an indication that these signals are generated by the coalescence of the phase arrivals from a large number of very small microearthquakes which are distributed over some finite area. Thus, this type of signal may be what one should expect from a "noisy" creep as illustrated in the introduction. These may be typical signals generated during episodes of subsidence. An interesting experiment would be to see if the occurrences of these events correspond with long-period tilt and/or strain steps locally.

A second type of signal which has been observed several times (all subsequent to the Phase II testing of the Pleasant Bayou No. 2 well) I refer to as harmonic tremor. The reason for this nomenclature comes from studies of volcanoes where harmonic tremor is commonly observed prior to eruption. The characteristic of harmonic tremor which is easily identified is a nearly purely monotonic vibration which is regionally pervasive. The source of these signals at volcanoes is still debated, but it is strongly argued that these signals are generated by fluid transport through a complex conduit system. An example of this phenomenon is illustrated in Figure 13b. Figure 13a illustrates the normal ambient condition for comparison. Characteristic ambient spectra at the Brazoria array for 8 August 1981 are illustrated in Figure 14a. Fourteen-minute time segments which were free from cultural and/or natural events were selected for analyses. The data for stations BEG1, BEG2, BEG3, and BEG5 were analyzed using a Hanning filter window with

TR 83-1

19:58:00 UCT (UNCORRECTED)

5 SEC

BCD TIME

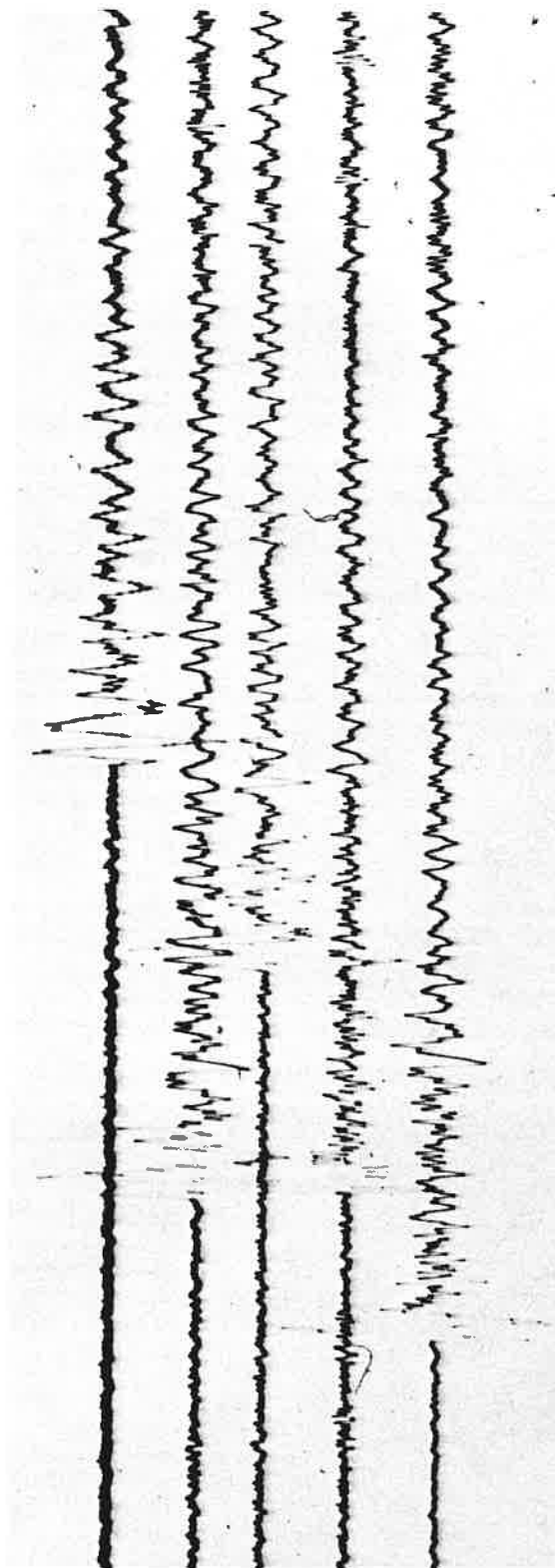LSU1 (67K)

LSU2 (62K)

LSU3 (60.5K)

LSU4 (60K)

LSU5 (60K)

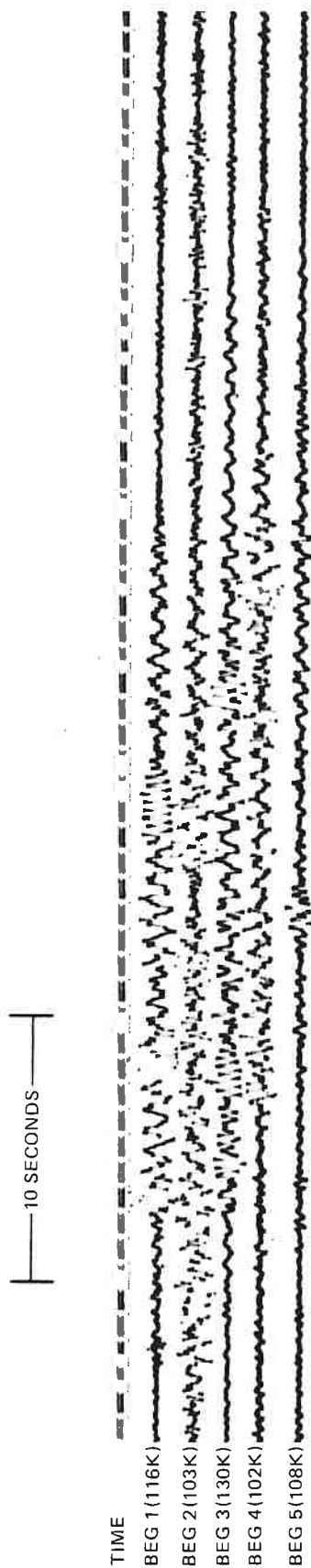FIGURE 11. EVENT 17 JANUARY 1982, IMPULSIVE RAYLEIGH ARRIVAL

G 12449

B-17

TR 83-1

FIGURE 12. RUMBLE EVENT 15 AUGUST 1981. DURATION 50 SECONDS.

G 12175

BEG1 (116K)
BEG2 (103K)
BEG3 (100K)
BEG4 (102K)
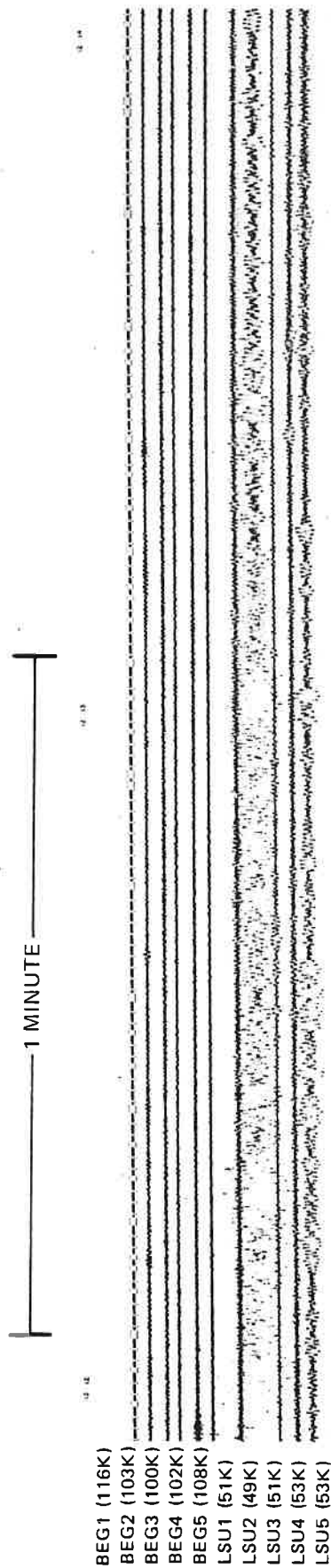BEG5 (108K)
LSU1 (51K)
LSU2 (49K)
LSU3 (51K)
LSU4 (53K)
LSU5 (53K)

— 1 MINUTE —

FIGURE 13a. NORMAL BACKGROUND AT THE BRAZORIA ARRAY. HIGH LEVEL NOISE AT THE
PARCPERDUE ARRAY TYPICAL WITH GULF STORMS.

BEG1 (116K)
BEG2 (103K)
BEG3 (100K)
BEG4 (102K)
BEG5 (108K)
LSU1 (51K)
LSU2 (49K)
LSU3 (51K)
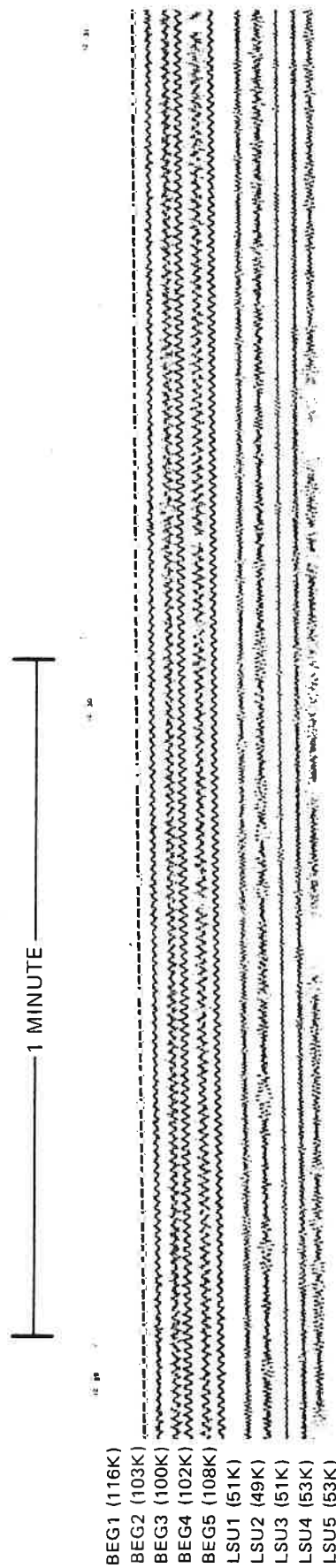LSU4 (53K)
LSU5 (53K)

— 1 MINUTE —

FIGURE 13b. HARMONIC TREMOR AT THE BRAZORIA ARRAY, AUGUST 4, 1981.
DURATION NINETY MINUTES FROM 12:19:24 UCT. MAXIMUM
GROUND DISPLACEMENT 6.5 NANOMETERS AT A PERIOD OF
0.8 ±0.05 SECOND.

G12176

B-19

linear summation of the eight-second block spectra for 105 blocks. The RMS amplitude spectra for the frequency range 0 through 3 seconds are illustrated in Figure 15a. All of the channels except BEG2 display RMS amplitude spectra in this frequency range which are approximately -50 dB. The general amplitude decrease with decreasing frequency is a characteristic of the instrumental frequency response. The higher amplitude lobe of energy on BEG2 at frequencies less than one hertz is caused by local drilling operations near that station. In comparison, the spectra displayed in Figure 14 were obtained for a fourteen-minute analysis period beginning12:19 UCT on 8 August during the time of the harmonic tremor. A boxcar filter window was used rather than a Hanning filter window to improve the amplitude accuracy. This filtering sacrificed the spectral resolution slightly which explains the more rounded appearance of spectra in Figure 14b compared with those of 14a. Note that the RMS amplitude of the harmonic tremor is 20 dB (10 times) above the ambient noise. The dominant frequency is 1.24 hertz, and the bandwidth is extremely narrow (indicating high selectivity of resonance or high Q, attenuation, away from the dominant resonant frequency). The offset of the spectra from BEG5 is due to higher magnification of this tape recorded channel and does not have any natural significance. The high-amplitude, narrow-frequency band spectrum is also characteristic of harmonic tremor observed at volcanoes.

During the duration of the main episode of harmonic tremor on 4 August 1981, two trains passed the array. The station nearest to the tracks is BEG1. Figure 14c illustrates the spectrum of the train passage at BEG1 for comparison with both 14a and 14b. Note that the passage of a train generally increases the amplitude throughout the frequency band from 0 to 3 hertz without producing a pronounced spectral peak at 1.24 hertz. I believe that this is additional evidence that the harmonic tremor is naturally and not culturally produced. Similarly, no teleseismic events nor Gulf of Mexico turbulence has been reported which might account for these signals; thus I conclude that these harmonic tremors which appear on all Brazoria stations are of local, natural origin.

A period of harmonic tremor on 2 October 1982, may have provided a key observation to understanding the origin of the harmonic tremor. Three microearthquakes occurred during the episode of harmonic tremor. Shortly following these three locatable microearthquakes, the harmonic tremor episode ceased. Although this may be purely coincidental, I believe that the two phenomena are related. The occurrence of these three events evidently changed subsurface conditions which caused the source of the harmonic tremor to stop emitting energy.

Returning to the events which can be located using standard techniques with body waves, it is interesting to note their distribution with respect to known tectonic features, i.e., growth faults. The six microearthquakes in 1981 located under these constraints at the Parcperdue, Louisiana, array are illustrated in Figure 15. Similarly, eight events at the Brazoria, Texas, site are illustrated in Figure 16. Note in both cases that the events have centroids which locate on or near growth faults. In the case of Parcperdue, events apparently are distributed on all growth faults surrounding the DOW-DOE L. R. Sweezy No. 1 well. At Brazoria, on the other hand, the seismic-
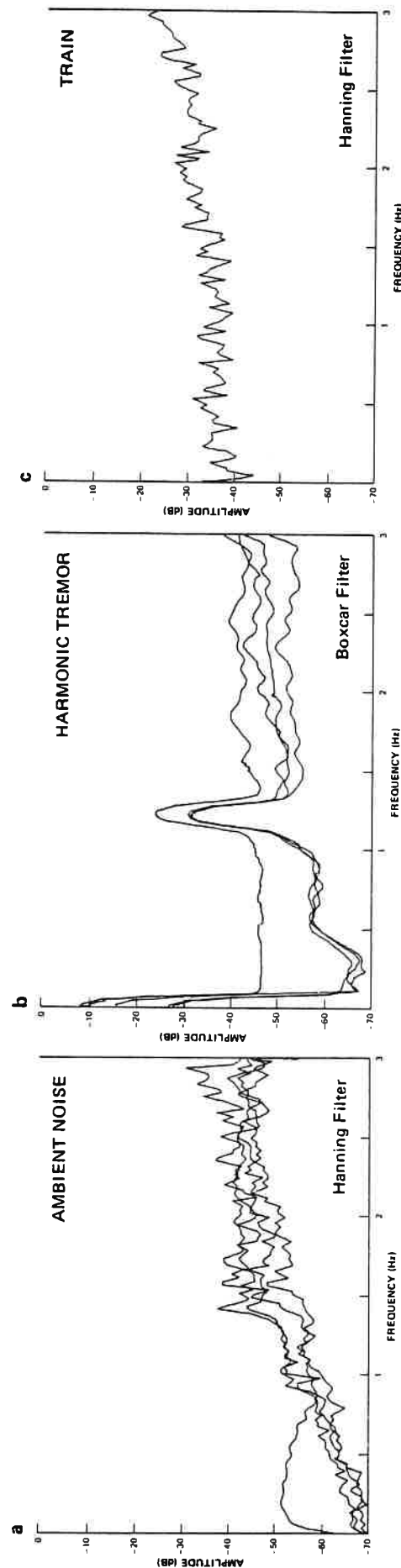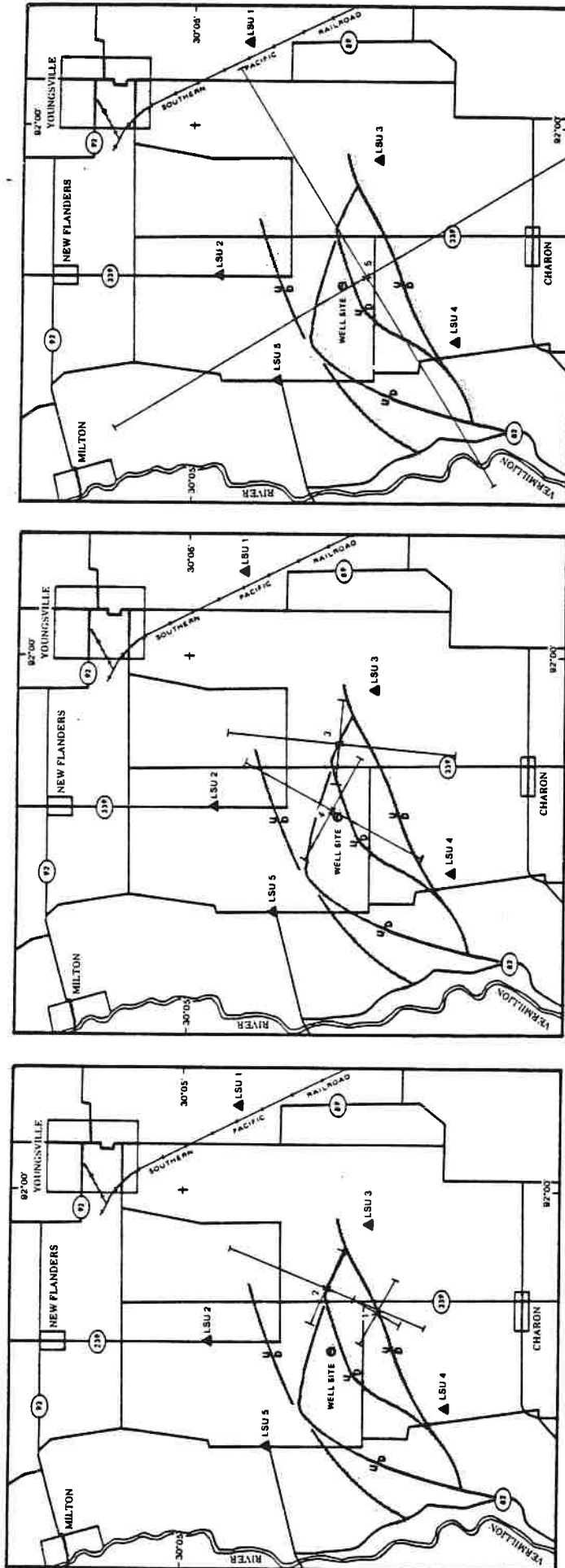
FIGURE 14. a. AMBIENT AMPLITUDE SPECTRA FOR BEG1, BEG2, BEG3, AND BEG5 FOR 8 AUGUST 1981. b. AMPLITUDE SPECTRA FOR BEG1, BEG2, BEG3, AND BEG5 FOR 8 AUGUST 1981 FROM 12:19 THROUGH 12:35 UCT DURING THE OCCURRENCE OF THE HARMONIC TREMOR c. AMPLITUDE SPECTRUM FOR BEG1 DURING THE PASSAGE OF A TRAIN ON 8 AUGUST 1981. SEE DISCUSSION FOR ADDITIONAL DETAILS.

G 12172

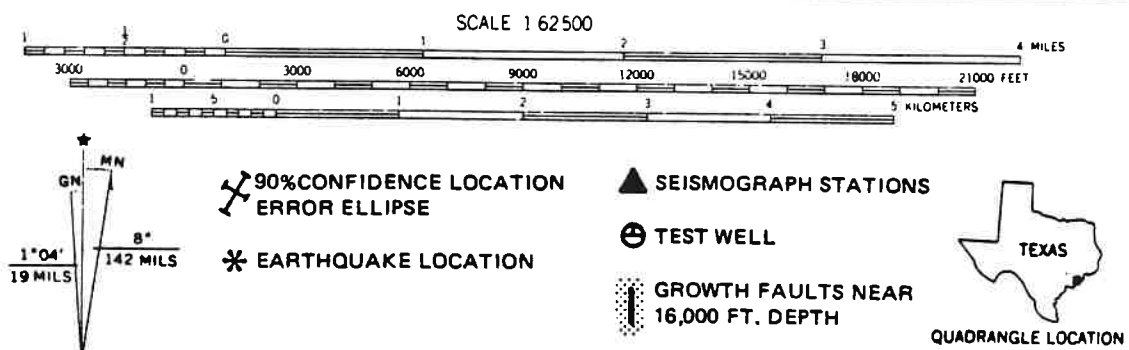FIGURE 15. EPICENTERS OF LOCAL EARTHQUAKES RECORDED DURING 1981
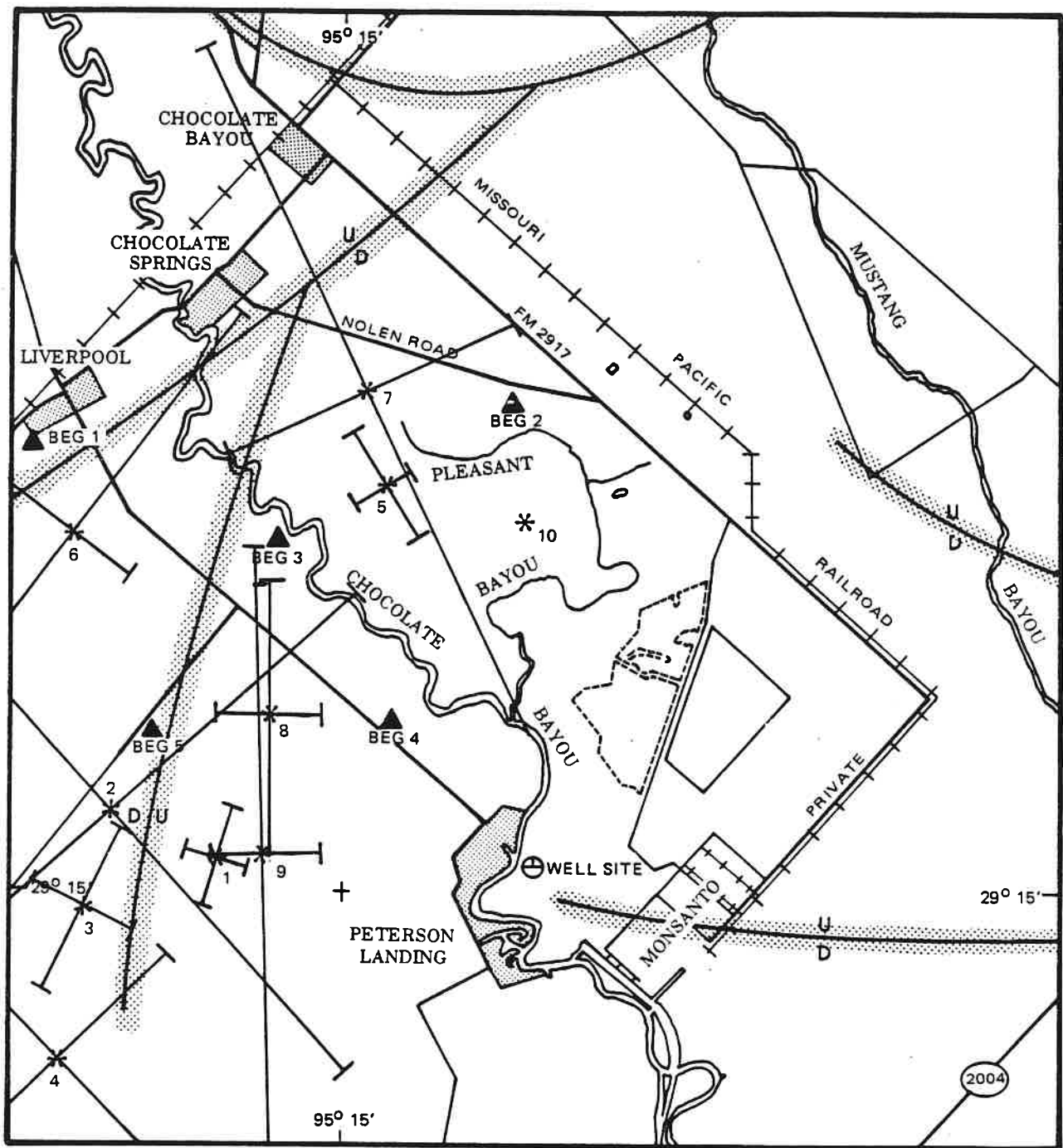
QUADRANGLE LOCATION   G 12362

▲ 90% CONFIDENCE LOCATION   ▲ SEISMOGRAPH STATIONS
  ERROR ELLIPSE   ⊕ TEST WELL

✱ EARTHQUAKE EPICENTER   GROWTH FAULTS NEAR
                            16,000 FT. DEPTH

B-22

FIGURE 16. RELOCATED EARTHQUAKES FOR 1981 (USING BODY WAVES)

G 11907 L

TR 83-1

ity clusters about only one regional growth fault, and the fault closest to the Pleasant Bayou No. 2 well does not appear to be active. Again, it is worth a precautionary note that this seismicity is dominantly ambient and not related to well production. Nevertheless, at Brazoria, the increased activity located using surface waves which are apparently related to production also clustered on this same fault. This strongly suggests that enhanced seismicity induced by well production will most likely associate with growth faults which are exhibiting unstable behavior during ambient conditions. In addition, induced seismicity at the Brazoria, Parcperdue and Sweet Lake Prospects (T. Statton, personal communication) are displaying temporal delays from gradients in production history which suggest a strain diffusion mechanism similar to hydrodynamic diffusion effects.

In conclusion, the results to date suggest a variety of types of fault behavior in the Gulf Coast. Both shear and dilatant behavior have been observed. There is an ambient seismicity related to growth faults movement in the absence of geopressured/geothermal well production. The number of events annually is six to ten, and the maximum magnitude observed has been 1.5. Development of the geopressured/geothermal wells results in increased seismicity approximately doubling or tripling the number of recorded events. Event magnitudes are all less than 1.5 indicating that conditions in the Gulf Coast sediments are such that strain accumulation sufficient to generate a large damaging earthquake is unlikely. Monitoring of the low-level activity, however, may provide important information about subsidence effects which in the long term are a more serious environmental and economical hazard of geopressured/geothermal well development as an alternative energy source.

Seismicity Induced by Geopressured/Geothermal Well Development in the Texas and Louisiana Gulf Coast

FREDERICK J. MAUK (Teledyne Geotech Geophysical Research Department, 3401
    Shiloh Road, Garland, Texas 75040)

R. ALAN DAVIS (Same as above)

Geopressured/geothermal brines, which may constitute an important future
energy alternative, are contained in Cretaceous and Tertiary-aged high-
permeability formations underlying the Texas and Louisiana Gulf Coasts.
Economic development of these resources necessitates production and subsur-
face disposal of the brines at individual well volumetric rates exceeding 3.2
x $10^3 m^3$/day). Such high volumetric transfer rates can alter substantially
the state of local geological stress and potentially result in induced
seismicity. To evaluate the potential cost/benefit of developing this
resource, the DOE in conjunction with state agencies in Texas and Louisiana
has been analyzing prototype development of a few design wells. Associated
microseismic monitoring with these well development programs has provided the
opportunity to analyze seismicity both prior to and post test production.
The results of these studies at the Pleasant Bayou, Texas and Parcperdue,
Louisiana design wells indicate that there is an ambient backbround of five
to ten events between magnitudes 0 and 2.0 per year. The frequency of
occurrence and characteristics of the events changes dramatically in post
production periods. Events prior to and post production periods cluster in
the vicinity of the same growth faults suggesting that high volume production
of wells in the Gulf Coast tends to enhance movement along faults which nor-
mally are active. Aspects of ambient and enhanced seismicity at these design
wells will be discussed.

TR 83-1

Technical Report No. 83-1

Microseismic Monitoring of Chocolate Bayou Texas
The Pleasant Bayou No. 2 Geopressured/Geothermal
Energy Test Well Program

1982 Annual Progress Report

Prepared by

Frederick J. Mauk, PhD and R. Alan Davis

Prepared for

The University of Texas at Austin
Bureau of Economic Geology
University Station, Box X
Austin, Texas 78712

CPT 264